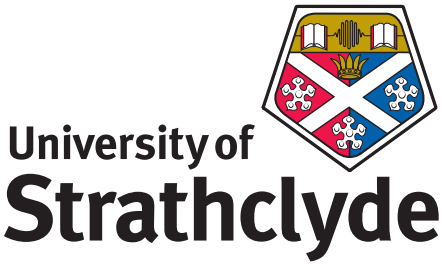

Fractional Derivative Models for the Spread of Diseases

Areej Abdullah Saleh Almuneef
Department of Mathematics and Statistics
University of Strathclyde
Glasgow, UK
March 2021

This thesis is submitted to the University of Strathclyde for the degree of Doctor of Philosophy in the Faculty of Science.

Acknowledgements

First and foremost, I would like to gratefully acknowledge my supervisor, Prof. Nigel Mottram, who gave me the golden opportunity to fulfill this thesis through his valuable guidance and useful suggestions.

I would like to also express my heartfelt thanks to my joint supervisor, D. Moustafa El-Shahed, who has always provided the kindest support, encouragement, and guidance throughout the accomplishment of this dissertation.

I am deeply grateful to the faculty teachers at University of Strathclyde and Princess Nourah bint Abdulrahman University who have helped me to do this research.

I am also indebted to my friend, Zuhur Alqahtani, for all her help, useful suggestions and for being there to listen when I needed an ear. She has been more like a sister than a friend to me.

Very special thanks to my husband, Mansour Ababutain, for all his help and support, for everything that he has done to make this work possible. His helping hand paved the way to the completion of this thesis.

Finally, many thanks to all my friends and colleagues for their help, cooperation and suggestions throughout the course of my research.

Abstract

This thesis considers the mathematical modelling of disease, using fractional differential equations in order to provide a tool for the description of memory effects. In Chapter 3 we illustrate a commensurate fractional order tumor model, and we find a critical value of the fractional derivative dependent on the parameter values of the model. For fractional derivatives of orders less than the critical value an unstable equilibrium point of the system becomes stable. In order to show changes in the observed areas of attraction of two stable points in the system, we then consider a fractional order SIR epidemic model and investigate the change from a monostable to a bistable system. Chapter 4 considers a model for virus dynamics where the fractional orders for populations are different, called an incommensurate system. An approximate analytical solution for the characteristic equation of the incommensurate model is found when the different fractional orders are similar and close to the critical value of the fractional order of the commensurate system. In addition, the instability boundary is found as a function of both parameters. A comparison between analytical and numerical results shows the high accuracy of this approximation. Chapter 5 consists of two parts, in the first part we generalise the integer Fisher's equation to be a space-time fractional differential equation and consider travelling wave solutions. In the second part we generalise an integer SIR model with spatial heterogeneity, which was studied by Murray [117], to a space-time fractional derivative model. We apply the (G'/G)-expansion method and find travelling wave solutions, although in this case we must consider the Jumarie's modified Riemann-Liouville fractional derivative. Finally, we consider the effect of changing the orders of time and space fractional derivatives on the location and speed of the travelling wave solution.

Contents

List of Figures

List of Tables

Chapter 1

Introduction

Programs to develop and improve sanitation, vaccination methods and the provision of antibiotics in the 20^{th} century have created confidence in the ability of human societies to control and eliminate many diseases. As a result, chronic diseases such as cancer or infectious diseases have received great attention in industrialized countries. These diseases have continued to spread in developing countries and have become the main causes of death and the suffering of people. In addition, diseases can adapt and develop, so that new diseases appear and existing diseases reappear [97]. The deterioration of ecosystems due to human or animal invasions, global warming, environmental debasement, expanded global travel, and changes in economic patterns also often allow new and existing illnesses to spread [108].

Emerging and reemerging diseases have been the focus of many researchers from numerous disciplines throughout the world. Mathematical models have played an important role in analysing and predicting the spread of diseases. The process of modelling uses various assumptions, variables, and parameters, and models can provide various useful outcomes, such as basic reproduction numbers, replacement numbers, thresholds, and contact numbers. Mathematical models and computer simulations are therefore helpful tools for building and testing speculations, evaluating quantitative guesses, responding to explicit inquiries, deciding sensitivities to changes in parameter values, and assessing key parameters from information. For instance, understanding the transmission qualities of disease in networks, locations, and nations can give better ways to deal with the transmission of these infections. The mathematical and statistical study of disease progression and transmission can add to epidemiological understanding, propose the essential information that ought to be gathered to distinguish patterns, make general forecasts, and evaluate the uncertainty in these forecasts [77, 78].

In many complex models, we move from a description of a real world system to an equation, often using a flow diagram as a visualisation and modelling tool. Flow diagrams are simple in design but structured to illustrate complicated phys-

ical aspects of the system and relationships or interactions between them. By allowing a logical analysis of the system, these diagrams assist us in formulating equations [148]. For each of the systems we consider in this thesis, we will use a flow diagram to visualise the model.

In this thesis we will consider a particular mathematical model of memory in biological systems, and the impact of memory on the behaviour of the system. For instance, human memory, and the behaviour that is affected by memory can impact the various processes, evolution and control of the spread of diseases within human populations. An individual's experience, knowledge and retrieved memory can affect their response during the spread of disease within the human populations [154].

Many different approaches to modelling memory effects have been used in mathematical models of disease spread. For instance, delay differential equations (DDEs) have often been exploited for modelling memory effects. In this type of system there are time delay terms which allow the current state of the system to depend on the state a fixed time in the past. However, DDEs are often only applicable if the memory effects need to reflect the dependence on a state at a specific time in the past. For instance, the modelling of a disease with an incubation period could allow the current infection rate to depend on the level of contact between the infected and non-infected population at fixed time (the incubation period) in the past. However, there is also a need for a model of continuous memory, i.e. an effect of experiences over a continuous period of time. Accordingly, fractional differential equations (FDEs) have been used [12], since they are non-local operators [154]. The fractional derivative of a function provides information about the function value at all times from an earlier point in time up to now, while an integer derivative provides information about the function's behaviour at only the current time [29].

In more general terms, fractional calculus is often used to generalise derivatives and integrals to an arbitrary order, integer or non-integer, real or complex. Although classical calculus provides powerful tools for modelling many phenomena studied in applied sciences, they do not allow rigorous consideration of some abnormal dynamics within certain complex systems encountered in nature. Experimental results show that several processes linked to these complex systems have a non-local dynamic behaviour, involving long-term effects, and fractional derivatives have been shown to have similarities with some of these characteristics [116].

Research on fractional calculus dates back more than three centuries. The concepts of fractional derivatives and integrals are often associated with Riemann and Liouville, although the generalisation of derivatives to fractional orders is older.

The beginnings of fractional calculus lie in a simple discussion between mathematicians when, in 1695, L'Hôpital raised a question with Leibniz inquiring about the significance of $d^n y/dx^n$ when $n = 1/2$. Leibniz, in his response, considered a possible theory of non-integer derivatives and wrote to L'Hôpital: 'An apparent paradox, from which one day useful consequences will be drawn.' It was not until 1990 that the first 'useful consequences' appeared [116].

Euler later considered this problem. In his article [55] where he introduces his famous Gamma function which generalises the factorial function, he considers rational numbers (termed fractional) and not arbitrary real numbers. The current denomination of derivatives as 'fractional' to express derivatives of an arbitrary order could thus find its historical origin in this work. The first real application of fractional calculus seems to be proposed by Abel in 1823 [2]. He showed that the generalised tautochrone problem might be written as a non-integer differential equation and expressed the solution using an integral equation. The first serious attempt to provide a logical definition for fractional derivatives is due to Liouville who published a series of nine research documents related to this subject between 1832 and 1837 [105]. Independently, Riemann proposed his own approach which was essentially the same as that of Liouville. Since that time this approach has been termed the 'Riemann-Liouville' approach.

Further approaches have been adopted to generalise the notion of derivatives to non-integer orders. For instance, the limit of the growth rate of a function is generalised in the Grunwald-Letnikov formula [70, 96], which is useful to obtain a numerical approximation of fractional derivatives and integrals [68]. The existence of different formulations raises the question of their equivalence. In fact, those of Grunwald-Letnikov and Riemann-Liouville are identical, although the proof is long and is presented in detail in the work of Samko, Kilbas and Marichev [134].

Heaviside provided the first concrete application of fractional calculus in 1892 in solving the one-dimensional heat equation. This approach was not rigorous (and was not justified until 1919) but nevertheless provides the correct solution to the problem. When considering periodic functions, it is useful to define fractional integral and derivative operations so that the period of the function is conserved after their application. Consequently, Weyl's definition was introduced [162]. Furthermore, the fractional integrals used in the Riemann-Liouville definition are defined on a bounded interval. However, for certain problems, defining fractional operators on an unbounded interval is required, and in this case, the Marchaud approach should be used [107].

Although fractional differentiation in the Riemann-Liouville sense was an important step forward in this field, several authors including Caputo realized that this definition must be revised. In fact, applications in visco-elasticity, mechan-

ics of solids and rheology require physically interpretable initial conditions which are not easy in the case of the Riemann-Liouville approach. The initial conditions in the sense of the Caputo approach [30] are expressed in terms of integer order derivatives, while those in the sense of Riemann-Liouville are expressed by fractional operators which may have no defined physical meaning [92], and this is often why the Caputo approach is preferred. Ishteva [81] examined the fundamental proprieties of Caputo derivatives and addressed this comparison in more detail.

Over the years many approaches to fractional calculus have been proposed, and Podlubny [125] provides a good review of these approaches, as well as several practical problems. There have been highly significant contributions by great mathematicians such as Lagrange in the eighteenth century, Laplace, Fourier, Hadamard and Heaviside in the nineteenth century, as well as Hardy, Littlewood and finally Riesz in the twentieth century. It seems that the many different, and often contradictory, definitions have prevented greater success of the theory, which has not yet been unified into a single approach. Moreover, the absence of a clear geometrical or physical interpretation of fractional derivatives has largely contributed to the fact that this field of research has remained on the sidelines.

Over recent years, interest in fractional differential equations has increased considerably, the first conference on fractional calculus and its applications taking place at the University of New Haven in 1974 [131]. The same year, Oldham and Spanier [120] published a key work which was totally devoted to fractional calculus, and where they summarised a wide range of concerns in relation to fractional calculus. In late 1996, a round table meeting was held on 'Physical and Geometrical Meaning and Applications of Fractional Calculus Operators', where the attendees conjectured about the existence of a geometrical representation of fractional derivatives [93]. In particular, fractional derivatives have been used as a tool to describe memory. In 2002, a physical interpretation of fraction derivatives as a model of memory was presented but was not compared to experimental results [126]. However, in [49] Du et al. noticed that a number of memory phenomena, from various disciplines such as biology, mechanics and psychology, are well modelled as two stage processes. Firstly a short permanent retention phase, and secondly a phase that is governed by a simple fractional derivative model. In this work they compared various models to experimental data and found that the memory phenomena are best fitted using the fractional derivative model. From the fitting of theoretical models to experimental data they found that the fractional derivative order can be interpreted physically as an index, or measure, of memory.

Several analytical methods such as Fourier transforms, model synthesis, eigenvector expansion, Laplace transforms, Mellin transforms, fractional Green's functions, and the power series method have been applied to solve FDEs. However, most of the aforementioned methods are only applicable to solve linear FDEs and

fail to solve the non-linear FDEs, some of which we consider in this thesis. Therefore, there has been an increasing interest in developing new numerical methods that could be applicable to both linear and non-linear FDEs, such as Podlubny's numerical method, the Predict Evaluate-Correct Evaluate (PECE) method, and the generalised Euler method. [42].

In this thesis we consider the application of fractional derivatives to model memory and spatial inhomogeneity in a number of biological systems. Indeed biology is an expanding field of application of fractional calculus. The qualitative behaviour of ordinary differential equation systems describing diseases and infections has been studied for a long time although researchers have encountered some difficulty in accurately understanding a number of results. Among those researchers are Ding and Ye [48] who obtained a system of fractional order derivatives to model HIV infection of $CD4^+$ T-cells after modifying a previous model proposed by Culshaw and Ruan [41]. Rihan [129] provided additional results after introducing a fractional model for describing the interaction of infection with the immune system, including a consideration of memory. One of the most frequently used models to interpret the characteristic of epidemic diseases is the Susceptible-Infected-Recovered (SIR) model, which was first introduced by Kermack and McKendrick [90]. Many different extensions of this model have since been employed to describe such epidemics. In [127], the authors discuss the insufficiency of classical models and thus propose a novel approach to a Dengue epidemic using fractional derivatives. This turns out to be a more accurate approach, and allows the authors to gain a deeper understanding and more realistic results concerning the transmission mechanism. Similar multi-compartmental models have also been proposed. In regard to epidemics that incorporate latency and recovery periods, it is appropriate to include a fourth compartment. For instance, González-Parra et al. [67] proposed a SEIR model (E for people incubating the virus) to test its agreement with real data for influenza A (H1N1). Estimating the model parameters allowed them to conclude that the choice of fractional order derivatives coincided closely with the realistic data. Against that background, Casagrandi et al. [32] introduced an alternative SIRC model (C for cross-immune individuals) to address epidemiological questions related to influenza A viruses. More results on that subject were discussed in the work of El-Shahed and Alsaedi [53].

This thesis is organized into six main chapters. Chapter 2 includes the basic concepts and mathematical principles of fractional derivatives, explains the specific approaches and tools needed to understand fractional calculus properties, as well as an introduction to the biological models we consider. Chapter 3 is in two parts, the first part presents the behaviour of a fractional order tumor model, and studies the properties of the system, where changing the parameters of the system leads to changes in stability, and the second part presents the behaviour of a fractional order SIR model, where non-linear interactions between individuals can

cause multiple stable states. In these systems we see that fractional derivatives can lead to multistability. In Chapter 4 we study a fractional system of viruses propagation, termed an incommensurate system, which means that the derivative orders of the individuals are different. Considering a perturbation of the solution to the characteristic equation of the commensurate system, we find an approximate analytical solution for the characteristic equation of the incommensurate system. The stability condition, which is a function of the fractional derivative orders in the incommensurate fractional system, is then found from the approximate analytical solution. A numerical method is also used to solve the incommensurate system, and to compare with the analytical solution for the virus propagation system. Chapter 5 discusses the existence of travelling wave solutions in fractional differential equations, and presents two models, the first one is the space-time fractional Fisher's equation, the second model is a space-time fractional SIR model. Through an attempt to model memory in a biological context, the use of fractional time derivatives was previously justified, and here we see the possibility of travelling waves in such a system. In Chapter 5 we use the (G'/G)-expansion method for determining new travelling wave solutions of the fractional PDEs, where we have used Jumarie's modified Riemann-Liouville derivatives. By plotting the location and speed of the travelling wave solution we find the effect of changing the time and space fractional derivatives on the travelling wave. Chapter 6 summarises the results and discusses further development and research extensions.

Chapter 2

Mathematical Background

2.1 Introduction

This chapter will be devoted to elementary definitions and basic concepts relating to fractional calculus and the models and methods we use in this thesis, including models of biological systems and various analytic and numerical methods we use to investigate these systems.

2.2 Basic Definitions

In this section, we give the most common definitions of fractional integrals and derivatives and then show that only certain properties of the classical derivatives can be generalised to the fractional case. Most of the definitions in this chapter are taken from [134] to which we refer the reader for an in-depth analysis of the subject, and we refer to [86, 120, 125] to introduce basic definitions and properties of fractional calculus theory.

2.2.1 The Mittag-Leffler Function

The exponential function, e^z, is very useful in the theory of integer order differential equations, forming the basis for eigenfunctions of the integer order derivative needed to investigate stability of equilibrium points. A generalisation of this function was introduced by Mittag-Leffler [54] and, as we will see later, it has been widely used in the context of fractional order differential equations.

Definition 2.2.1 *Let $z \in \mathbb{C}$. The Mittag-Leffler function with parameter α is defined as*

$$E_\alpha(z) = \sum_{k=0}^{\infty} \frac{z^k}{\Gamma(k\alpha + 1)},$$

where $\alpha > 0$ and $\Gamma(.)$ is the Gamma function.

The Mittag-Leffler function with two parameters, α and β, has the form

$$E_{\alpha,\beta}(z) = \sum_{k=0}^{\infty} \frac{z^k}{\Gamma(k\alpha + \beta)},$$

where $\alpha > 0$ and $\beta > 0$.

Using these definitions we see that $E_\alpha(z) = E_{\alpha,1}(z)$ and $E_1(z) = E_{1,1}(z) = e^z$. As we will see below, when considering fractional order differential equations, the Mittag-Leffler function serves a similar purpose as the exponential function for integer order derivatives.

2.2.2 Grunwald-Letnikov Fractional Derivative

The Grunwald-Letnikov fractional derivative [92] of order α of a function f where $f : [a, \infty) \to \mathbb{R}$ is defined by

$$f^{(\alpha)}(x) = D^\alpha f(x) = \lim_{h \to 0} h^{-\alpha} \sum_{k=0}^{\infty} (-1)^k \begin{pmatrix} \alpha \\ k \end{pmatrix} f(x - kt),$$

where $\begin{pmatrix} \alpha \\ k \end{pmatrix} = \dfrac{\Gamma(\alpha + 1)}{\Gamma(k + 1)\Gamma(\alpha - k + 1)}$. Since the summation upper limit is infinity then the derivative $f^{(\alpha)}(x)$ takes information from an infinite number of times before. We see from the coefficient $h^{-\alpha} \begin{pmatrix} \alpha \\ k \end{pmatrix}$ that if $\alpha = 1$ then the fractional derivative takes present time and time before but everything else equal to zero. As α decreases, the fractional derivative places more weight on information from further back in time. Therefore, α gives a measure of how important previous information is. If α changes, the weighting of previous time changes. Thus, variation of α will model changes in memory from long memory (when $\alpha \to 0$) to short memory (when $\alpha \to 1$). So α is a simple description of how far back in time the system can remember.

2.2.3 Riemann-Liouville Fractional Integral and Derivative

Some of the original, and most used, forms of fractional operators were developed by Riemann and Liouville. Here we will summarise these definitions and list various useful properties. First we consider the Riemann-Liouville fractional integral. Let f be a continuous function on the interval $[a, b]$, and let us consider the integral

$$I_a^1 f(x) = \int_a^x f(t)dt.$$

The second integral of f is then given by

$$I_a^2 f(x) = \int_a^x \Big(\int_a^u f(t)dt \Big) du.$$

Exchanging the order of integration we obtain

$$\begin{aligned} I_a^2 f(x) &= \int_a^x \Big(\int_t^x du \Big) f(t)dt. \\ &= \int_a^x (x-t) f(t)dt. \end{aligned}$$

We can then define the n^{th} iteration of the operator I,

$$I_a^n f(x) = \int_a^x dx_1 \int_a^{x_1} dx_2 ... \int_a^{x_{n-1}} f(x_n)dx_n = \frac{1}{(n-1)!} \int_a^x (x-t)^{n-1} f(t)dt.$$

Using the well-known property of the Gamma function, $\Gamma(n) = (n-1)!$, finally gives

$$I_a^n f(x) = \frac{1}{\Gamma(n)} \int_a^x (x-t)^{n-1} f(t)dt.$$

This formula makes sense even for non-integer values of n, and so we are able to define a fractional version of I, which is termed the Riemann-Liouville integral.

Definition 2.2.2 *The Riemann-Liouville integral is*

$$I_a^\alpha f(x) = \frac{1}{\Gamma(\alpha)} \int_a^x (x-t)^{\alpha-1} f(t)dt,$$

where $\alpha \in \mathbb{R}$.

There are several possible definitions of fractional derivatives [92, 125] and we will discuss three of these in the section below. We first introduce possibly the most frequently used, the Riemann-Liouville derivative.

Definition 2.2.3 *If we consider the classical relation* $\dfrac{d}{dx} = \dfrac{d^2}{dx^2} \circ I^1$, *we define a fractional derivative with order* $0 < \alpha \leq 1$ *as*

$$\frac{d^\alpha}{dx^\alpha} = \frac{d}{dx} \circ I^{1-\alpha},$$

where $I^{1-\alpha}$ *is the Riemann-Liouville integral. More generally, if* $\alpha > 0$ *and* $m = [\alpha] + 1$ *where* $[\alpha]$ *denotes the floor function value of* α, *we have*

$$\frac{d^\alpha}{dx^\alpha} = \frac{d^m}{dx^m} \circ I^{m-\alpha}, \tag{2.1}$$

and therefore we obtain the definition of the Riemann-Liouville fractional derivative

$${}^{RL}D_a^\alpha f(x) = D^m I_a^{m-\alpha} f(x) = \frac{d^m}{dx^m} \circ I_a^{m-\alpha} f(x),$$

where $m - 1 < \alpha \leq m$, $\alpha > 0$ *and* $x \geq a$.

Equivalently, we distinguish two cases, where $\alpha \neq m$ or where $\alpha = m$, so that,

$$ {}^{RL}D_a^\alpha f(x) = \begin{cases} \dfrac{1}{\Gamma(m-\alpha)} \dfrac{d^m}{dx^m} \displaystyle\int_a^x (x-t)^{m-\alpha-1} f(t)dt, & \text{if } m-1 < \alpha < m \\ \dfrac{d^m}{dx^m} f(x), & \text{if } \alpha = m \end{cases} $$

where $x \geq a$, $\alpha > 0$ and $m \in \mathbb{N}$.

Riemann-Liouville fractional derivatives have many properties,

1. The differential operator ${}^{RL}D^\alpha$ is a left inverse of the integral operator I^α, so that ${}^{RL}D_a^\alpha(I_a^\alpha f(x)) = f(x)$.
2. If $\alpha = 0$ we have ${}^{RL}D_a^0 f(x) = f(x)$, the identity operator.
3. The classical composition property is not true ${}^{RL}D_a^\alpha({}^{RL}D_a^\beta f(x)) \neq {}^{RL}D_a^{\alpha+\beta} f(x)$.
4. Left composition with an integer order derivative is true but it is non-commutative,

   $$ {}^{RL}D_a^m({}^{RL}D_a^\alpha(f(x))) = {}^{RL}D_a^{m+\alpha}(f(x)) \neq {}^{RL}D_a^\alpha({}^{RL}D_a^m(f(x))), $$

   for $m \in \mathbb{N}$.
5. The operator ${}^{RL}D$ is linear so that

   $$ {}^{RL}D_a^\alpha(\lambda f(x) + \gamma g(x)) = \lambda {}^{RL}D_a^\alpha f(x) + \gamma {}^{RL}D_a^\alpha g(x), $$

   where λ and $\gamma \in \mathbb{C}$.
6. The fractional derivative of $f(t) = (x-a)^\gamma$, for $\gamma > -1$, is

   $$ {}^{RL}D_a^\alpha (x-a)^\gamma = \frac{\Gamma(\gamma+1)}{\Gamma(\gamma-\alpha+1)} (x-a)^{\gamma-\alpha}. $$

7. The fractional derivative of $f(t) = c$, where c is constant, is

   $$ {}^{RL}D_a^\alpha(c) = \frac{c}{\Gamma(1-\alpha)} (x-a)^{-\alpha}. $$

8. The Laplace transform of ${}^{RL}D_a^\alpha(f)$ is

   $$ L({}^{RL}D_a^\alpha(f(x)))(s) = s^\alpha F(s) - \sum_{k=0}^{m-1} s^k({}^{RL}D_a^{\alpha-k-1}(f(a))). $$

   Although this transfomation has been reported frequently in the literature [120, 131], its practical application is limited by the absence of physical interpretation of the limit values of fractional derivatives at the lower bound, $x = 0$.

The Riemann-Liouville derivative plays a significant role in the development of the theory of fractional differentiation and it is widely employed in pure mathematics. However, practical applications of the theory require dealing with initial conditions of concrete physical sense, which this approach does not allow. A certain solution for this conflict was proposed, in the sixties, by Caputo [31], which we will discuss below.

2.2.4 Caputo Fractional Derivative

The Caputo fractional derivative of order α of a function f where $f : [a, \infty) \to \mathbb{R}$ is defined by

$$ {}^{C}D_a^{\alpha} f(x) = \frac{1}{\Gamma(m-\alpha)} \int_a^x (x-t)^{m-\alpha-1} f^{(m)}(t) dt, $$

where $\alpha > 0$ such that: $m - 1 < \alpha \leq m$, $m \in \mathbb{N}$, and $f^{(m)}(t) = \frac{d^m}{dt^m} f(t)$. In this thesis, we consider $m = 1$, and for simplicity of notation we denote ${}^{C}D_a^{\alpha}$ as D_a^{α}.

Definition 2.2.4 *A simple reverse operation of the compositions in (2.1) allows the definition of the Caputo fractional derivative as*

$$ D_a^{\alpha} f(x) = I^{m-\alpha} \circ \frac{d^m}{dx^m} f(x), $$

where $x \geq a$, $\alpha > 0$ and $m \in \mathbb{N}$, $m - 1 < \alpha \leq m$.

Equivalently, we distinguish two cases, where $\alpha \neq m$ and where $\alpha = m$,

$$ D_a^{\alpha} f(x) = \begin{cases} \dfrac{1}{\Gamma(m-\alpha)} \displaystyle\int_a^x (x-t)^{m-\alpha-1} f^{(m)}(t) dt, & \text{if } m-1 < \alpha < m \\ \dfrac{d^m}{dx^m} f(x), & \text{if } \alpha = m \end{cases} $$

where $x \geq a$, $\alpha > 0$ and $m \in \mathbb{N}$.

Caputo fractional derivatives have many properties,

1. If $\alpha = 0$ we have $D_a^0 f(x) = f(x)$, the identity operator.
2. The classical composition property is not true $D_a^{\alpha}(D_a^{\beta} f(x)) \neq D_a^{\alpha+\beta} f(x)$.
3. Left composition with an integer order derivative is true but it is non-commutative,

   $$ D_a^{\alpha}(D_a^m(f(x))) = D_a^{\alpha+m}(f(x)) \neq D_a^m(D_a^{\alpha}(f(x))), $$

   for $m \in \mathbb{N}$.

4. The operator D^α is linear so that

$$D_a^\alpha(\lambda f(x) + \gamma g(x)) = \lambda D_a^\alpha f(x) + \gamma D_a^\alpha g(x)),$$

where λ and $\gamma \in \mathbb{C}$.

5. The fractional derivative of $f(t) = (x-a)^\gamma$, for $\gamma > -1$, is

$$D_a^\alpha (x-a)^\gamma = \frac{\Gamma(\gamma+1)}{\Gamma(\gamma-\alpha+1)}(x-a)^{\gamma-\alpha}.$$

6. The fractional derivative of $f(t) = c$, where c is constant, is $D_a^\alpha(c) = 0$.

7. The Laplace transform of $D_a^\alpha(f)$ is

$$L(D_a^\alpha(f(x)))(s) = s^\alpha F(s) - \sum_{k=0}^{m-1} s^{\alpha-k-1}(D_a^k(f(a))).$$

The important differences between the Riemann-Louiville and Caputo approaches are that, firstly, the initial conditions of a fractional order differential equation using Caputo derivatives can be written in the form of evaluations of the functions and integer derivatives of the function. Secondly, the Caputo fractional derivative of a constant function $f(t) = c$ equals zero, while it equals $c(x-a)^{-\alpha}/\Gamma(1-\alpha)$ in the sense of the Riemann-Louiville derivative.

2.2.5 Jumarie's Modified Riemann-Liouville Derivative

With the aim of correcting the problem of the Riemann-Liouville derivative of a constant, which for many reasons we would like to be zero, Jumarie [84] introduced a revised definition of the Riemann-Liouville derivative.

Definition 2.2.5 *Jumarie's modified Riemann-Liouville derivative of order α is defined by*

$$D_a^\alpha f(x) = \begin{cases} \dfrac{1}{\Gamma(-\alpha)} \displaystyle\int_a^x (x-t)^{-\alpha-1} f(t)dt, & \alpha < 0 \\ \dfrac{1}{\Gamma(1-\alpha)} \dfrac{d}{dx} \displaystyle\int_a^x (x-t)^{-\alpha}(f(t)-f(a))dt, & 0 < \alpha < 1 \\ (f^n(x))^{\alpha-n}, & n \le \alpha < n+1, n \ge 1. \end{cases}$$

We note that the above expression coincides with the Riemann-Liouville definition in the case $\alpha < 0$.

Jumarie's modified Riemann-Liouville derivative has many properties [21, 85],

1. The fractional derivative of $f(t) = c$ where c is a constant is $D_a^\alpha(c) = 0$, $\alpha > 0$.

2. The fractional derivative of $f(x) = x^v$ where $v > 0$ is

$$D_a^\alpha x^v = \frac{\Gamma(1+v)}{\Gamma(1+v-\alpha)} x^{v-\alpha}.$$

3. The fractional derivative of $cf(x)$ where c is a constant is

$$D_a^\alpha(cf(x)) = cD_a^\alpha f(x),\ \alpha > 0.$$

4. The operator D_a^α is linear, so that $D_a^\alpha(af(x)+bg(x))) = aD_a^\alpha f(x)+bD_a^\alpha g(x)$, where a and b are constants.

5. The operator D_a^α satisfies the product and chain rule,

$$\begin{aligned} D_a^\alpha(f(x)g(x)) &= g(x)D_a^\alpha f(x) + f(x)D_a^\alpha g(x), \\ D_a^\alpha f[g(x)] &= f'[g(x)]D_a^\alpha g(x) = D_a^\alpha f(g)(g'(x))^\alpha. \end{aligned}$$

2.3 Mathematical Models of Biological Systems

Mathematical models provide a way to describe the interaction between species whether the species are animal or human populations, natural resources, or cells [161]. However, in real life it is difficult to study the behaviour of interactions between species over long periods of time, and for this reason mathematical models are often useful. A simple single-species model might be

$$\frac{dN}{dt} = \text{births} - \text{deaths} + \text{migration}, \tag{2.2}$$

where $N(t)$ is the species' population at time t [118]. We will now consider various possible forms of the terms for birth, death and migration.

2.3.1 Malthusian Growth

Malthus [104] proposed the simplest model of the form (2.2) when there is no migration as follows,

$$\frac{dN}{dt} = \underbrace{bN}_{\text{births}} - \underbrace{dN}_{\text{deaths}} = (b-d)N = rN, \tag{2.3}$$

where $r = b - d$. The solution is then

$$N(t) = N_0 e^{rt},$$

where $N(0) = N_0$ is the initial population. For this simple model we see that if $r < 0$ ($b < d$) then the population decreases exponentially, if $r = 0$ ($b = d$) the population remains constant at its initial value, and if $r > 0$ ($b > d$) the population increases exponentially.

2.3.2 Logistic Growth

It is unrealistic to consider a population's growth as always growing and there will always be a limit, or carrying capacity, to exponential growth. A logistic growth model can be used as a way to describe the population's limited growth. From [43], the classical logistic equation is

$$\frac{dN}{dt} = rN\left(1 - \frac{N}{K}\right), \tag{2.4}$$

where N is the population size, $r = b - d$ is the difference between natural birth and death rates, and K is a carrying capacity of the population. This equation has solution

$$N(t) = \frac{KN(0)}{N(0) + (K - N(0))e^{-rt}}.$$

Figure 2.1 indicates the behaviour of the solution to equation (2.4). At first when $N(0) \ll K$ the growth is exponential and then when the population size approaches the carrying capacity the growth rate approaches zero. For a large initial population, i.e. $N(0) > K$, the population will decline until the carrying capacity is approached.

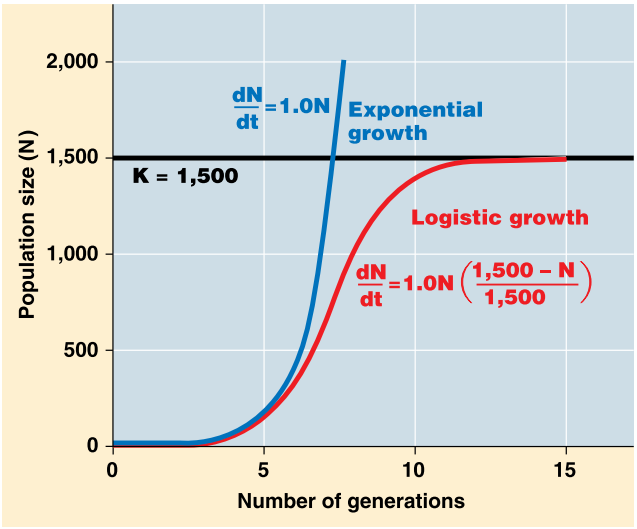

Figure 2.1: Logistic growth (red curve) compared to exponential growth (blue curve), from [43].

2.3.3 Functional Response

Functional response is a term denoting how two species can interact in a predator-prey system [50]. It describes the dependency of the predator consumption rate on both the density of the prey. Holling (1959) introduced three forms of functional response as follows

$$\begin{aligned} f(R) &= aR, \\ f(R) &= a\frac{R}{h+R}, \\ f(R) &= a\frac{R^2}{h^2+R^2}, \end{aligned}$$

called Holling type I, II and III respectively, where R is the population of prey, $f(R)$ is the rate of prey consumption, a is a maximum consumption rate, and h is the density of the prey when the consumption per capita is half the maximum value. In Holling type I, the feeding rate does not saturate as the prey density increases, which means the consumption has a linear form, and a is the constant predation rate, as used by Lotka and Volterra in the standard form of the integer system, see Figure 2.2 (a). In Holling type II, as the number of prey increases, the feeding rate saturates, with a maximum growth rate a. This maximum depends on the handling time, so that, even if the number of prey is very large the predator cannot eat the prey fast enough because of the time needed to handle and eat the prey, see Figure 2.2 (b). Holling type III has a similar behaviour to the Holling type II except, for low numbers of prey, the predators will rarely find prey (the so called search time), so the form of the predation rate reduces to zero, see Figure 2.2 (c).

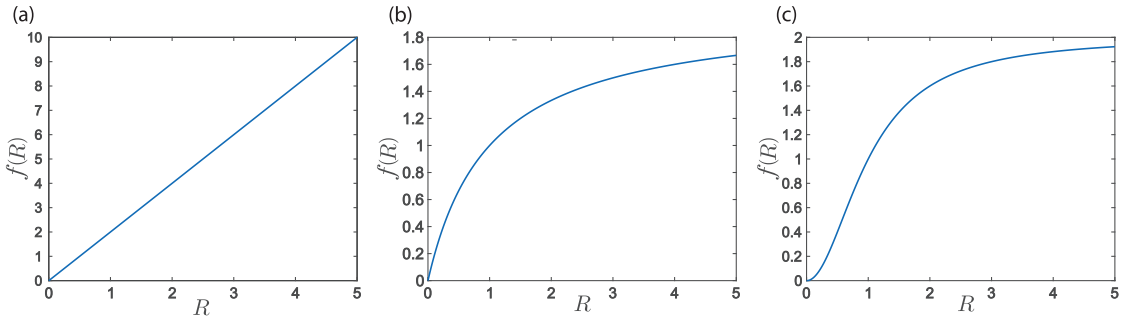

Figure 2.2: Plots of the functional response for (a) Holling type I, (b) II and (c) III.

2.3.4 SIR Models

For models of the spread of infectious diseases, it is common to suppose that the population can be divided into three compartments: the susceptible, S, who can

catch the disease, the infected, I, who have caught and can transmit the disease, and the recovered (or removed) population, R, who have recovered from the disease and are now immune, or who have isolated until they have recovered, or who have died due to the disease [117]. The assumptions made about the transmission of the infection and incubation period are that the incubation period is short enough to be negligible, and that the epidemic is of short duration so that the population can be taken to be uniform. A simple dynamic model based on the above assumptions is then

$$\begin{aligned} \frac{dS}{dt} &= -rSI, && (2.5)\\ \frac{dI}{dt} &= rSI - aI, && (2.6)\\ \frac{dR}{dt} &= aI, && (2.7) \end{aligned}$$

where $r > 0$ is the infection rate of the susceptible population and $a > 0$ is the recovery or removal rate of infected population. Note that

$$\frac{d}{dt}(S + I + R) = 0 \Rightarrow S + I + R = N, \tag{2.8}$$

so that the total population N is a constant. The initial conditions are

$$\begin{aligned} S(t = 0) &= S_0 > 0, && (2.9)\\ I(t = 0) &= I_0 > 0, && (2.10)\\ R(t = 0) &= 0. && (2.11) \end{aligned}$$

In this simple model it is clear from (2.5) that

$$\frac{dS}{dt} = -rSI \leq 0, \tag{2.12}$$

so that S decreases from its initial value, $S \leq S_0$. From equation (2.6) we see that

$$\begin{aligned} \frac{dI}{dt} &= I(rS - a) > 0 \quad \text{if} \quad S > \frac{a}{r},\\ \frac{dI}{dt} &= I(rS - a) < 0 \quad \text{if} \quad S < \frac{a}{r}. \end{aligned} \tag{2.13}$$

Therefore, if $S_0 < a/r$, then I will decrease for all time and $I(t) \to 0$ as $t \to \infty$. However, if $S_0 > a/r$ then I will initially increase and then later, when S has reduced to a/r, will start to decrease.

The maximum infected population can also be calculated. From (2.5) and (2.6), we see

$$\frac{dI}{dS} = -\frac{(rS - a)}{rS} = -1 + \frac{\rho}{S}, \tag{2.14}$$

where $\rho = a/r$. Integrating and knowing that $S = S_0$ when $I = I_0$ gives

$$I \;=\; -S + \rho \ln S + I_0 + S_0 - \rho \ln S_0.$$

If there is a maximum value of I for $t > 0$, i.e. when $S_0 \geq \rho$, then we see from (2.6) that maximum, $I_{\max}$, occurs at $S = \rho$. We therefore have,

$$I_{\max} = \begin{cases} \rho \ln \rho - \rho + I_0 + S_0 - \rho \ln S_0, & S_0 \geq \rho. \\ I_0, & S_0 \leq \rho. \end{cases}$$

2.4 Stability for Integer Systems

In this section we will consider the standard approach to finding equilibrium points and the stability of these points for dynamical systems. This approach, using the eigenvalues of the Jacobian matrix [118], will be the basis for our study of the fractional systems that we will study later in this thesis. We consider a system of ODEs, $\dot{x} = f(x)$, where $f : \mathbb{R}^n \to \mathbb{R}^n$ and $x \in \mathbb{R}^n$, i.e.

$$\frac{d}{dt} \begin{bmatrix} x_1 \\ x_2 \\ \vdots \\ x_n \end{bmatrix} = \begin{bmatrix} f_1(x_1, \ldots, x_n) \\ f_2(x_1, \ldots, x_n) \\ \vdots \\ f_n(x_1, \ldots, x_n) \end{bmatrix}, \tag{2.15}$$

where $f_i : \mathbb{R}^n \to \mathbb{R}$. We then make the following definitions,

Definition 2.4.1 *An equilibrium (fixed) point of (2.15) is a point $x_\star \in \mathbb{R}^n$ that satisfies $f_i(x_\star) = 0$ for all $1 \leq i \leq n$.*

Definition 2.4.2 *A solution $x(t)$ of (2.15) with initial condition $x(t = 0) = x_0$ is stable if $\forall \epsilon > 0$, there exists $\delta(\epsilon) > 0$ such that if $\bar{x}(t)$ is another solution of (2.15) with $\bar{x}(t = 0) = \bar{x}_0$ and $\|\bar{x}_0 - x_0\| < \delta(\epsilon)$, then*

$$\|\bar{x}(t) - x(t)\| < \epsilon, \quad \forall t \geq 0.$$

Definition 2.4.3 *A solution of (2.15) is unstable if it is not stable.*

Definition 2.4.4 *A solution $x(t)$ of (2.15) with initial condition $x(t = 0) = x_0$ is asymptotically stable if: (a) it is stable, and (b) there exists $\gamma > 0$ such that $\|\bar{x}_0 - x_0\| < \gamma \implies \|\bar{x}(t) - x(t)\| \to 0 \quad as \quad t \to \infty$.*

Linearisation of the system of ODEs about an equilibrium point will lead to

$$\frac{dx}{dt} = Jx, \tag{2.16}$$

where J is the Jacobian matrix evaluated at the equilibrium point. The solutions of (2.16) are then

$$x = x_0 e^{\lambda t}, \tag{2.17}$$

where x_0 is a fixed vector and the eigenvalues λ are the roots of the characteristic equation

$$|J - \lambda I| = 0, \tag{2.18}$$

where I is the identity matrix.

Theorem 2.4.1 *For the system of linear ODEs (2.16), if all the eigenvalues, λ, have negative real parts, then the solution is stable. If at least one eigenvalue, λ, has a positive real part, then the solution is unstable.*

For example, consider the system of two ODEs

$$\frac{d}{dt}\begin{bmatrix} x(t) \\ y(t) \end{bmatrix} = J\begin{bmatrix} x(t) \\ y(t) \end{bmatrix}, \tag{2.19}$$

where J is the Jacobian matrix evaluated at the equilibrium point. The stability of the solution therefore depends on the eigenvalues, λ_1, λ_2 of J. The possible behaviours of the solutions depend on the eigenvalues, and whether they are real or complex, with negative or positive real parts. Table 2.1 shows all the possible solution behaviours, termed node, saddle, spiral or centre. Figures 2.3, 2.4 and 2.5 illustrate these behaviours as plots of the xy-plane, the phase portraits.

Eigenvalues	Type of Equilibrium Point	Stability
$\lambda_1 > \lambda_2 > 0$	Node	Unstable
$\lambda_1 < \lambda_2 < 0$	Node	Asymptotically stable
$\lambda_2 < 0 < \lambda_1$	Saddle point	Unstable
$\lambda_1 = \lambda_2 > 0$	Degenerate node	Unstable
$\lambda_1 = \lambda_2 < 0$	Degenerate node	Asymptotically stable
$\lambda_1, \lambda_2 = r \pm i\mu$	Spiral (or Focus) point	
$r > 0$		Unstable
$r < 0$		Asymptotically stable
$\lambda_1 = i\mu, \lambda_2 = -i\mu$	Centre	Stable

Table 2.1: The kinds of stability or instability corresponding to the eigenvalues of the Jacobian matrix J.

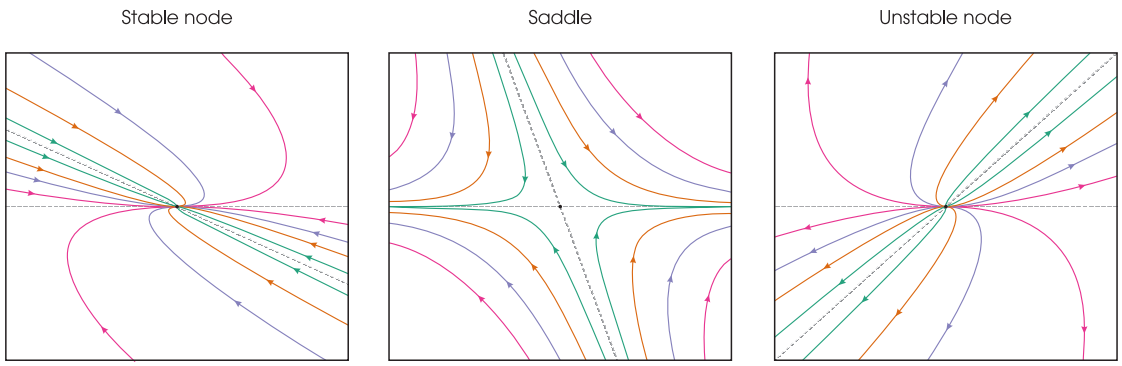

Figure 2.3: Qualitative behaviour when the matrix J in equation (2.19) has two different nonzero real eigenvalues, $\lambda_1 < \lambda_2 < 0$, $\lambda_2 < 0 < \lambda_1$ and $\lambda_1 > \lambda_2 > 0$ respectively.

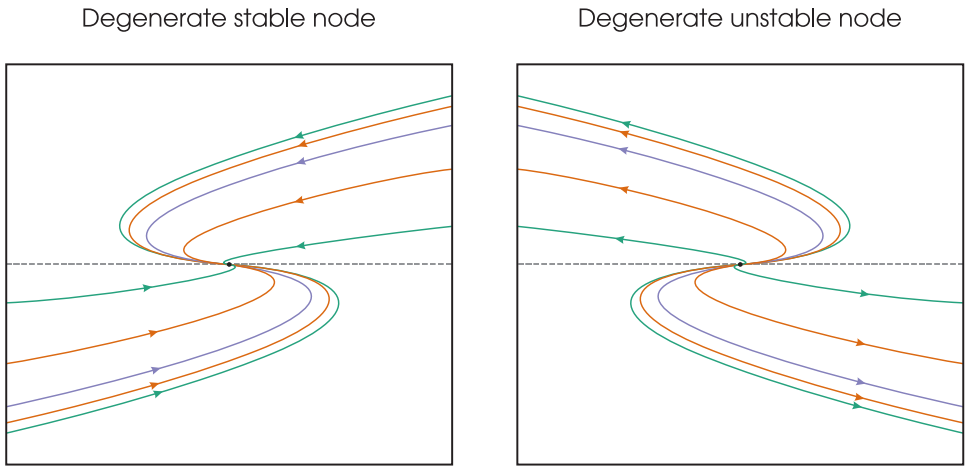

Figure 2.4: Qualitative behaviour when the matrix J in equation (2.19) has repeated real eigenvalue, $\lambda_1 = \lambda_2 < 0$ and $\lambda_1 = \lambda_2 > 0$ respectively.

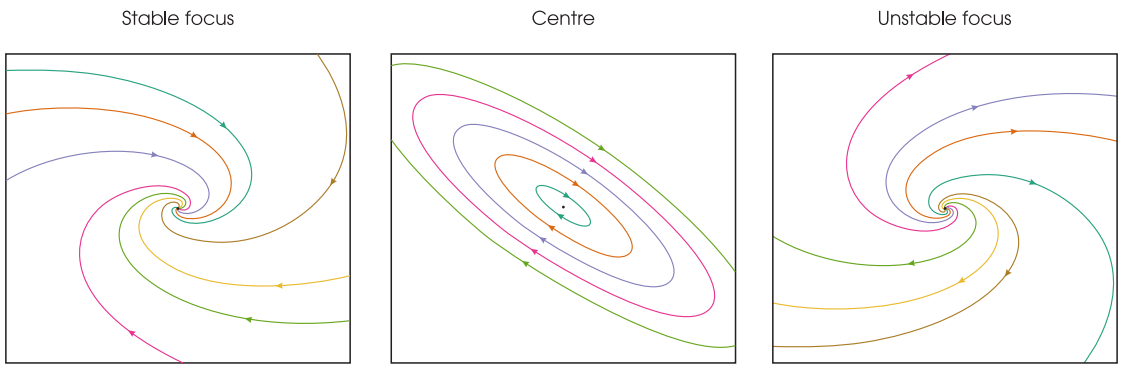

Figure 2.5: Qualitative behaviour when the matrix J in equation (2.19) has complex-conjugate eigenvalue pair $\lambda = r \pm i\mu$, $r < 0$, $r = 0$, and $r > 0$ respectively.

2.4.1 Routh-Hurwitz Conditions

Given the stability criteria discussed in the last section, in the subsequent chapters we will be interested in the number of eigenvalues with negative real parts, to ensure stability. One method we will consider, uses the Routh-Hurwitz conditions [118]. If the system (2.16) is of n^{th} order, then the characteristic equation is

$$P(\lambda) = \lambda^n + a_1\lambda^{n-1} + \cdots + a_n = 0, \tag{2.20}$$

where $a_i, i = 1, \ldots, n$ are real. The necessary and sufficient conditions on the a_i such that the roots of $P(\lambda)$ have $\mathrm{Re}\,\lambda < 0$ are the Routh-Hurwitz conditions,

$$\begin{gathered} D_1 = a_1 > 0, \quad D_2 = \begin{vmatrix} a_1 & a_3 \\ 1 & a_2 \end{vmatrix} > 0, \quad D_3 = \begin{vmatrix} a_1 & a_3 & a_5 \\ 1 & a_2 & a_4 \\ 0 & a_1 & a_3 \end{vmatrix} > 0, \\ D_k = \begin{vmatrix} a_1 & a_3 & \cdot & \cdot & \cdot & \cdot \\ 1 & a_2 & a_4 & \cdot & \cdot & \cdot \\ 0 & a_1 & a_3 & \cdot & \cdot & \cdot \\ 0 & 1 & a_2 & \cdot & \cdot & \cdot \\ 0 & 0 & \cdot & \cdot & \cdot & a_k \end{vmatrix} > 0, \quad k = 4, \ldots, n, \end{gathered} \tag{2.21}$$

where $a_i = 0$ for $i > n$. For example, for the cubic equation

$$\lambda^3 + a_1\lambda^2 + a_2\lambda + a_3 = 0,$$

The condition $\mathrm{Re}\ \lambda < 0$ is satisfied if

$$a_1 > 0, \quad a_1a_2 - a_3 > 0, \quad a_3 > 0.$$

Definition 2.4.5 *[6] The discriminant $D(f)$ of a polynomial*

$$f(x) = x^n + c_1x^{n-1} + c_2x^{n-2} + \ldots\ldots + c_n,$$

is defined by $D(f) = (-1)^{n(n-1)/2}R(f, f')$, where f' is the derivative of f, and for $g(x) = x^l + d_1x^{l-1} + d_2x^{l-2} + \ldots\ldots + d_l$, $R(f, g)$ is the determinant of the corresponding Sylvester $(n+l) \times (n+l)$ matrix. The Sylvester matrix is formed by filling the matrix beginning with the upper left corner with the coefficients of $f(x)$ and then shifting down one row and one column to the right and filling in the coefficients starting there until they hit the right side. The process is then repeated for the coefficients of $g(x)$.

2.5 Stability for Fractional Systems

In this thesis we will use either the Caputo derivative or Jumarie's modified Riemann-Liouville fractional derivative. For these definitions, the derivative of a constant is zero and so the equilibrium points for the fractional systems will be the same as the equilibrium points for the integer system.

The general form of any fractional system, that has x_k species with initial conditions $x_k(t_0) = b_k$, $k = 1, ..., n$, is

$$D^{\alpha_k} x_k(t) = f_k(x_1, x_2, ..., x_n), \tag{2.22}$$

where α_k are the fractional derivative orders. When all the species have the same memory, so that all fractional derivatives are of order α, the system is called commensurate. When the species have different memory, and so not all α_k are equal, the system is called incommensurate.

2.5.1 Asymptotic Stability for a Commensurate Fractional Differential Equation System

In this section we will introduce results related to the stability of a commensurate fractional system. We first introduce a lemma that relates the stability of a commensurate fractional system to the eigenvalues of the equivalent integer derivative system. The proof of this result is relatively straightforward, and makes use of the Mittag-Leffler function as the eigenfunction of the fractional system, and can be found in [38] as well as other standard textbooks in the area.

Lemma 2.5.1 *[38] Let x^* be an equilibrium of the nonlinear system $D_t^\alpha x = f(x)$, then x^* is locally asymptotically stable if*

$$|arg\lambda| > \alpha\frac{\pi}{2},$$

for all eigenvalues λ of the Jacobian matrix $J(x^*)$.

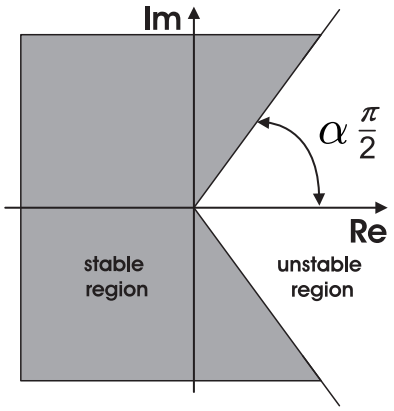

Figure 2.6: The stability region for a fractional system, from [29].

2.5.2 Asymptotic Stability for an Incommensurate Fractional Differential Equation System

In this section we will introduce the lemma that is related to the stability of an incommensurate fractional system. A proof of this result can be found in [144].

Lemma 2.5.2 *[144] Suppose that $x = x^*$ is an equilibrium point of the system*

$$D_t^{\alpha_i} x = f(x), \tag{2.23}$$

where $i = 1, 2, ...n$, and the fractional derivatives orders $\alpha_i \in \mathbb{Q}$ are not necessarily equal. Suppose also that M is the lowest common multiple of the denominators u_i of the α_i, where $\alpha_i = v_i/u_i$, the greatest common divisor of u_i and v_i is 1, and $u_i, v_i \in \mathbb{Z}^+$. Then the equilibrium point is asymptotically stable if

$$|arg(\lambda_i)| > \frac{\pi}{2M}, \tag{2.24}$$

for all roots λ_i of the equation

$$det(J - diag[\lambda^{M\alpha_1}, \lambda^{M\alpha_2}, ..., \lambda^{M\alpha_n}]) = 0, \tag{2.25}$$

where J is the Jacobian matrix of (2.23) at the equilibrium point x^*.

2.6 Numerical Methods for Solving Fractional Differential Equations

Numerical methods have been widely used to solve all types of fractional differential equations. Several numerical methods, such as the variational iteration method [141], least squares method [113], Galerkin method [22], Euler's method

[147], and Runge Kutta method [25], have all been successfully applied. In this thesis, we use a method based on the Adams-Bashforth-Moulton approach, which has been previously used for the numerical solution of similar differential equations of fractional order. The Adams method is a multi-step method using a predictor-corrector algorithm. Each of the methods in the multi-step class of numerical methods can be either explicit or implicit [15], where the explicit type is known as the Adams-Bashforth method, and the implicit type is known as the Adams-Moulton method. Within the predictor-corrector scheme we use, the explicit formula is used to predict the value, while the implicit formula is used to correct this prediction, and this method is therefore called Adams-Bashforth-Moulton method. Standard and higher orders of Adams-Bashforth-Moulton are widely adopted for fractional differential equations [123], and Diethelm et al. [46, 47] provide more detailed description of this method and its error analysis.

Here we use Matlab to encode this numerical method. Specifically, the Matlab code flmm2 was used for solving the commensurate system in Chapter 3. This code was initially developed by Lubich [72] and studied for stability by Garrappa [63], where three different implicit methods were considered, the classical trapezoidal rule or Tustin method, the Newton-Georgy formula and the backward differentiation formula [64]. Similarly, we use the FDE-PI1-Ex code for solving equations that describe the incommensurate system in Chapter 4, which was also described in detail by Garrappa in [64].

2.7 Description of (G'/G)-Expansion Method

In Chapter 5 of this thesis we will investigate travelling waves in fractional differential equations. In order to construct solutions we will use the (G'/G)-expansion method, first introduced by Wang et al. [155] to find the travelling wave solutions of various nonlinear PDEs. The method was then extended by Bin [23] for solving nonlinear fractional PDEs. Here we will outline this method. Suppose that a fractional PDE is given by

$$P(u, D_t^{\alpha}u, D_x^{2\beta}u, D_y^{2\gamma}u) = 0, \tag{2.26}$$

where $u = u(t, x, y)$ is an unknown function, $0 < \alpha, \beta, \gamma \leq 1$, are fractional derivative orders and P is a polynomial in $u(t, x, y)$ and fractional partial derivatives of u.
Step 1: Eq.(2.26) can be converted to an ordinary differential equation,

$$Q(u, u', u'') = 0, \tag{2.27}$$

by the fractional transformation [75, 100], $u(t, x, y) = u(Z)$, where

$$Z = -\frac{Lt^{\alpha}}{\Gamma(\alpha + 1)} + \frac{Kx^{\beta}}{\Gamma(\beta + 1)} + \frac{My^{\gamma}}{\Gamma(\gamma + 1)}, \tag{2.28}$$

and L, K, and M are arbitrary constants.
Step 2: Eq.(2.27) is then integrated as many times as possible using known conditions to determine constants of integration.
Step 3: Suppose that the solution of the resulting equation can be expressed as a polynomial of (G'/G) in the form

$$u(Z) = \sum_{i=0}^{m} \alpha_i \left(\frac{G'}{G}\right)^i, \tag{2.29}$$

where α_i $(i = 0, 1, ...m)$ are constants, and $G = G(Z)$ is the solution of the following second order linear ODE,

$$G''(Z) + \lambda G'(Z) + \mu G(Z) = 0, \tag{2.30}$$

where λ and μ are, as yet unknown, constants.
Step 4: The positive integer m can be determined by using the homogeneous balance between the highest order derivatives and the nonlinear terms appearing in the equation found in Step 2.
Step 5: Substituting eq.(2.29) and eq.(2.30) into eq.(2.27), and equating the coefficients of the obtained polynomial, gives a set of algebraic equations for α_i $(i = 0, 1, ...m,)$ L, K, M, λ, and μ.
Step 6: The general solution of eq.(2.30) is then

$$\frac{G'}{G} = \begin{cases} \dfrac{-\lambda}{2} + \dfrac{\sqrt{\lambda^2 - 4\mu}}{2} \left(\dfrac{c_1 \sinh\left(\frac{Z\sqrt{\lambda^2-4\mu}}{2}\right) + c_2 \cosh\left(\frac{Z\sqrt{\lambda^2-4\mu}}{2}\right)}{c_1 \cosh\left(\frac{Z\sqrt{\lambda^2-4\mu}}{2}\right) + c_2 \sinh\left(\frac{Z\sqrt{\lambda^2-4\mu}}{2}\right)} \right), & \text{if } \lambda^2 - 4\mu > 0, \\ \dfrac{-\lambda}{2} + \dfrac{\sqrt{4\mu - \lambda^2}}{2} \left(\dfrac{-c_1 \sin\left(\frac{Z\sqrt{4\mu-\lambda^2}}{2}\right) + c_2 \cos\left(\frac{Z\sqrt{4\mu-\lambda^2}}{2}\right)}{c_1 \cos\left(\frac{Z\sqrt{4\mu-\lambda^2}}{2}\right) + c_2 \sin\left(\frac{Z\sqrt{4\mu-\lambda^2}}{2}\right)} \right), & \text{if } \lambda^2 - 4\mu < 0, \\ \dfrac{-\lambda}{2} + \dfrac{c_2}{c_1 + c_2 Z}, & \text{if } \lambda^2 - 4\mu = 0. \end{cases} \tag{2.31}$$

Step 7: By substituting α_i $(i = 0, 1, ...m)$, L, K, M, into eq.(2.31) and then into eq.(2.29), the solution of eq.(2.26) can be obtained.

Chapter 3

Commensurate Models

In this chapter, we consider two models: the first is a fractional order model for the tumor-immune system using a prey-predator-like model, and the second is a fractional SIR epidemic model with saturated treatment rate. We obtain all the conditions of the existence of equilibrium points, and the asymptotic stability of these points is studied, along with a numerical simulation.

3.1 A Fractional Order Model for the Tumor-Immune System Response

This section deals with a fractional order model that explores the immune response to a tumor, that can be modelled as a prey-predator system. As discussed in Chapter 1, fractional order derivatives can be used to model a form of system memory, which may be more realistic compared to the integer order, because of the non-local properties of fractional derivatives. The model considered in the present study is a generalisation of that introduced by Kaur and Ahmad [89], changing the order of the model from integer to fractional. Local asymptotic stability of the possible equilibrium points is studied and the generalised Adams-Bashforth-Moulton method is then used to numerically solve and simulate the system.

3.1.1 Introduction

Cancer is a group of diseases involving abnormal cell growth, with the potential to invade or spread to other parts of the body and form tumors, which can be benign (non-cancerous) or malignant (cancerous). It has been observed that cancer cell populations decrease considerably due to the proliferation of lymphocytes mediated by immunotherapy. We can therefore control the cancer cell population relatively easily if the form of cancer is immunogenic, that is, the cells possess distinctive surface markers called tumor-specific antigens [4].

Recent progress in mathematical biology, especially in the field of cancer, mean that mathematical models of tumor growth can give analytical insight into the elements of the human immune system that influence cancer treatment. Mathematical models also help us understand the growth mechanisms of the tumor in order to predict its future behaviour. However, the problem lies in formulating mathematical models that preserve a realistic dynamic nature of such real-life systems. It has been shown that ordinary differential equations sometimes fail to capture real world data due to the lack of non-local effects [66]. For this reason, the concept of fractional calculus has been introduced, since it involves differentiation using non-local operators. Fractional derivatives have the capacity of representing dissipative effects and capturing the memory effects which are detected in many biological systems.

Possibilities for research in this field are wide reaching. Some researchers have studied the interaction between the immune system cells and cancer cells. For instance, Ucar et al. [150] used the Caputo fractional derivative to generalise the integer order model presented by Castiglione and Piccoli [33] in order to analyse the activities and behaviour of cells through the modification of the fractional derivative parameter. As with many authors, they obtained numerical solutions for this type of system by applying the Adams-Bashforth-Moulton algorithm. Their main focus was on dendritic cells and IL-2, although, the model also tested how CD4+ T cells and CD8+ T cells fight tumor cells. They studied the interaction between cancer cells and immune systems cells and demonstrated that for some values of the fractional order the effectiveness of both types of cells varies. Specifically, cancer cells noticeably decrease as the fractional order decreases. Balci et al. [17] have compared Caputo and conformable fractional derivative models to determine which is better suited to model the interaction between immune system cells and cancer cells. They proved that the discrete version of the conformable fractional order model depicts a wider class of tumor growth dynamics than those of the Caputo fractional order model and is a more convenient model due to the chaotic and oscillatory tumor growth prior to treatment. For treatment and chemotherapy of tumors in the case of bladder cancer, Baba [16] studied the effect of Bacillus Calmette-Guerin (BCG) on the control of bladder cancer and developed a model that demonstrated effects seen in experiments. The author obtained two equilibrium points, a tumor-free equilibrium and an endemic equilibrium. Unfortunately, the author demonstrated that the cancer-free equilibrium is unstable. However, he proved that BCG is quite effective in controlling bladder cancer. Akman Yildiz et al. [8] presented a novel mathematical model to describe the effect of obesity on malignant tumor growth during the course of chemotherapy and immunotherapy. They described an optimal control problem in order to diminish the tumor population and decrease drug dose over a finite duration using the Caputo time fractional derivative. The authors demonstrated the existence and stability of two

equilibrium points, a tumor-free equilibrium and coexisting equilibrium, and used a specific method to discretize the cancer-obesity model.

In Rihan et al. [130], the authors proved that fractional order differential equations are, at their worst, as stable as their integer-order equivalents when modelling immune system behaviour. However, an increase in the complexity of the monitored behaviour was noted as their calculations constantly relied on all prior states of the solution. Gomez-Aguilar et al. [66] offered an analysis of a three-dimensional fractional-order dynamical model for the evolution of cancer growth. The model used the Caputo-Fabrizio-Caputo derivative and a new fractional derivative with a Mittag-Leffler kernel in the Liouville-Caputo derivative. They obtained the solution through an interactive approach that involved using the Laplace transform and, for the Atangana-Baleanu-Caputo fractional order derivative, using the Sumudu transform.

Mathematical models have also been used to analyse the possible causative mechanisms of cancer, escape from immune-induced dormancy, and decaying efficacy in both immune predation and immune recruitment are analysed with results suggesting that decline in recruitment is a stronger determinant of escape than increased resistance to predation [163].

Also, Iyiola et al. [82] investigated the need for fractional order derivatives as compared to the classical first order derivative for cancer tumor models. Numerical simulations have also confirmed the advantages of using fractional-order differential models in biological systems over differential equations with integer order such as dynamics of tumor-immune system and HIV infection of CD4+ T cells [129].

In this section, we will consider a fractional order model for the tumor-immune system response, based on a prey-predator model. We give a detailed analysis for the asymptotic stability of the model.

3.1.2 Model Formulation

Kaur and Ahmad [89] studied the interaction between tumor cells, modelled as prey, and the immune systems resting and hunting cells, modelled as predators, as follows,

$$\begin{aligned}
\frac{dT}{dt} &= q + r_1 T\Big(1 - \frac{T}{k_1}\Big) - \alpha_1 TH, \\
\frac{dH}{dt} &= \beta HR - d_1 H - \alpha_2 HT, \\
\frac{dR}{dt} &= r_2 R\Big(1 - \frac{R}{k_2}\Big) - \beta HR - d_2 R + \frac{\rho TR}{T+\eta},
\end{aligned} \tag{3.1}$$

where $T(t)$ is the concentration of tumor cells in the given area at time t, $H(t)$ the concentration of hunting T cells, and $R(t)$ the concentration of resting T cells, the parameter q is the conversion rate of normal cells into tumor cells, r_1 is the growth rate of tumor cells, k_1 is the maximum carrying capacity of tumor cells, α_1 is the rate of predation of tumor cells by hunting cells, β is the conversion rate of resting cells into hunting cells, d_1 is the apoptosis rate of hunting cells, α_2 is the rate of predation of hunting cells by tumor cells, r_2 is the growth rate of resting cells, k_2 is the maximum carrying capacity of resting cells, d_2 is the apoptosis rate of resting cells, ρ is the proliferation rate of resting cells, and η is the half-saturation for the proliferation term. See Figure 3.1 for a schematic description of the process modeled by the system (3.1).

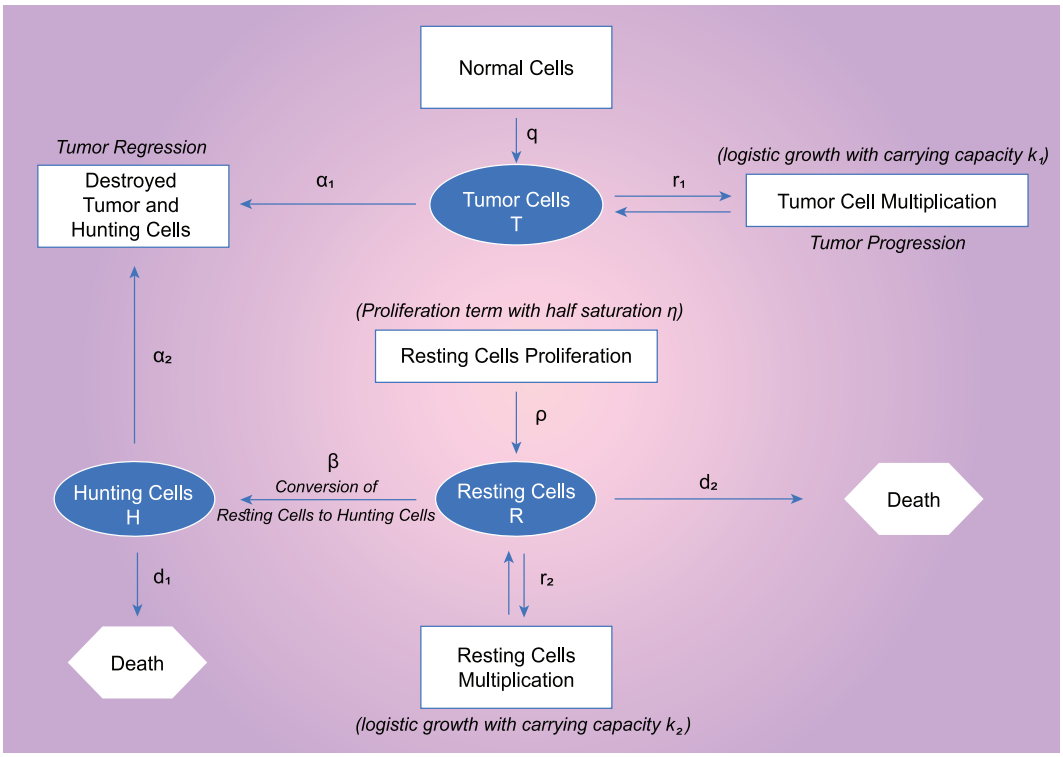

Figure 3.1: Schematic diagram of the system (3.1).

The following dimensionless variables can be defined to reduce the number of system parameters $t^* = qt/k_1$, $T^* = T/k_1$, $H^* = \alpha_1 k_1 H/q$, $R^* = R/k_2$.

Dropping the stars yields the following model:

$$\begin{aligned}
\frac{dT}{dt} &= 1 + a_1 T(1-T) - TH, \\
\frac{dH}{dt} &= a_2 HR - a_3 H - a_4 HT, \\
\frac{dR}{dt} &= a_5 R(1-R) - a_6 HR - a_7 R + \frac{a_8 TR}{T+K},
\end{aligned} \tag{3.2}$$

where

$$\begin{aligned}
&a_1 = r_1 k_1/q, && a_2 = \beta k_1 k_2/q, && a_3 = k_1 d_1/q, \\
&a_4 = \alpha_2 k_1^2/q, && a_5 = r_2 k_1/q, && a_6 = \beta/\alpha_1, \\
&a_7 = k_1 d_2/q, && a_8 = k_1 \rho/q, && K = \eta/k_1.
\end{aligned} \tag{3.3}$$

We will now introduce fractional order derivatives to the ODE model (3.2), leading to a new system described by the following set of equations:

$$\begin{aligned}
D_t^\alpha T &= 1 + a_1 T(1-T) - TH, \\
D_t^\alpha H &= a_2 HR - a_3 H - a_4 HT, \\
D_t^\alpha R &= a_5 R(1-R) - a_6 HR - a_7 R + \frac{a_8 TR}{T+K},
\end{aligned} \tag{3.4}$$

where D_t^α is the Caputo fractional derivative defined in Definition (2.2.4). In the next few sections we consider the equilibrium points of the system (3.4) and the conditions of the existence and stability of these points.

3.1.3 Equilibrium Points

To evaluate the equilibrium points of the system (3.4) we set $D_t^\alpha T = 0$, $D_t^\alpha H = 0$, $D_t^\alpha R = 0$, and solve equations (3.4) to give the equilibrium points:
$E_1(T_1, 0, 0)$ where $T_1 = \frac{1}{2}\Big(1 + \sqrt{1 + \frac{4}{a_1}}\Big)$ so there are no hunting or resting cells.
$E_2(T_2, 0, R_2)$ where $T_2 = \frac{1}{2}\Big(1 + \sqrt{1 + \frac{4}{a_1}}\Big)$, $R_2 = \frac{1}{a_5}\Big(a_5 - a_7 + a_8 T_2/(T_2 + K)\Big)$ so there are no hunting cells.
$E_3(T_3, H_3, 0)$ where $T_3 = -\dfrac{a_3}{a_4}$, $H_3 = \dfrac{1}{T_3} + a_1(1 - T_3)$ so there are no resting cells.
$E_4(T_4, H_4, R_4)$ where $R_4 = \frac{1}{a_2}(a_3 + a_4 T_4)$, $H_4 = \frac{1}{a_6}\Big(a_5 - \frac{a_5}{a_2}(a_3 + a_4 T_4) - a_7 + a_8 T_4/(T_4 + K)\Big)$ and T_4 satisfies the following cubic equation:

$$c_3 T_4^3 + c_2 T_4^2 + c_1 T_4 + c_0 = 0, \tag{3.5}$$

where

$$\begin{aligned} c_3 &= a_1a_6 - \frac{a_4a_5}{a_2}, \\ c_2 &= a_5 - a_7 + a_8 - \frac{a_5}{a_2}(a_3 + a_4K) - a_1a_6(1-K), \\ c_1 &= a_5K - \Big(a_7K + \frac{a_5a_3K}{a_2} + a_6(a_1K+1)\Big), \\ c_0 &= -a_6K < 0. \end{aligned}$$

To be a physically realistic equilibrium point, each of the concentrations $T(t)$, $H(t)$, $R(t)$ must be greater or equal to zero. The equilibrium point E_1 is always physical since $a_1 > 0$, so $T_1 > 0$. The equilibrium point E_2 is physical if $a_5 + a_8T_2/(T_2+K) > a_7$ to ensure that R_2 is positive. However, the equilibrium point E_3 is always unphysical since $a_3 > 0$, $a_4 > 0$, so $T_3 < 0$. The existence of the equilibrium point E_4 depends on the positivity of T_4, H_4 and R_4, which is more complicated and is now discussed in detail.

For a physically realistic state we must, as well as having $T_4 > 0$, which automatically ensure that $R_4 > 0$, have $a_5 + a_8T_4/(T_4+K) > \frac{a_5}{a_2}(a_3 + a_4T_4) + a_7$ to ensure that $H_4 > 0$. In order to understand the positivity of T_4 we must determine the number of real roots of the cubic equation (3.5), which we will do by considering the discriminant of the equation (see Definition (2.4.5)), namely

$$\Delta = -\begin{vmatrix} c_3 & c_2 & c_1 & c_0 & 0 \\ 0 & c_3 & c_2 & c_1 & c_0 \\ 3c_3 & 2c_2 & c_1 & 0 & 0 \\ 0 & 3c_3 & 2c_2 & c_1 & 0 \\ 0 & 0 & 3c_3 & 2c_2 & c_1 \end{vmatrix} = 18c_3c_2c_1c_0 + (c_2c_1)^2 - 4c_1^3c_3 - 4c_2^3c_0 - 27c_3^2c_0^2. \tag{3.6}$$

If $\Delta > 0$, then there are three real roots and if $\Delta < 0$ then there is only one real root [152]. The number of real and positive roots of (3.5) can be found by using the sign of the discriminant in (3.6) together with Descartes' Rule of Signs [14]. We will concentrate on the equilibrium point E_4 because, as we will see later, there are more possibilities for stable equilibria. In particular, we will later see that the stability of E_1 and E_2 are not affected by changing the fractional order α, but a change of stability is possible for E_4 by changing α. From the discriminant and using Descartes' Rule of Signs we find that it is possible to have three positive real roots or one positive real root for the cubic equation (3.5), when $\Delta > 0$ and the change of signs in the equation is equal to three, i.e. $c_3 > 0$, $c_2 < 0$, $c_1 > 0$, which is equivalent to a condition on the growth rate of tumor cells, $\max(M_1, M_2) < a_1 < M_3$ if $K < 1$ or $M_1 < a_1 < \min(M_2, M_3)$ if $K > 1$,

where

$$\begin{aligned} M_1 &= \frac{a_4 a_5}{a_2 a_6}, \\ M_2 &= \frac{a_2(a_5 - a_7 + a_8) - a_5(a_3 + a_4 K)}{a_2 a_6(1-K)}, \\ M_3 &= \frac{a_5 - a_7}{a_6} - \frac{a_5 a_3}{a_2 a_6} - \frac{1}{K}. \end{aligned}$$

However, these conditions for finding three real roots for the cubic equation (3.5) are necessary but not sufficient, so if these conditions are met, we might not have three real roots (there could be only one positive root). We also find that the equation (3.5) has one positive real root when the change of signs in the equation is equal to one, i.e. $c_3 > 0$, which is equivalent to the condition on the growth rate of tumor cells, $a_1 > M_1$. In addition, we find that there are three possibilities to have two positive real roots or no positive real root for the cubic equation (3.5), when $\Delta > 0$ and the change of signs in the equation is equal to two: $c_3 < 0$, $c_2 > 0$, $c_1 < 0$, which is equivalent to a condition on the growth rate of tumor cells, $M_3 < a_1 < \min(M_1, M_2)$ if $K < 1$ or $\max(M_2, M_3) < a_1 < M_1$ if $K > 1$; $c_3 < 0$, $c_2 < 0$, $c_1 > 0$, which is equivalent to a condition on the growth rate of tumor cells, $M_2 < a_1 < \min(M_1, M_3)$ if $K < 1$ or $a_1 < \min(M_1, M_2, M_3)$ if $K > 1$; $c_3 < 0$, $c_2 > 0$, $c_1 > 0$, which is equivalent to a condition on the growth rate of tumor cells, $a_1 < \min(M_1, M_2, M_3)$ if $K < 1$ or $M_2 < a_1 < \min(M_1, M_3)$ if $K > 1$.

3.1.4 Stability

The local asymptotic stability analysis of the equilibrium points can be investigated by using the Jacobian matrix of (3.2),

$$J(T,H,R) = \begin{bmatrix} a_1 - 2a_1 T - H & -T & 0 \\ -a_4 H & a_2 R - a_3 - a_4 T & a_2 H \\ \dfrac{a_8 R K}{(T+K)^2} & -a_6 R & a_5 - 2a_5 R - a_6 H - a_7 + \dfrac{a_8 T}{T+K} \end{bmatrix}.$$

Lemma 2.5.1 will now be used to define the conditions of the stability for each of the equilibrium points.

For E_1, the Jacobian matrix $J(E_1)$ is

$$J(E_1) = \begin{bmatrix} -a_1\sqrt{1+\frac{4}{a_1}} & -\frac{1}{2}\left(1+\sqrt{1+\frac{4}{a_1}}\right) & 0 \\ 0 & -a_3 - \frac{a_4}{2}\left(1+\sqrt{1+\frac{4}{a_1}}\right) & 0 \\ 0 & 0 & a_5 - a_7 + \dfrac{\frac{a_8}{2}\left(1+\sqrt{1+\frac{4}{a_1}}\right)}{\frac{1}{2}\left(1+\sqrt{1+\frac{4}{a_1}}\right)+K} \end{bmatrix},$$

and E_1 is locally asymptotically stable if all the eigenvalues, λ_{1i}, $i = 1, 2, 3$, of the Jacobian satisfy the condition $|\arg(\lambda_{1i})| > \alpha\pi/2$. However, all the eigenvalues are real,

$$\begin{aligned}
\lambda_{11} &= -a_1\sqrt{1+\frac{4}{a_1}} < 0, \\
\lambda_{12} &= -\left(a_3 + \frac{a_4}{2}\left(1+\sqrt{1+\frac{4}{a_1}}\right)\right) < 0, \\
\lambda_{13} &= a_5 - a_7 + \frac{\frac{a_8}{2}\left(1+\sqrt{1+\frac{4}{a_1}}\right)}{\frac{1}{2}\left(1+\sqrt{1+\frac{4}{a_1}}\right)+K} > 0.
\end{aligned}$$

The eigenvalues λ_{11} and λ_{12} are negative, but the sign of λ_{13} depends on the existence condition of E_2. We see that $\lambda_{13} > 0$, so that E_1 is unstable, if E_2 exists, and E_1 is stable if E_2 does not exist.

For E_2, the Jacobian matrix $J(E_2)$ is

$$J(E_2) = \begin{bmatrix} a_1 - 2a_1T_2 & -T_2 & 0 \\ 0 & a_2R_2 - a_3 - a_4T_2 & 0 \\ \dfrac{a_8R_2K}{(T_2+K)^2} & -a_6R_2 & a_5 - 2a_5R_2 - a_7 + \dfrac{a_8T_2}{T_2+K} \end{bmatrix}.$$

As with E_1, the eigenvalues are real,

$$\begin{aligned}
\lambda_{21} &= -a_1\sqrt{1+\frac{4}{a_1}} < 0, \\
\lambda_{22} &= a_2R_2 - a_3 - a_4T_2, \\
\lambda_{23} &= -\left(a_5 - a_7 + \frac{a_8T_2}{T_2+K}\right).
\end{aligned}$$

The eigenvalue $\lambda_{21} < 0$ and the sign of λ_{23} depends only on the existence condition of E_2. We see that $\lambda_{23} < 0$ if we assume that E_2 exists. Therefore, the stability of E_2 depends only on the sign of λ_{22}, so that E_2 is stable if $\lambda_{22} < 0$ and unstable if $\lambda_{22} > 0$.

For E_4, the Jacobian matrix $J(E_4)$ is

$$J(E_4) = \begin{bmatrix} a_1 - 2a_1T_4 - H_4 & -T_4 & 0 \\ -a_4H_4 & a_2R_4 - a_3 - a_4T_4 & a_2H_4 \\ \dfrac{a_8R_4K}{(T_4+K)^2} & -a_6R_4 & a_5 - 2a_5R_4 - a_6H_4 - a_7 + \dfrac{a_8T_4}{T_4+K} \end{bmatrix},$$

and the eigenvalues are solutions of the equation

$$\lambda^3 + A_1\lambda^2 + A_2\lambda + A_3 = 0, \tag{3.7}$$

where

$$\begin{aligned} A_1 &= -(A+B), \\ A_2 &= AB + a_2a_6R_4H_4 - a_4H_4T_4, \\ A_3 &= a_4BH_4T_4 + \frac{a_2a_8KH_4T_4R_4}{(T_4+K)^2} - a_2a_6AH_4R_4, \end{aligned}$$

where $A = a_1 - 2a_1T_4 - H_4$ and $B = a_5 - 2a_5R_4 - a_6H_4 - a_7 + a_8T_4/(T_4+K)$. Therefore, E_4 is locally asymptotically stable if all the roots of this polynomial equation (3.7) satisfy $|\arg(\lambda_{4i})| > \alpha\pi/2$, $i = 1, 2, 3$. No serious analytical progress can be made in this case, and so we will later investigate the existence and stability of these equilibrium points numerically.

To summarise, the equilibrium point E_1 is always unstable (a saddle point) if the equilibrium point E_2 exists and, therefore, E_1 and E_2 cannot be stable for the same parameter values. We also found that E_2 is locally asymptotically stable if the eigenvalue λ_{22} is negative. However, the equilibrium point E_4 is only locally asymptotically stable if all the roots of the polynomial equation (3.7) satisfy $|\arg(\lambda_{4i})| > \alpha\pi/2$, $i = 1, 2, 3$.

3.1.5 Numerical Simulation

This section is devoted to the numerical study of the mathematical model presented in (3.4), using Matlab and Maple, and taking the values of our parameters from reference [89], $a_1 = 1.82$, $a_2 = 0.239$, $a_3 = 0.2$, $a_4 = 0.04$, $a_5 = 0.0191$, $a_6 = 0.5$, $a_7 = 0.01$, $a_8 = 2$ and $K = 1$. We also compare between our parameters and the parameters in references [44, 136, 137]. From reference [44], the parameters K and a_8 are exactly same our parameters K and a_8. From reference [136], by comparing their model with our model we found that $q = 10$, $r_1 = 0.9$, $k_1 = 0.8$, $\alpha_1 = 0.3$, $\beta = 0.1$, $d_1 = 0.02$, $r_2 = 0.8$, $k_2 = 0.7$ and $d_2 = 0.03$. Substituting these values into our dimensionless variables (3.3), we found $a_1 = 0.072$, $a_2 = 0.0056$, $a_3 = 0..0016$, $a_5 = 0.064$, $a_6 = 0.33$ and $a_7 = 0.0024$, these results were similar to our parameters. We also nondimensionalise the model in [137] and use their parameters we found $a_1 = 1.82$, $a_2 = 1.30$, $a_3 = 0.416$, $a_4 = 0.173$, $a_5 = 1.055$, $a_6 = 0.392$ and $a_7 = 0.416$, these results were almost equal our parameters. Figures 3.2 - 3.4 have been obtained for different values of α. In these figures we have taken the initial conditions $T(0) = 1$, $H(0) = 1$ and $R(0) = 1.5$, and our parameter values as mention above. For these parameter values, the positive equilibrium points will

be $E_1 = (1.39, 0, 0)$, $E_2 = (1.39, 0, 61.45)$ and $E_4 = (0.77, 1.72, 0.97)$. It should be noted here that the equilibrium point E_4 has the lowest concentration of tumor cells, and so we take particular notice of when this solution is a stable equilibrium. For the integer system (3.2), E_1 and E_2 are unstable, and E_4 is unstable because two of the eigenvalues of the Jacobian matrix are complex with positive real parts. The instability of E_4 in the integer system is shown in Figure 3.2 where we see that a limit cycle is approached as $t \to \infty$.

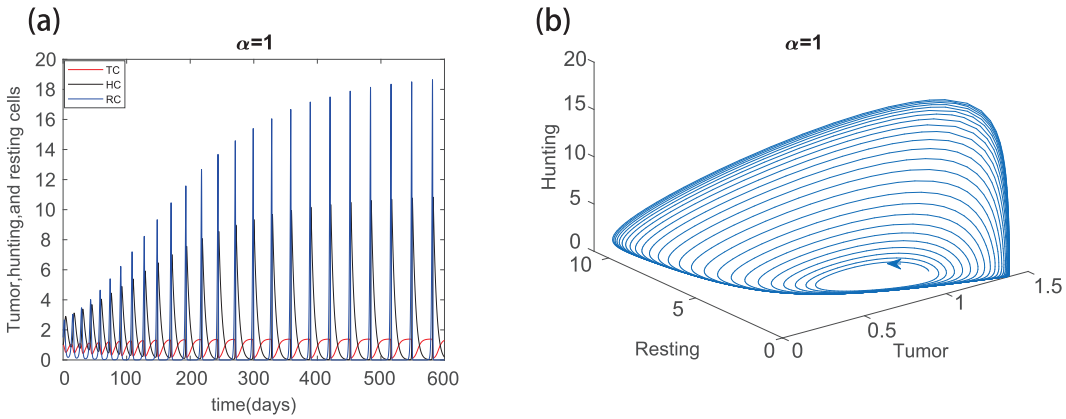

Figure 3.2: The instability of the integer system (3.2) around E_4, (a) tumor, hunting and resting cell concentration as a function of time showing the convergence to a limit cycle. (b) The phase plane plot of (a).

To study the stability of E_4 for the fractional system (3.4), we know from Lemma 2.5.1 that the equilibrium point is locally asymptotically stable if all the eigenvalues of the Jacobian matrix of E_4 satisfy the condition $|\arg(\lambda_{4i})| > \alpha\pi/2$, $i = 1, 2, 3$. For the complex eigenvalue with positive real part, namely λ_{41}, we obtain a critical value of the fractional order $\alpha^* = \frac{2}{\pi}|\arg(\lambda_{41})| = 0.984$, and therefore the system will be stable about E_4 if $\alpha < \alpha^*$. We see from Figure 3.3 for $\alpha > \alpha^*$, i.e. $\alpha = 0.992$ and $\alpha = 0.989$, E_4 remains unstable, but from Figure 3.4 when α is below α^*, i.e. $\alpha = 0.94$ and $\alpha = 0.9$, the equilibrium point becomes stable.

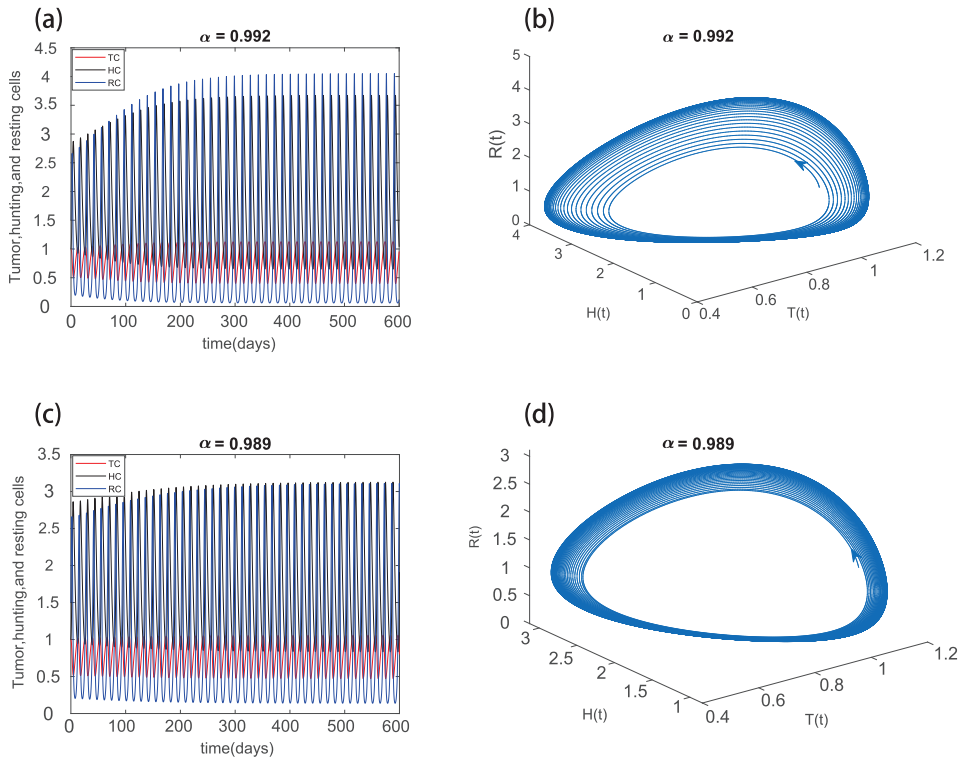

Figure 3.3: The instability of the fractional system (3.4) around E_4 when (a) $\alpha > \alpha^* = 0.984$, i.e. $\alpha = 0.992$, tumor, hunting and resting cell concentration as a function of time showing the convergence to a limit cycle. (b) The phase plane plot of (a). The instability of the fractional system (3.4) around E_4 when (c) $\alpha > \alpha^* = 0.984$, i.e. $\alpha = 0.989$, tumor, hunting and resting cell concentration as a function of time showing the convergence to a limit cycle. (d) The phase plane plot of (c).

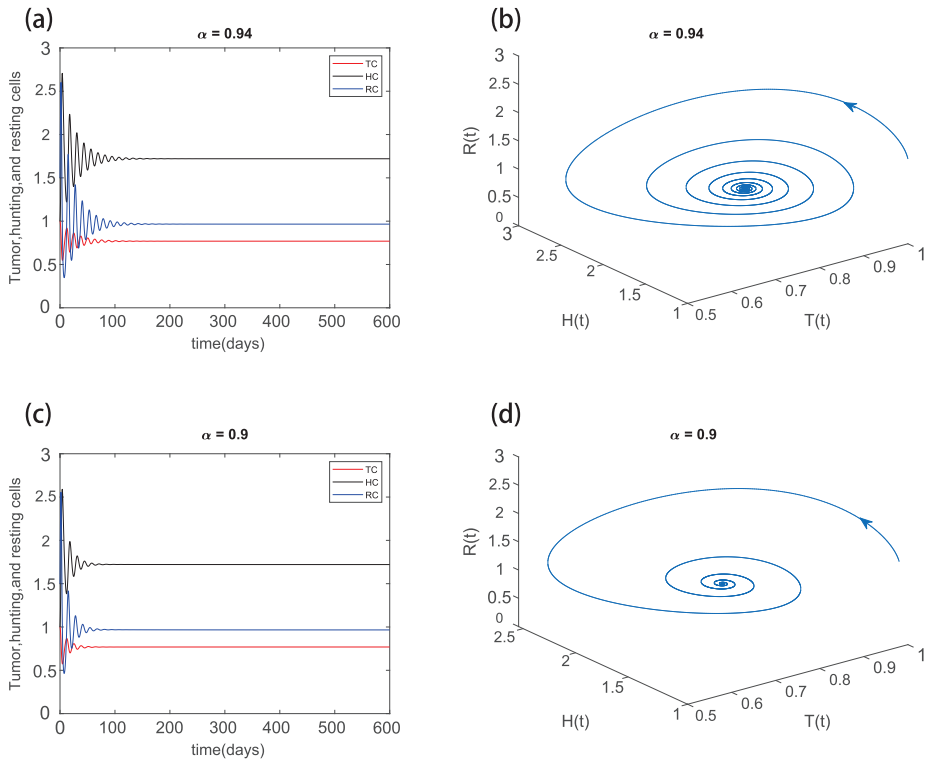

Figure 3.4: The stability of the fractional system (3.4) around E_4 when (a) $\alpha < \alpha^* = 0.984$, i.e. $\alpha = 0.94$, tumor, hunting and resting cell concentration as a function of time showing the convergence to E_4. (b) The phase plane plot of (a). The stability of the fractional system (3.4) around E_4 when (c) $\alpha < \alpha^* = 0.984$, i.e. $\alpha = 0.9$, tumor, hunting and resting cell concentration as a function of time showing the convergence to E_4. (d) The phase plane plot of (c).

It is clear that if we wish to ensure the stability of the low-tumor cell concentration state, E_4, we are interested in mechanisms that either allow α to be reduced to below α^*, or for α^* to be increased above the intrinsic value of α for the system. This latter possibility is investigated in the following section.

3.1.6 Parameter Dependence of α^*

In this section we consider the dependency of α^* on the parameter values a_1 - a_8 and K. In each situation we keep all but one parameter constant, using the values in Section 3.1.5. We can classify our results under three major groups: the first group includes a_1, a_3, a_5 and a_7, the second includes a_2, a_4 and a_8, and finally the third includes a_6 and K. Each of the accompanying figures (Figures

3.5 - 3.7) includes two columns; the first shows the eigenvalue of the integer system (the red line), while the second shows the value of α^* as one parameter is varied (the blue line) and the red line indicates the integer, $\alpha = 1$, bound. For the region below the blue line the system will exhibit a stable E_4 equilibrium point.

The dependency of α^* on parameters in the first group, a_1, a_3, a_5 and a_7 is shown in Figure 3.5. As we can see from Figure 3.5 (a, c, e, g), the integer system is unstable when approximately $a_1 < 5$, $a_3 < 2.5$, $a_5 < 0.04$ and $a_7 < 0.7$ respectively. On the other hand, for the fractional system we can see from Figure 3.5 (b, d, f, h) that if the values of a_1, a_3, a_5 and a_7 increase, then α^* will increase. Therefore, for the parameters a_1, a_3, a_5 and a_7 a reduction in the parameter value will tend to destabilise the system, with a reduction in α delaying this destabilisation to lower parameter values.

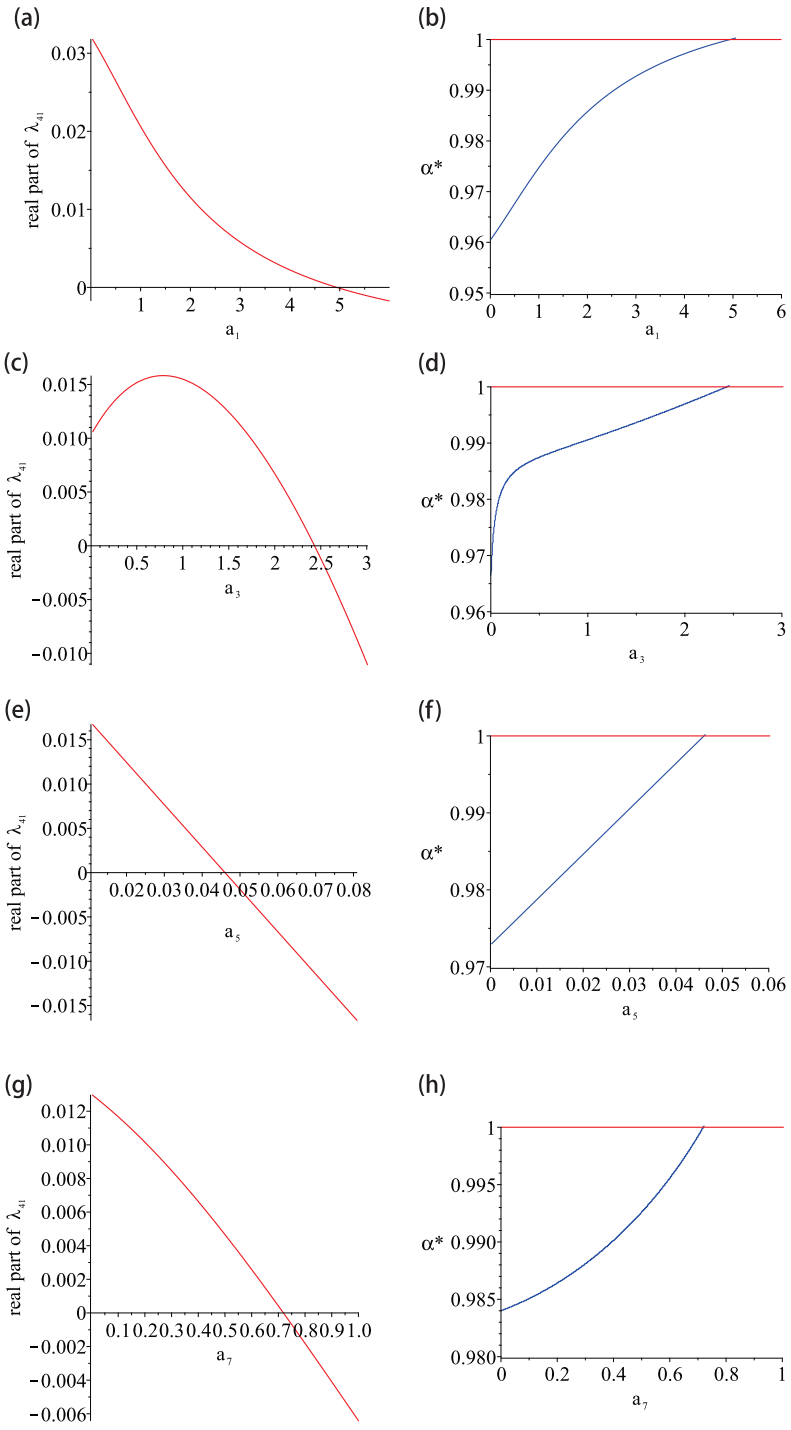

Figure 3.5: (a), (c), (e) and (g) are the real part of the eigenvalue of E_4 of the integer system (3.2) for different values of a_1, a_3, a_5 and a_7 respectively. (b), (d), (f) and (h) are the dependency of α^* on the growth rate of tumor cells, a_1, the apoptosis rate of hunting cells, a_3, the growth rate of resting cells, a_5, and the apoptosis rate of resting cells, a_7, for the fractional system (3.4) respectively.

The dependency of α^* on parameters in the second group, a_2, a_4 and a_8 is shown in Figure 3.6. As we can see from Figure 3.6 (a, c, e), the integer system is unstable when $a_2 > 0.1$ and $a_8 > 0.9$ approximately, and the integer system is unstable for all values of a_4. Furthermore, for the fractional system we can see from Figure 3.6 (b, d, f) that if the values of a_2, a_4 and a_8 increase, then α^* decreases and so the stability of the system decreases. For a_2, a_4 and a_8 an increase in the parameter value will destabilise the system although a lower value of α will delay that destabilisation to higher values of a_2, a_4 and a_8.

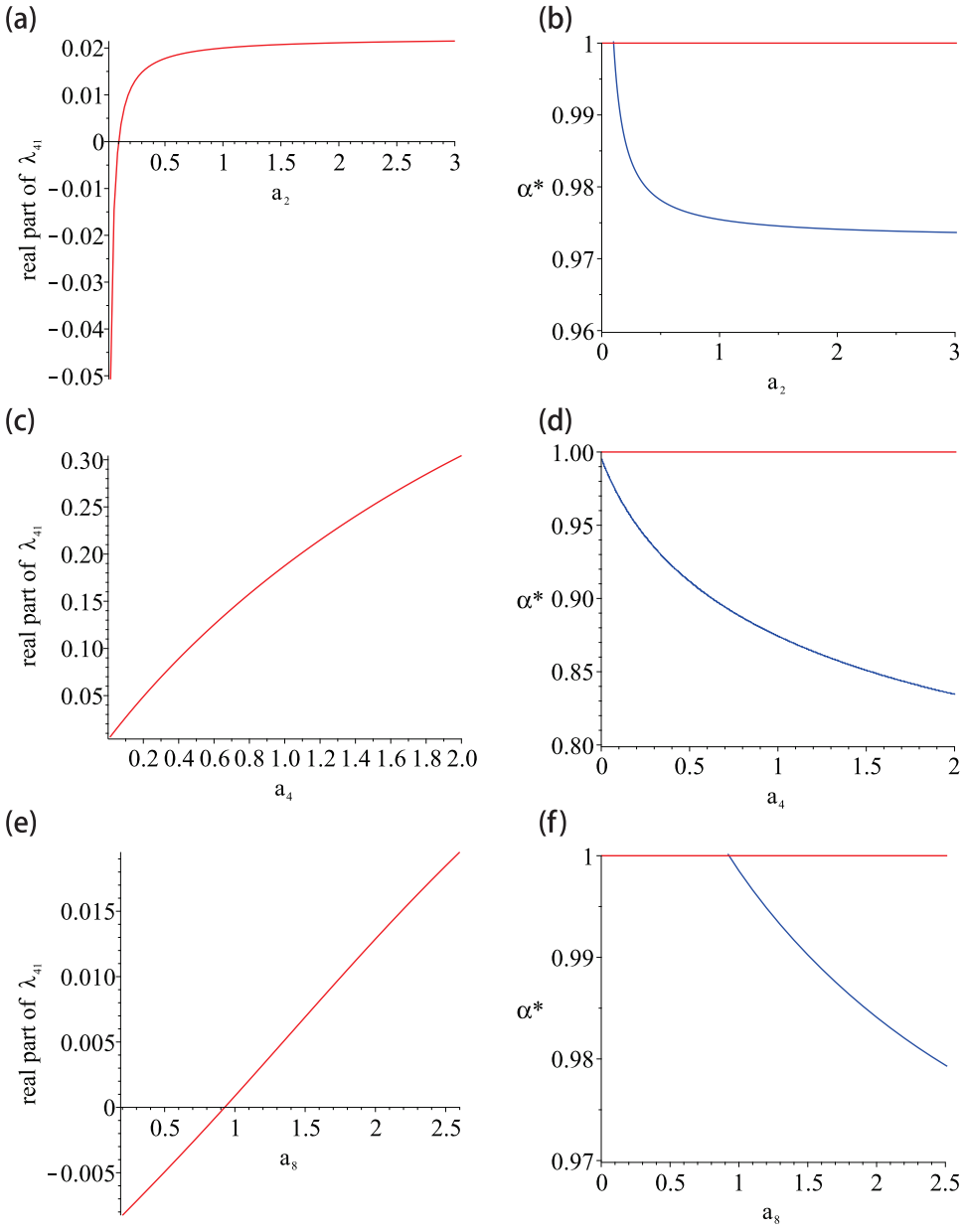

Figure 3.6: (a), (c) and (e) are the real part of the eigenvalue of the equilibrium point E_4 of the integer system (3.2) for different values of a_2, a_4 and a_8 respectively. (b), (d) and (f) are the dependency of α^* on the conversion rate of resting cells into hunting cells, a_2, the rate of predation of hunting cells by tumor cells, a_4, and the proliferation rate of resting cells, a_8, for the fractional system (3.4) respectively.

The dependency of α^* on parameters in the third group, a_6 and K is shown in Figure 3.7. As we can see from Figure 3.7 (a, c), the integer system is unstable when approximately $0.1 < a_6 < 1.5$ and $K < 4$ respectively. Furthermore, for the fractional system we can see from Figure 3.7 (b, d) that for these parameters the dependency of α^* is non-monotonic. For a fixed value of α it is therefore possible

to obtain a stable E_4 state for both low and high values of the parameters. This is a particularly interesting result and it would be useful to test this further to gain biological insight, from considering these two possible areas of stability.

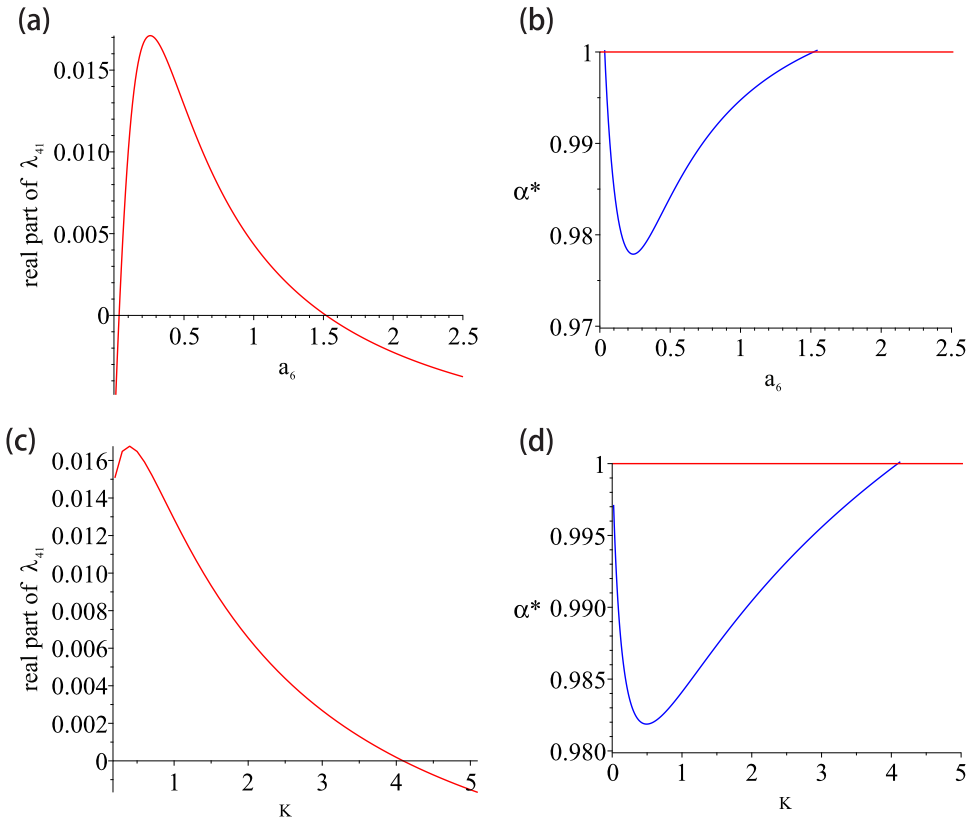

Figure 3.7: (a) and (c) are the real part of the eigenvalue of the equilibrium point E_4 of the integer system (3.2) for different values of a_6 and K respectively. (b) and (d) are the dependency of α^* on the ratio of conversion rate of resting cells into hunting cells to the rate of predation of tumor cells by hunting cells, a_6, and the half- saturation for proliferation term, K, for the fractional system (3.4) respectively.

3.2 A Fractional SIR Epidemic Model with Saturated Treatment Rate

As mentioned previously, fractional-order derivative models can be used to try and capture memory effects. One important area where memory effects could be influential is in epidemiology. In this case human memory may affect the speed of disease in a population. The literature includes many epidemiological models involving fractional-order derivatives, many of which are related to SIR-type models. In this section, we consider a fractional order model of a SIR epidemic model with a saturated treatment rate. This is a generalisation of Zhonghua and Yaohong [180], and consists of three component populations: susceptible, infected, and recovered. We have obtained the conditions for the existence and stability of equilibrium points, and the generalised Adams-Bashforth-Moulton method is then used to numerically solve the system of fractional differential equations.

3.2.1 Introduction

Mathematical modelling is a valuable approach in epidemiology, and it has been possible to restrict and reduce the outbreak of epidemic diseases such as measles, tuberculosis, and flu by analysing various treatment functions. In SIR models there are many different ways that treatment, such that infected individuals are moved to the recovered state, can be incorporated. This removal rate of infected individuals is often assumed to be directly proportional to the size of the infected population. Thus, resources such as medications, drugs, hospital capacity, and isolation chambers are presumed adequate. However, this assumption does not take into account the challenge that each community has a different, and limited capacity for treatment. To examine the impact of such a limited treatment capacity on the propagation of epidemic diseases, Wang and co-workers considered both a constant treatment rate [158]

$$h(I) = \begin{cases} \beta, & I > 0 \\ 0, & I = 0 \end{cases}$$

and a limited capacity treatment rate [156]

$$h(I) = \begin{cases} \beta I, & 0 \leq I \leq I_0 \\ \beta I_0, & I > I_0 \end{cases}$$

where I_0 represents the level of infection at which the health care system reaches its maximum capacity. Therefore, the treatment rate is proportional to the number of the infected I only until the maximum treatment capacity is attained, taking the maximum value βI_0 thereafter.

Zhang and Liu [177] proposed a continuously differentiable version of such a treatment function

$$h(I) = \frac{\beta I}{1 + kI},$$

where $\beta > 0$, is the treatment rate as $I \to 0$ and $k = 1/I_0$ models the delay in treating the infected. The treatment function $h(I)$ approaches βI when I is sufficiently small, and approaches $\beta/k = \beta I_0$ in the event that I is large. This model is more faithful to a real situation and has the advantage of being continuous and differential. Similar treatment functions have been used by Zhou and Fan [181] and Zhang et al. [175].

3.2.2 Model Formulation

In this section we will consider the SIR model used in Zhonghua and Yaohong [180]

$$\begin{aligned} \frac{dS}{dt} &= A - dS - \lambda SI, \\ \frac{dI}{dt} &= \lambda SI - (d + \gamma)I - \frac{\beta I}{1 + kI}, \\ \frac{dR}{dt} &= \gamma I + \frac{\beta I}{1 + kI} - dR, \end{aligned} \tag{3.8}$$

where S, I, and R denote the numbers of the susceptible, infected and recovered individuals at time t, A is the recruitment rate of the population, d is the natural death rate of the population, γ is the natural recovery rate of the infected individuals, λSI is the bilinear transmission term, λ being the average number of contacts per infected person per unit time. In this model, the term $\beta I/(1 + kI)$ models the treatment of the infected individuals, where β is the treatment rate when the number of infected is low, and k is a measure of the extent of the infected being delayed for treatment and β/k is the maximum treatment rate. See Figure 3.8 for a description of the process modeled by (3.8).

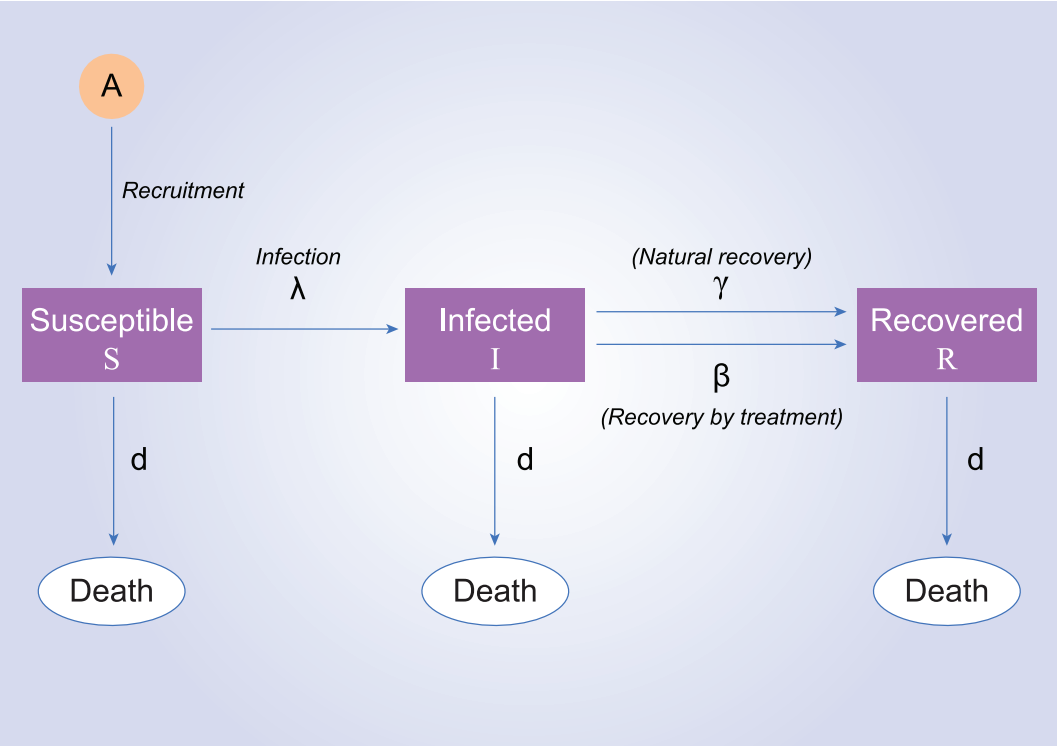

Figure 3.8: Schematic diagram of the system (3.8).

As noted in [180], the first two equations are independent of the third equation, so we may focus on the subsystem

$$\begin{aligned} \frac{dS}{dt} &= A - dS - \lambda SI, \\ \frac{dI}{dt} &= \lambda SI - (d+\gamma)I - \frac{\beta I}{1+kI}. \end{aligned} \tag{3.9}$$

In order to model memory effects, we will introduce fractional order derivatives to the ODE model (3.9), leading to the system

$$\begin{aligned} D_t^\alpha S &= A - dS - \lambda SI, \\ D_t^\alpha I &= \lambda SI - (d+\gamma)I - \frac{\beta I}{1+kI}, \end{aligned} \tag{3.10}$$

where D_t^α is the Caputo fractional derivative defined in Definition (2.2.4). In the next few sections we consider the equilibrium points of the system (3.10) and the conditions of the existence and stability of these points.

3.2.3 Equilibrium Points

Setting $D_t^\alpha S = 0$, $D_t^\alpha I = 0$, we find three possible equilibrium points: a disease free equilibrium $E_0(A/d, 0)$, i.e. where $S = A/d$ and $I = 0$, and two endemic

equilibria $E_1(S_1^*, I_1^*)$ and $E_2(S_2^*, I_2^*)$, where $S_j^* = A/(d + \lambda I_j^*)$, $j = 1, 2$, and I_j^* satisfies the equation

$$(n\lambda k)I^{*2} + (-\lambda Ak + ndk + n\lambda + \beta\lambda)I^* + (-\lambda A + nd + \beta d) = 0, \tag{3.11}$$

where we have set $n = d + \gamma$. The solutions for I^* are

$$I_1^* = \frac{\lambda Ak - ndk - (\beta + n)\lambda + \sqrt{\Delta}}{2n\lambda k}, \tag{3.12}$$

$$I_2^* = \frac{\lambda Ak - ndk - (\beta + n)\lambda - \sqrt{\Delta}}{2n\lambda k}, \tag{3.13}$$

where

$$\Delta = (-\lambda Ak + ndk + (\beta + n)\lambda)^2 + 4n\lambda k(\lambda A - (\beta + n)d). \tag{3.14}$$

These solutions for I^* can be rewritten as

$$I_1^* = \frac{2}{kb^2}\left(\frac{R_1 - 1}{R_1} + \sqrt{\Big(\frac{R_1 - 1}{R_1}\Big)^2 + b^2\Big(\frac{R_0 - 1}{R_0}\Big)}\right), \tag{3.15}$$

$$I_2^* = \frac{2}{kb^2}\left(\frac{R_1 - 1}{R_1} - \sqrt{\Big(\frac{R_1 - 1}{R_1}\Big)^2 + b^2\Big(\frac{R_0 - 1}{R_0}\Big)}\right), \tag{3.16}$$

where

$$R_0 = \lambda A/(d(\beta + n)), \tag{3.17}$$

which we prove below is the basic reproduction number,

$$R_1 = \lambda Ak/(ndk + \lambda(\beta + n)), \tag{3.18}$$

and

$$b = 2\sqrt{n/(Ak)}. \tag{3.19}$$

These equilibria will only exist in the real world if $S > 0$, $I > 0$. The equilibrium point E_0 is physical since $A > 0$ and $d > 0$, but to discuss the existence of E_1 and E_2, we must consider the parameters R_0, R_1 and $b = 2\sqrt{n/(Ak)}$.
We first show that $R_0 = \lambda A/(d(\beta + n))$ is the basic reproduction number. Using the next generation method [76] to find the basic reproduction number for the system (3.10), we consider the system of the form

$$\frac{dx}{dt} = f(x) - v(x),$$

where $x = [S, I]^T$,

$$f(x) = \begin{bmatrix} f_1 \\ f_2 \end{bmatrix} = \begin{bmatrix} \lambda SI \\ 0 \end{bmatrix}, \; v(x) = \begin{bmatrix} v_1 \\ v_2 \end{bmatrix} = \begin{bmatrix} nI + \dfrac{\beta I}{1+kI} \\ -A + dS + \lambda SI \end{bmatrix}.$$

The Jacobian matrices of $f(x)$ and $v(x)$ at E_0 are then given by

$$F(x) = \begin{bmatrix} \dfrac{\lambda A}{d} & 0 \\ 0 & 0 \end{bmatrix}, V(x) = \begin{bmatrix} n+\beta & 0 \\ \dfrac{\lambda A}{d} & d \end{bmatrix}.$$

The eigenvalues of $F \cdot V^{-1}$ are then $\delta_1 = \lambda A / \left(d\left(n+\beta\right)\right)$ and $\delta_2 = 0$. The basic reproduction rate is given by $R_0 = \max\left(\delta_i\right)$, $i = 1, 2$, so that $R_0 = \lambda A / \left(d\left(n+\beta\right)\right)$.

E_0 is always physical, but $E_{1,2}$ are physical if they are real and positive. $E_{1,2}$ are real if

$$\Big(\frac{1-R_1}{R_1}\Big)^2 + b^2\Big(\frac{R_0-1}{R_0}\Big) \geq 0,$$

or equivalently

$$R_0 \geq \frac{b^2 R_1^2}{R_1^2(1+b^2) - 2R_1 + 1} = F(R_1),$$

where $b = 2\sqrt{n/(Ak)}$. Note that $F \to b^2/(1+b^2)$ as $R_1 \to \infty$. Table 3.1 shows when E_1, E_2 are positive from the expression for I_1^* and I_2^*, i.e. equations (3.15) and (3.16).

	$R_1 < 1$	$R_1 = 1$	$R_1 > 1$
$R_0 > 1$	$E_1 > 0, E_2 < 0$	$E_1 > 0, E_2 < 0$	$E_1 > 0, E_2 < 0$
$R_0 = 1$	$E_1 = 0, E_2 < 0$		$E_1 > 0, E_2 = 0$
$R_0 < 1$	$E_1 < 0, E_2 < 0$		$E_1 > 0, E_2 > 0$

Table 3.1: The signs of E_1 and E_2 depending on the expressions for I_1^* and I_2^*.

Figure 3.9 summarises the physical states, i.e. real and positive equilibrium points for the system, where the blue curve denotes $R_0 = F(R_1)$. E_1 and E_2 above the blue curve are real-valued equilibrium points, but E_1 and E_2 below the blue curve have non-zero imaginary components and so are not physically realistic equilibrium points. So E_1 and E_2 may exist only above the blue curve.

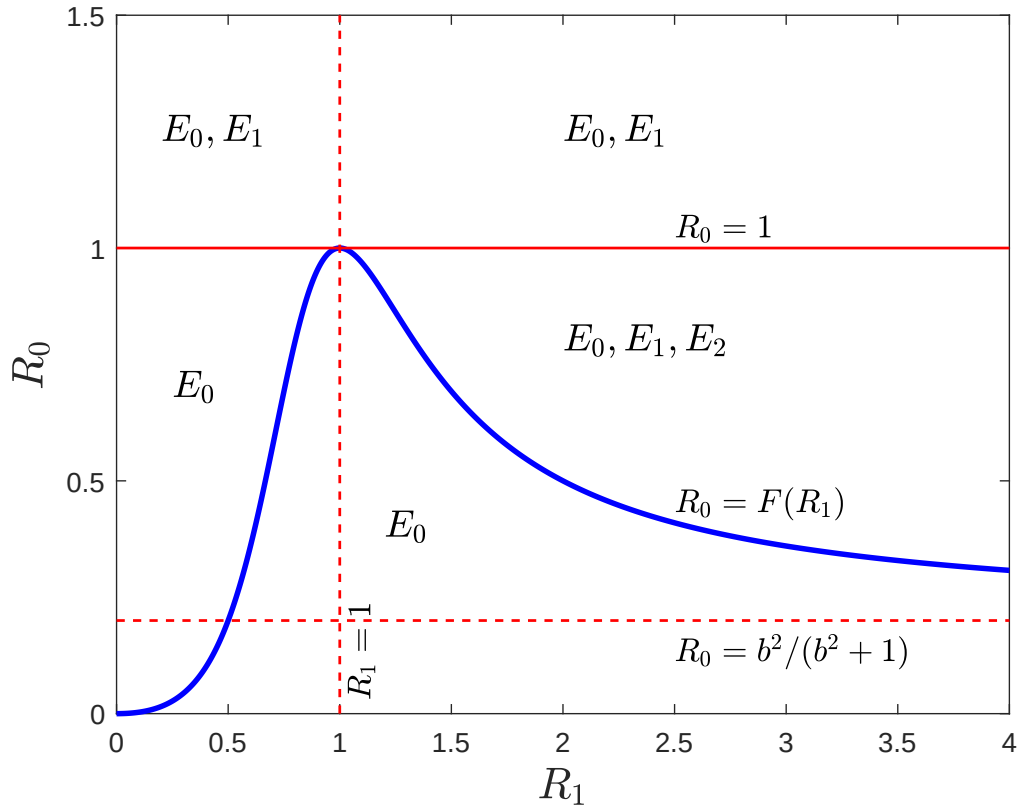

Figure 3.9: Diagram showing physical states of the system (3.10) as a function of R_0 and R_1.

3.2.4 Stability

As discussed in Chapter 2, the local asymptotic stability analysis of the equilibrium points can be investigated by using the Jacobian matrix of the system. From (3.10) the Jacobian is

$$J(S^*, I^*) = \begin{bmatrix} -d - \lambda I^* & -\lambda S^* \\ \lambda I^* & \lambda S^* - n - \dfrac{\beta}{(1+kI^*)^2} \end{bmatrix}.$$

From the equilibrium form of the second equation in (3.10), we have $\lambda S^* - n = \beta/(1+kI^*)$, so that

$$J(S^*, I^*) = \begin{bmatrix} -d - \lambda I^* & -\lambda S^* \\ \lambda I^* & \dfrac{k\beta I^*}{(1+kI^*)^2} \end{bmatrix}.$$

As mentioned in Chapter 2, an equilibrium point is asymptotically stable if the eigenvalues of the Jacobian, θ_i, satisfy $|\arg(\theta_i)| > \alpha\pi/2$, $i = 1, 2$. For E_0, the

Jacobian matrix $J(E_0) = J(A/d, 0)$ is

$$J(E_0) = \begin{bmatrix} -d & -\dfrac{\lambda A}{d} \\ 0 & (\beta + n)(R_0 - 1) \end{bmatrix},$$

for which the eigenvalues are real, $\theta_{01} = -d < 0$ and $\theta_{02} = (n+\beta)(R_0 - 1)$. Hence if $R_0 < 1$ the disease free equilibrium E_0 is asymptotically stable, while if $R_0 > 1$ the disease free equilibrium E_0 is unstable. Since the eigenvalues of the Jacobian of the disease free equilibrium E_0 are always real, then $\arg(\theta_{0i}) = 0$ or π and its stability will be unaffected by the fractional derivative order.

In contrast to the disease free equilibrium E_0, the stability of the endemic equilibrium points E_1 and E_2 can be affected by the fractional derivative order. The characteristic equation of $J(E_i)$ is

$$\theta^2 + f_i\theta + g_i = 0, \tag{3.20}$$

where

$$f_i = d + \lambda I_i^* - \frac{k\beta I_i^*}{(1 + kI_i^*)^2}, \tag{3.21}$$

$$g_i = \frac{\lambda^2 A}{d + \lambda I_i^*} I_i^* \left(1 - \frac{k\beta(d + \lambda I_i^*)^2}{\lambda^2 A(1 + kI_i^*)^2}\right). \tag{3.22}$$

The stability condition of the endemic equilibrium points E_i, $i = 1, 2$, therefore depends on f_i and g_i.

Using the Routh-Hurwitz criterion and Lemma 2.5.1 mentioned in Chapter 2, we find that

1. If $f_i > 0$ and $g_i > 0$, then (3.20) has no changes of sign of the coefficients and so there are two roots with negative real parts, and the equilibrium point is asymptotically stable for all $\alpha \in (0, 1]$.

2. If $f_i > 0$ and $g_i < 0$, and so $g_i < f_i^2/4$, then (3.20) has real roots. Since there is one change of sign of the coefficients of (3.20), there is one positive real root, and the equilibrium point is unstable for all $\alpha \in (0, 1]$.

3. If $f_i < 0$ and $0 < g_i < f_i^2/4$, then (3.20) has real roots, and since there are two changes of sign of the coefficients of (3.20), so there are either two or zero positive real roots. Since the roots are real the fractional order will not change the stability.

4. If $f_i < 0$ and $g_i > f_i^2/4$, then (3.20) has two complex conjugate roots with real part $-f_i/2$, which is positive since $f_i < 0$. Then the condition of stability of the fractional system is $|\arg(\theta_{ij})| = \cos^{-1}(-f_i/(2\sqrt{g_i})) > \alpha\pi/2$, $j = 1, 2$, $\alpha \in (0, 1]$, and the maximum value of α, for which stability is ensured, occurs at

$$\alpha^* = \frac{2}{\pi}\cos^{-1}\left(\frac{-f_i}{2\sqrt{g_i}}\right). \tag{3.23}$$

Here we will rewrite f_i and g_i as only functions of R_0, R_1, b, d, n. Using equations (3.15) - (3.18), f_i and g_i can be rewritten as

$$f_i = d + \frac{dyz}{4nR_1} - \frac{2z\left(\frac{y}{2R_1} - nR_0\right)}{b^2R_0\left(\frac{2z}{b^2} + 1\right)^2}, \tag{3.24}$$

$$g_i = \frac{d^2y^2z}{2R_1(dyz + 4dnR_1)} - \frac{b^2}{R_0(2z + b^2)^2}\left(2z\left(\frac{y}{2R_1} - nR_0\right)\left(\frac{dyz}{4nR_1} + d\right)\right), \tag{3.25}$$

where

$$y = \frac{4n}{b^2}\left(R_0 + \sqrt{R_0^2 - b^2R_1^2R_0}\right), \tag{3.26}$$

$$z = \frac{R_1 - 1}{R_1} + \sqrt{\left(\frac{R_1 - 1}{R_1}\right)^2 + b^2\left(\frac{R_0 - 1}{R_0}\right)}. \tag{3.27}$$

We can summarise all these stability results in Figure 3.10, where we have taken parameters from Case 1 in Section 3.2.5, i.e. $A = 76.5$, $d = 0.5$, $n = 7.5$, and $k = 0.5$. Using equation (3.19) we have $b = 0.8856$. The green area indicates the area in which $f_i > 0$ and $g_i > 0$ together, and the cyan area indicates the area where $f_i < 0$ and $g_i > f_i^2/4$ together.

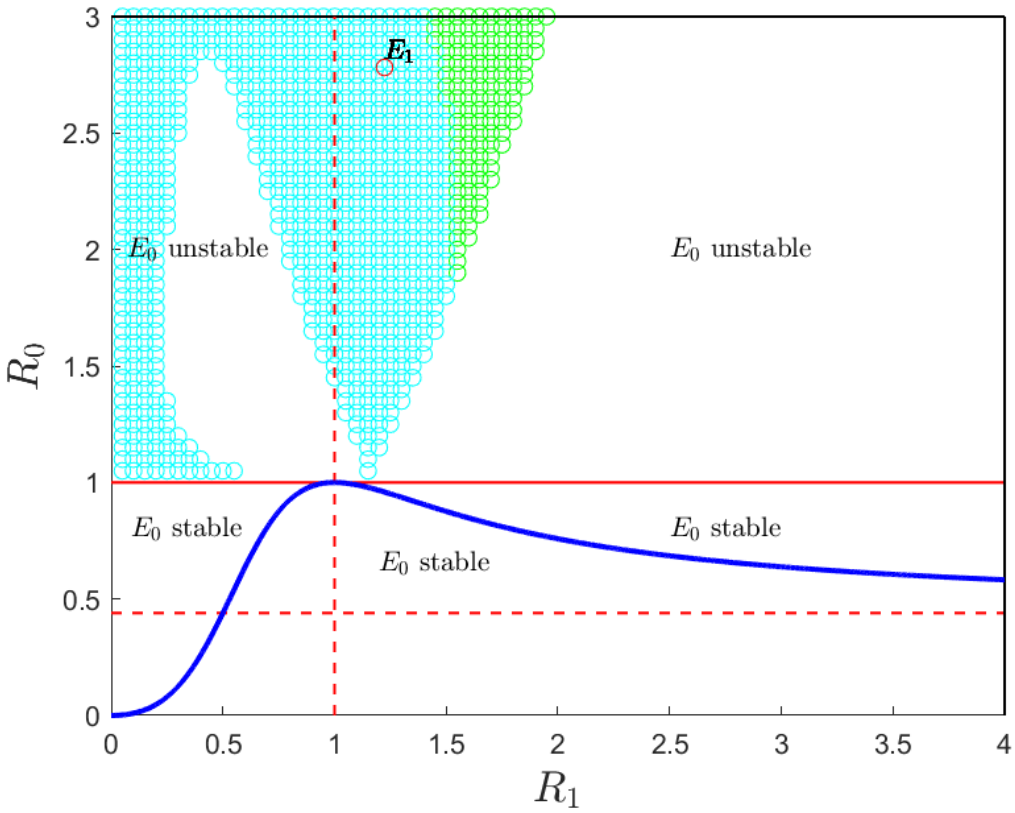

Figure 3.10: Diagram showing stability regions of equilibrium points for Case 1 in the numerical simulation. The green area shows the area that satisfies $f_i > 0$ and $g_i > 0$ together, so that E_1 is stable, the cyan area shows the area that satisfies $f_i < 0$ and $g_i > f_i^2/4$ together, so that E_1 is stable if $\alpha < 2/\pi \cos^{-1}(-f_i/(2\sqrt{g_i}))$. E_0 is unstable in the area $R_0 > 1$. The red circle in the cyan area indicates the stable equilibrium point E_1 in this case.

Similarly, for Figure 3.11, where we have taken parameters from Case 2 in Section 3.2.5, i.e. $A = 3$, $d = 0.01$, $n = 0.08$, and $k = 0.8$. Using equation (3.19) we have $b = 0.3651$. The green area indicates the area in which $f_i > 0$ and $g_i > 0$ together, and the cyan area indicates the area where $f_i < 0$ and $g_i > f_i^2/4$ together.

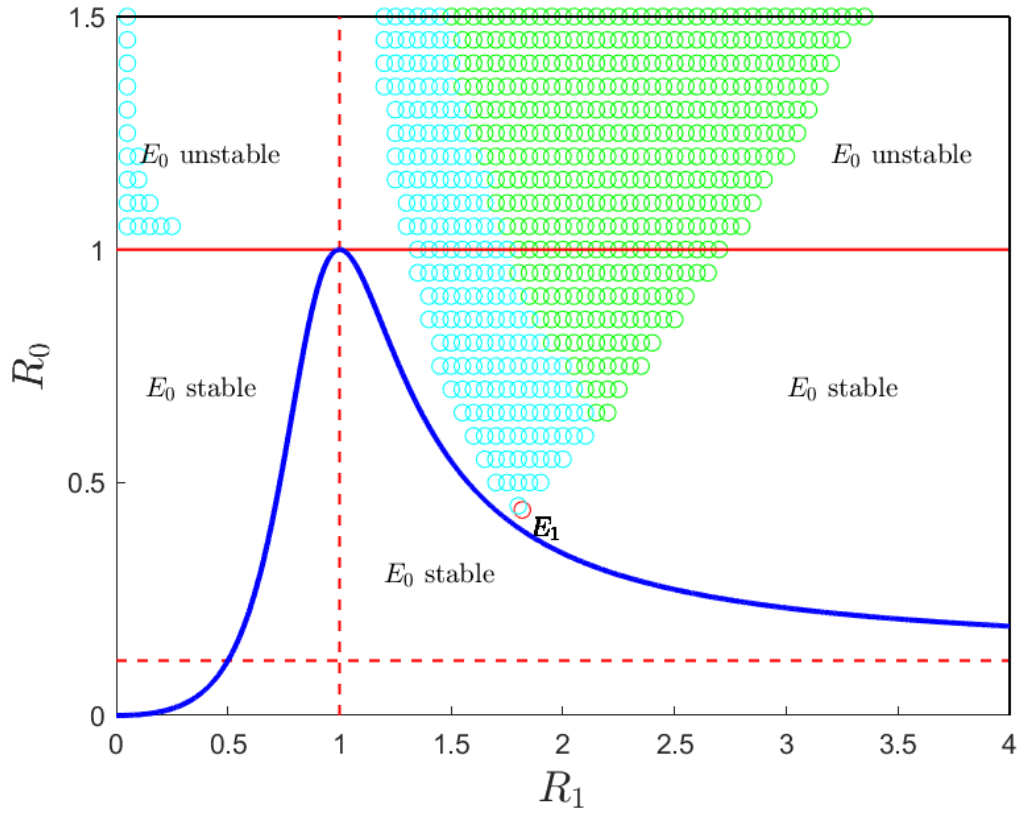

Figure 3.11: Diagram showing stability regions of equilibrium points for Case 2 in the numerical simulation. The green area shows the area that satisfies $f_i > 0$ and $g_i > 0$ together, so that E_1 or E_2 are stable, the cyan area shows the area that satisfies $f_i < 0$ and $g_i > f_i^2/4$ together, so that E_1 or E_2 are stable if $\alpha < 2/\pi \cos^{-1}(-f_i/(2\sqrt{g_i}))$. E_0 is stable in the area $R_0 \leq 1$. The red circle in the cyan area indicates the particular stable equilibrium point E_1 for the parameters used in this case.

In the integer system it was previously reported that, when both endemic equilibria exist, i.e. when $R_0 < 1$, $R_1 > 1$, and $\Delta > 0$, either one of the two endemic equilibria is asymptotically stable and the other endemic equilibrium is unstable or both of them are unstable [180]. Therefore, in the integer system it is not possible to have both endemic equilibria stable for the same parameter values. However, due to the stabilising effects of reducing the fractional derivative order α, it is possible for the system to exhibit two stable endemic equilibria. Having two stable endemic equilibria is significant for the possible control of the spread of a disease using hysteresis behaviour of a bistable system. On the other hand, if the disease-free equilibrium is the unique stable equilibrium of the system, then the system will converge to the stable disease-free equilibrium from any starting initial condition [128]. In a bistable system the choice between two endemic equi-

libria will depend on the initial state. Since the initial state could be manipulated (by harvesting, culling and control of the disease) it will be possible to determine which stable state the system approaches in the long-term [157].

3.2.5 Numerical Simulation

In this section we numerically solve the fractional differential equations (3.10) using the Adams-Bashforth-Moulton method described in Chapter 2. We consider two cases:

Case 1: E_0 is unstable and E_1 is unstable for integer order derivatives but can be stabilised by reducing the fractional derivative order, but E_2 does not exist.

Case 2: E_0 is stable and both E_1 and E_2 exist and are unstable in the integer order system. However, reducing the fractional order leads to E_1 becoming stable. In this case we therefore have the possibility of two stable equilibria, one disease free and one endemic.

For Case 1 we have chosen parameters $A = 76.5$, $d = 0.5$, $\lambda = 0.5$, $n = 7.5$, $\beta = 20$ and $k = 0.5$ that satisfy the conditions $R_0 = 2.78 > 1$, $R_1 = 1.23 > 1$, $f_1 = -1.37 < 0$, $g_1 = 19.6 > 0$, $g_1 > f_1^2/4$. The positive equilibrium points are $E_0 = (153, 0)$ and $E_1 = (27, 4.667)$, and the second endemic equilibrium point does not exist because it is negative $E_2 = (-85, -2.8)$. The eigenvalues of $J(E_0)$ are $\theta_{01} = 49$ and $\theta_{02} = -0.5$, so E_0 is unstable, and the eigenvalues of $J(E_1)$ are $\theta_{11} = 0.68 + 4.4i$ and $\theta_{12} = 0.68 - 4.4i$, so, for an integer system E_1 is unstable. However, as described in the previous section, E_1 can be stabilised by reducing the fractional order to below a critical value α^*. For these parameters we found that $\alpha^* = 0.9$. Figures 3.12 and 3.13 show the numerical solutions for $S(t)$ and $I(t)$ for $\alpha = 0.99$, $\alpha = 0.85$ and $\alpha = 0.75$, with the initial conditions $S(0) = 40$, $I(0) = 1$. From these figures we see that while for that system (3.8) considered by Zhonghua and Yaohong [180], E_1 is unstable, the fractional system (3.10) is stable for $\alpha = 0.85$ and 0.75. When α is increased above α^*, the equilibrium point loses its stability through a Hopf-like bifurcation and what appears to be a limit cycle occurs in the neighborhood of the equilibrium point.

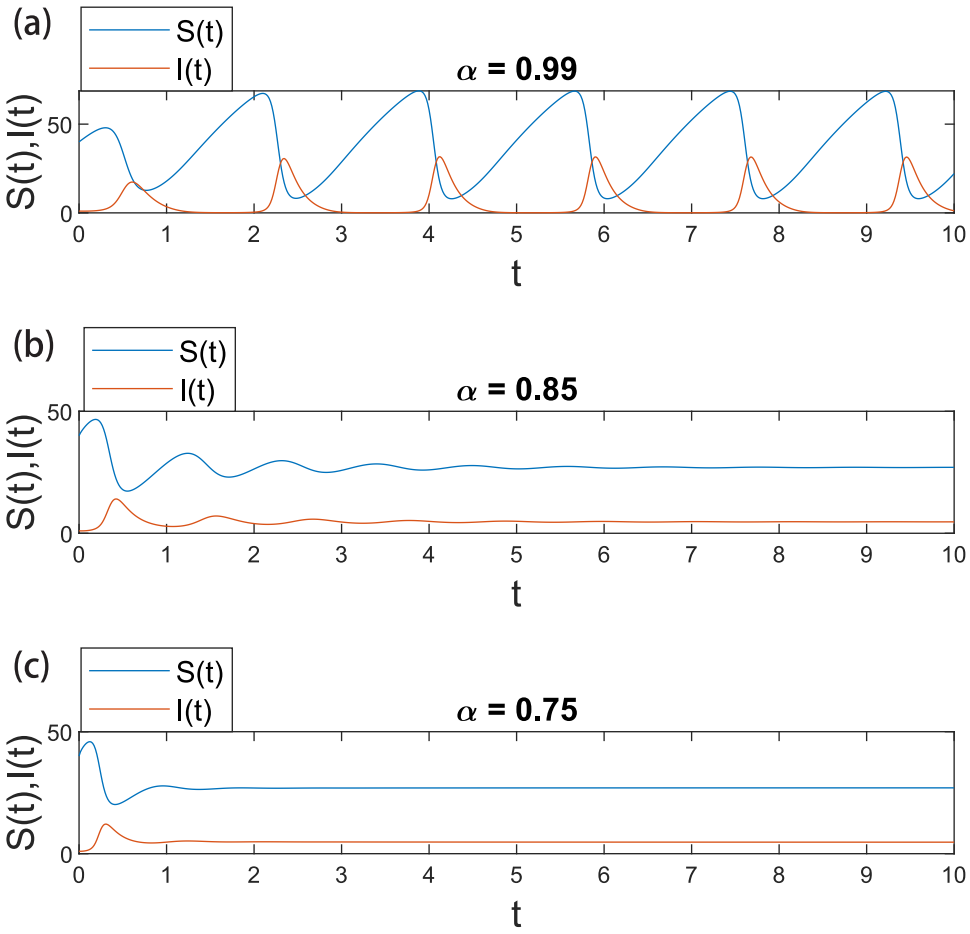

Figure 3.12: Numerical solutions of $S(t)$ and $I(t)$ for the system (3.10). (a) For $\alpha = 0.99$ E_1 is unstable and the system converges to a limit cycle, (b) when $\alpha = 0.85$ and (c) $\alpha = 0.75$ the system converges to $E_1 = (27, 4.667)$.

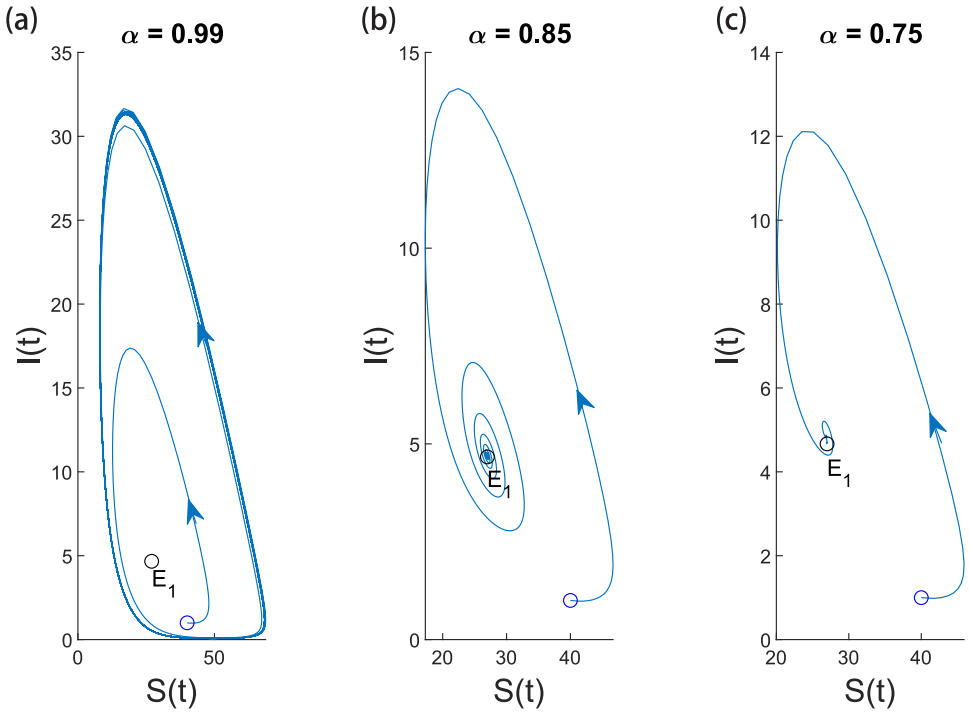

Figure 3.13: Phase portraits corresponding to the solutions shown in Figure 3.12. (a) When $\alpha = 0.99$ E_1 is unstable and the system converges to limit cycle, (b) when $\alpha = 0.85$ and (c) $\alpha = 0.75$ the system converges to $E_1 = (27, 4.667)$.

In Case 2 we have chosen parameters $A = 3$, $d = 0.01$, $\lambda = 0.001$, $n = 0.08$, $\beta = 0.6$ and $k = 0.8$ which satisfies the conditions $R_0 = 0.44 < 1$, $R_1 = 1.818 > 1$, $f_1 = -0.03 < 0$, $g_1 = 0.0005 > 0$, $g_1 > f_1^2/4$. The positive equilibrium points are then $E_0 = (300, 0)$, $E_1 = (137, 11.9)$ and $E_2 = (200, 5)$. The eigenvalues of $J(E_0)$ are $\theta_{01} = -0.38$ and $\theta_{02} = -0.01$, so E_0 is stable. The eigenvalues of $J(E_2)$ are $\theta_{21} = 0.09$ and $\theta_{22} = -0.005$, so E_2 is unstable, and the eigenvalues of $J(E_1)$ are $\theta_{11} = 0.015 + 0.02i$ and $\theta_{12} = 0.015 - 0.02i$. Therefore, although in the integer system E_1 will be unstable, in the fractional system this equilibrium point can be stabilised by reducing α. The red circle in Figure 3.11 indicates the stable equilibrium point E_1 in this case. For these parameters we find the critical value of the fractional order, $\alpha^* = 0.53$. Figures 3.14 and 3.15 illustrate the behaviour of the system (3.10) with two stable equilibrium points. Figure 3.14 shows that E_1 is stable for $\alpha < \alpha^*$ but, importantly, it also shows that for the same initial conditions, as α decreases the stable equilibrium point that the system will approach at long time can change. For $\alpha = 0.6$ the system approaches E_0 while for $\alpha = 0.4$ the system approaches E_1. In order to investigate this effect further we will analyse the system response to variations of the initial values measuring the final state at $t = t_{end} = 120000$. We mark the initial values according to whether the final state is closest to E_0 or E_1. Figures 3.16 and 3.17 highlight our findings; the blue colour indicates that a system with this initial state is eventually closest to E_0 and

a yellow colour is closest to E_1. These figures make it possible to illustrate how modifying the fractional derivative order may affect the effective domain of attraction of the equilibrium points. We use the term 'effective domain of stability' since we measure proximity to the equilibrium points at $t = t_{end}$. The actual stability region, i.e. the initial states that leads to convergence to an equilibrium point as $t \to \infty$ will not depend on α. However, in a real system the state will need to be measured at particular times and will never reach a $t \to \infty$ state. As seen in Figures 3.16 and 3.17 the transient 'effective' domain of attraction are dependent on α. Figures 3.16 and 3.17 indicate that if the order is lower than the critical value the system shifts between the two states at $t = t_{end}$. If the order goes above the critical value, the equilibrium E_1 becomes unstable and thus the yellow region is expected to collapse. However, since the regions are labelled according to the state at $t = t_{end}$ and because of transient oscillating movement around E_1, the system is maintained close to E_1 for a range of initial conditions.

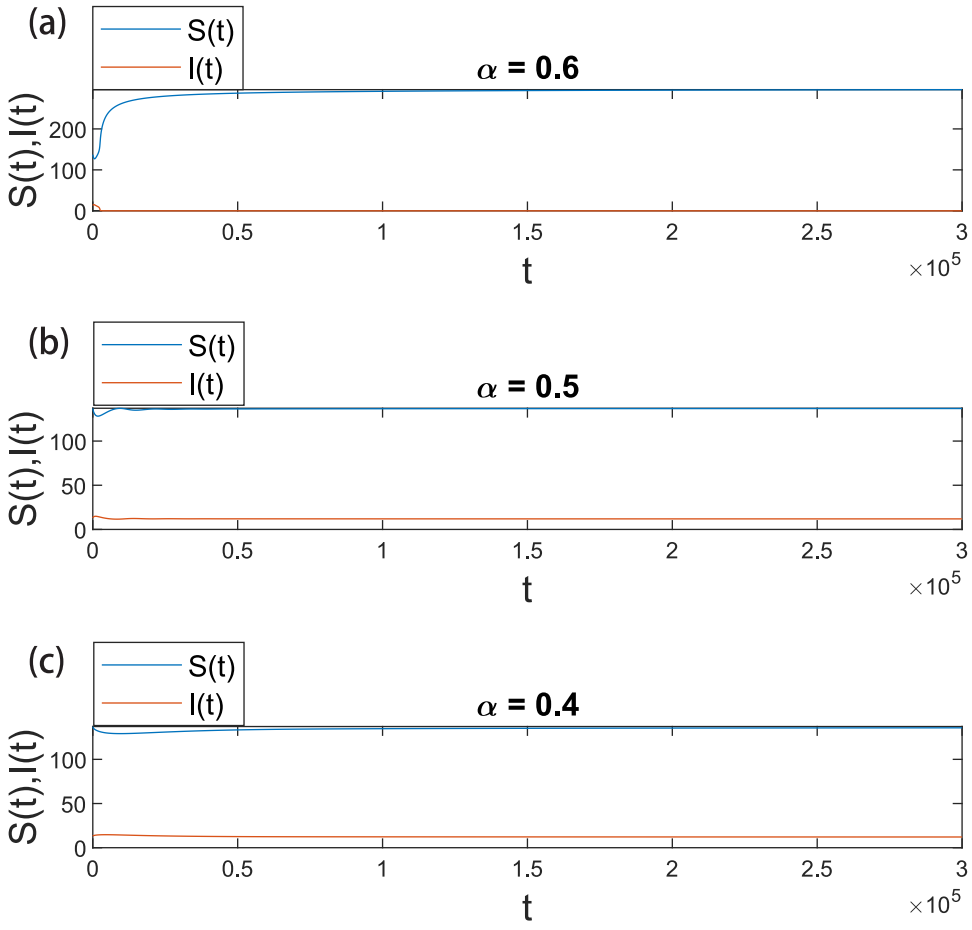

Figure 3.14: Numerical solutions of $S(t)$ and $I(t)$ for the system (3.10). (a) For $\alpha = 0.6$ the system converges to $E_0 = (300, 0)$, (b) when $\alpha = 0.5$ and (c) $\alpha = 0.4$ the system converges to $E_1 = (137, 11.9)$.

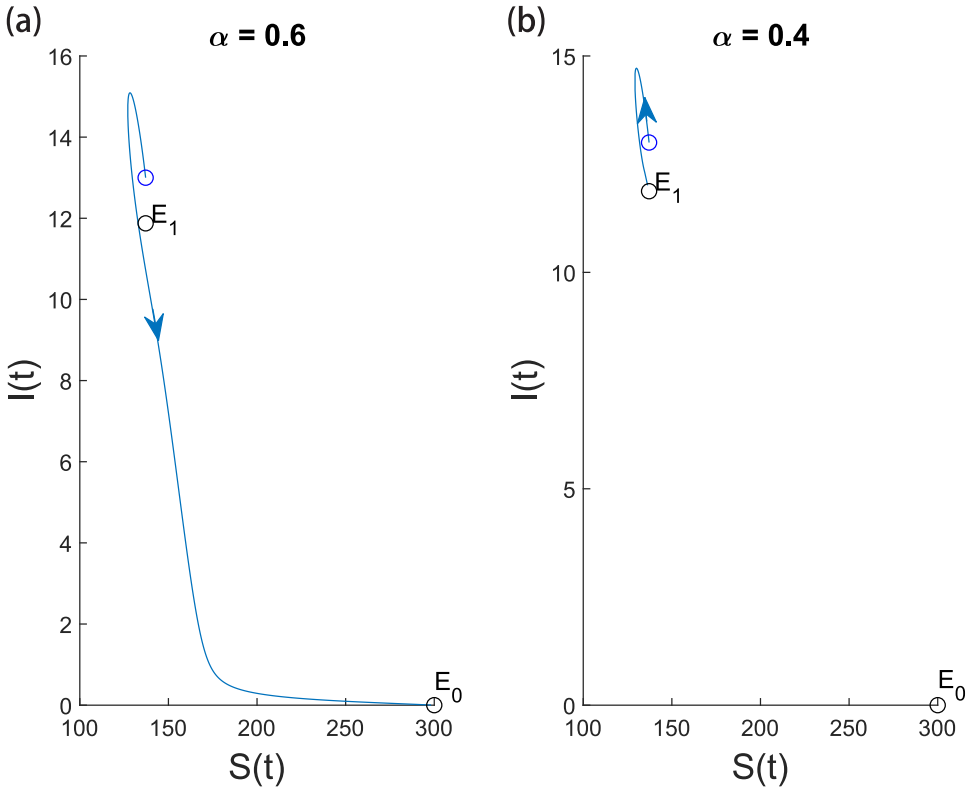

Figure 3.15: Phase portraits corresponding to the solutions shown in Figure 3.14. (a) When $\alpha = 0.6$ the system converges to $E_0 = (300, 0)$, (b) when $\alpha = 0.4$ the system converges to $E_1 = (137, 11.9)$.

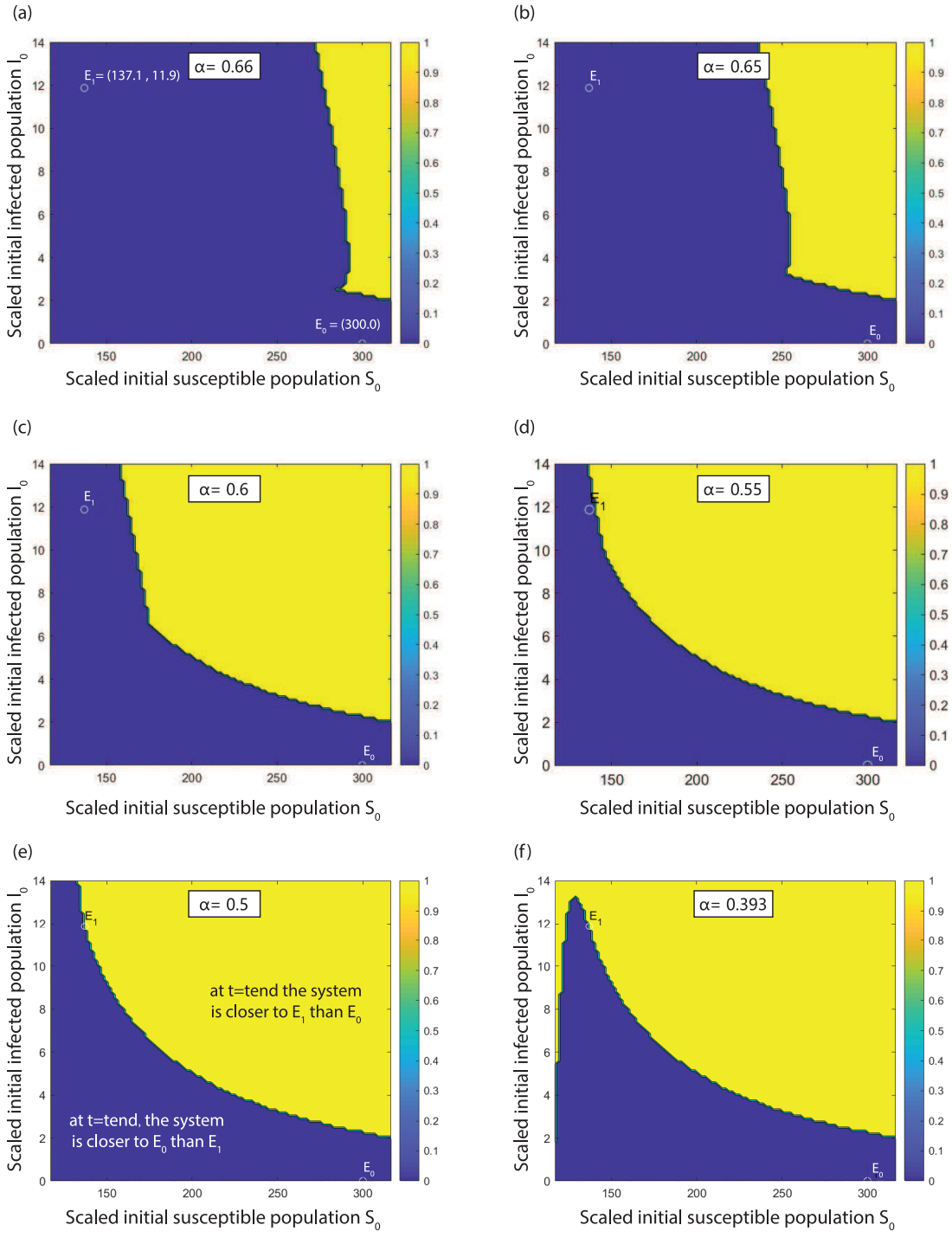

Figure 3.16: Effective domain of attraction for different values of α. If the initial states S_0, I_0 are chosen from the blue region the system remains relatively close to E_0 at $t = t_{end}$. For (a) to (d), E_1 is unstable, but for (e) and (f), E_1 is stable.

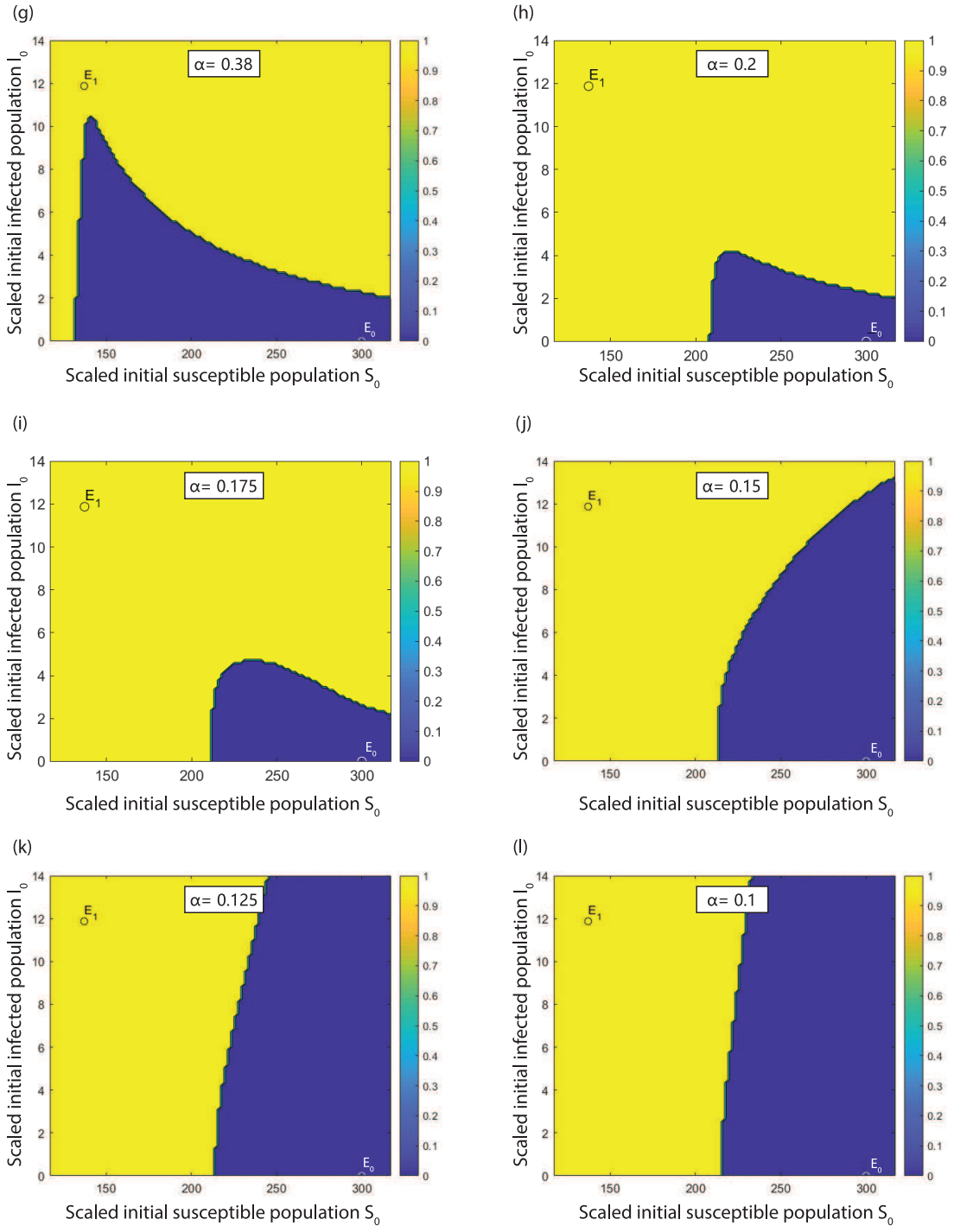

Figure 3.17: Effective domain of attraction for different values of α. For (g) to (l), E_0 and E_1 are stable, so if the initial states S_0, I_0 are chosen from the blue region the system remains relatively close to E_0. For initial states within the yellow region the system remains relatively close to E_1, at $t = t_{end}$.

3.3 Conclusion

In this chapter, we have considered two fractional order models. The first model is the tumor-immune system prey-predator model. We have obtained the conditions of the existence and studied stability conditions for the equilibrium points. We have also illustrated the effect of changing α on the stability and Hopf-bifurcation using a numerical simulation. Finally, we have investigated the dependency of α^* on all the parameters in the system (3.4). In the second model, relevant conditions of stability and bifurcation are laid down for the SIR system under consideration. Importantly, it has been shown how the variation of the fractional order could generate a monostable to bistable transition. Particular interest was paid to the model and parameters in [180]. However, it should be noted that these main effects, both on stability and on domains of attraction, emanating from the variation of the fractional order, would occur for any analogous system that has more than one stable state. In particular, Figure 3.16 and Figure 3.17 provide key information on the significant link between the values of the fractional order, compared to the critical value α^*, and the resulting domain of attraction. Within a concrete ecological framework, the value of α which models the memory characteristics of species may be fixed, or it may vary (i.e. with age). Figure 3.16 and Figure 3.17, and plots such as Figure 3.15, demonstrate that the long-term evolution of the system may depend significantly on α, and may therefore be unpredictable.

Chapter 4

Stability in an Incommensurate Fractional-Order Model

4.1 Introduction

Over the last two decades, many researchers have been concerned with the study of commensurate order systems, where the fractional orders of all time derivatives are the same, as compared with incommensurate orders. Stability and stabilisation issues were particularly addressed and most of the results were obtained based on the Matignon criterion [110]. This theorem is the starting point for many results in this field of study, for instance, in the work of Momani and Hadid [115], and Matignon and Prieur [111].

Very few studies have investigated stability issues for incommensurate models. One of the first attempts to investigate the stability of incommensurate fractional systems was conducted by Bonnet and Partington in [26] which included consideration of time delays. The authors were concerned with BIBO (Bounded-Input Bounded-Output) stability in the general case and managed to establish links between stability conditions and system pole locations. Later, Deng et al. [45] extended the study for systems with numerous time delays. Stability conditions were proved and the results were confirmed through illustrative examples. The case of distributed delay systems was examined in [153], where, after considering the Cauchy problem for a linear system, the authors proved the existence and uniqueness of solutions. Both Caputo and Riemann-Liouville cases of fractional derivatives have been considered when investigating the stability of the base solution of such systems.

BIBO stability issues were also investigated in the case of fractional systems with incommensurate orders by Jiao and Chen [83] who considered a fractional system with double incommensurate orders and, by using Laplace transforms, proposed sufficient and necessary conditions to ensure the stability of such sys-

tems and then improved their results by proposing a stability testing algorithm. Sabatier et al. [133] also conducted BIBO stability analysis and applied Cauchy's argument principle to establish a graphical test allowing the evaluation of incommensurate system stability. Despite the accuracy of the test in several examples, it is challenging to implement such complicated procedures. Petras [124] has also reported further findings about stability issues of incommensurate systems.

Several works have been interested in considering chaotic behaviour in incommensurate fractional order systems. For instance, Tavazoei and Haeri [144] used basic stability results to propose a necessary condition under which incommensurate order systems could generate scroll chaotic attractors. Additional numerical evaluations were performed to improve the reliability of the analytical method in detecting chaotic behaviour. The control and the stabilisation of such chaotic systems remains one of the major challenges when studying chaotic dynamics of such systems. Zhang and Yang [132] tried to address this challenge by proposing a systematic model capable of stabilising incommensurate fractional order chaotic systems. The method was implemented on the basis of the Lyapunov stability criterion and a substitution method, using only one state variable. It should be noted that the simplicity of this method and its usefulness for both commensurate and incommensurate systems means it is widely applicable.

Chaotic synchronization of fractional dynamics has attracted considerable attention in recent times. An interesting scheme was introduced in [109], with the aim of estimating state variables for incommensurate fractional order systems. Although the authors applied the methodology to incommensurate chaotic models, the proposed scheme may apply to a wide class of systems. Similarly, Chen et al. [35] proposed a second order sliding mode control (SOSM) to allow chaos synchronization of an incommensurate fractional order system, taking into account uncertainty and the presence of external disturbances. The ability of this second order algorithm to cancel chattering effects as well as its asymptotic stability was proved using the Lyapunov theorem.

In this chapter we will generalise the commensurate fractional order model of virus propagation in [52] to become an incommensurate model. We will find approximate analytical solutions for the eigenvalues of the characteristic equation of this model and compare to the numerical results.

4.2 Model Formulation

Following [151, 180], the mathematical model for virus propagation in a situation where treatment can assist recovery of the infected population can be written as

a set of three coupled nonlinear ordinary differential equations as follows:

$$\begin{aligned} \frac{dS}{dt} &= A - \mu S - bSI + \omega R, \\ \frac{dI}{dt} &= bSI - (\mu + g + \delta)I - \frac{\epsilon I}{1 + qI}, \\ \frac{dR}{dt} &= gI + \frac{\epsilon I}{1 + qI} - (\mu + \omega)R, \end{aligned} \tag{4.1}$$

where S, I and R denote the numbers of the susceptible, infected and recovered individuals at time t, respectively. In the equation for the evolution of the susceptible population, the parameter A denotes the recruitment or birth rate of the population, μ is the natural death rate of the population, bSI is the bilinear transmission term between susceptible and infected populations, b being the average number of contacts per infected person per unit time, and due to the loss of immunity, at any time the recovered population becomes susceptible with constant probability ω. Additional parameters in the evolution equation for the infected population are g, the natural recovery rate of the infected individuals, δ the death due to infection, and $\epsilon I/(1+qI)$ models the treatment of the infected individuals, where ϵ is the treatment rate when the number of infected is low, and q measures the extent of the infected being delayed for treatment and ϵ/q is the maximal treatment resources supplied per unit time. All the parameters A, μ, b, g, δ, ω, ϵ and q are positive and the Figure 4.1 shows a pictorial representation of the process modeled by the system (4.1).

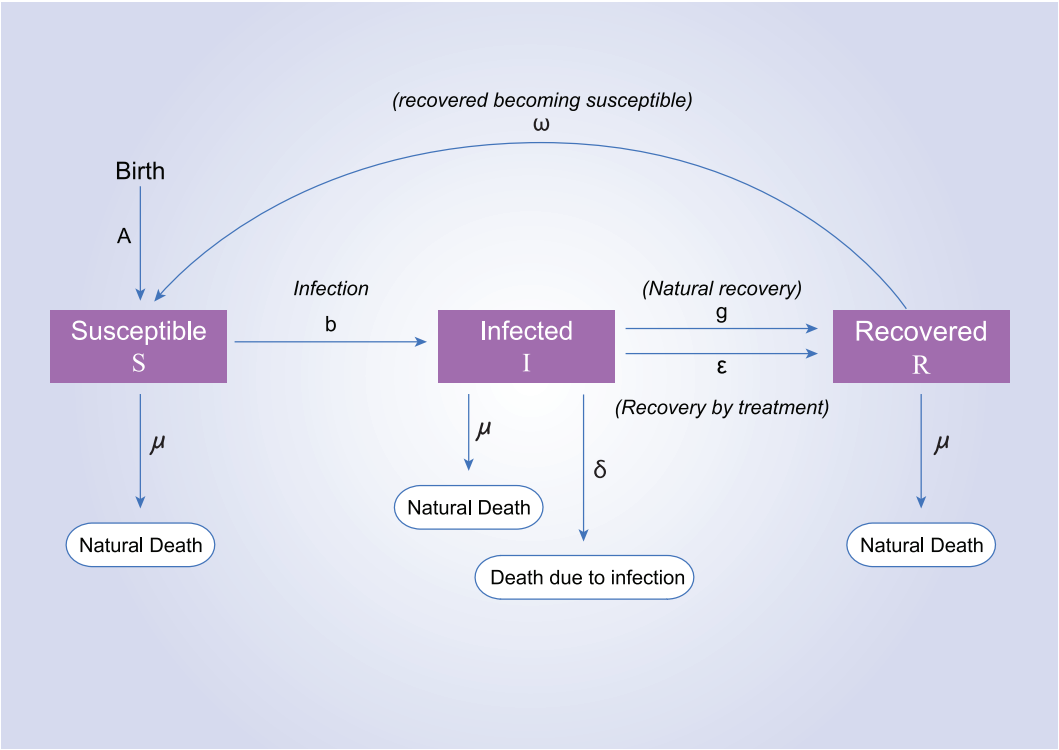

Figure 4.1: Schematic diagram of the system (4.1).

El-Shahed and Alissa [52] investigated the equivalent commensurate fractional system of differential equations:

$$\begin{aligned} D_t^\alpha S &= A - \mu S - bSI + \omega R, \\ D_t^\alpha I &= bSI - (\mu + g + \delta)I - \frac{\epsilon I}{1+qI}, \\ D_t^\alpha R &= gI + \frac{\epsilon I}{1+qI} - (\mu + \omega)R, \end{aligned} \tag{4.2}$$

where D_t^α is the Caputo fractional derivative defined in Definition (2.2.4). They studied the stability of equilibrium points and proved that a small change in the fractional order, α, may affect the stability. The trajectories converge to the equilibrium point when $\alpha < \alpha^*$ whereas when α is increased above α^* the equilibrium point loses its stability.

Here we describe the incommensurate system by the following set of fractional order differential equations:

$$\begin{aligned} D_t^\alpha S &= A - \mu S - bSI + \omega R, \\ D_t^\beta I &= bSI - (\mu + g + \delta)I - \frac{\epsilon I}{1+qI}, \\ D_t^\gamma R &= gI + \frac{\epsilon I}{1+qI} - (\mu + \omega)R, \end{aligned} \tag{4.3}$$

where α, β and γ are the fractional orders of the Caputo time derivatives related to the susceptible, infected and recovered populations. As discussed in the next few sections we consider the equilibrium points of the system (4.3) and the conditions of the existence and stability of these points.

4.3 Equilibrium Points

The equilibrium points of the system (4.3) are the same equilibrium points of the system (4.1) that have already been written in [52]. Setting derivatives to zero, we find three equilibrium points, namely, a disease free equilibrium $E_0(A/\mu, 0, 0)$, with no infected or recovered individuals, and two endemic equilibria $E_1(S_1^*, I_1^*, R_1^*)$ and $E_2(S_2^*, I_2^*, R_2^*)$, where

$$\begin{aligned} S_j^* &= \frac{\Psi}{b} + \frac{\epsilon}{b(1+qI_j^*)}, \\ R_j^* &= \frac{I_j^*}{\theta}\Big(g + \frac{\epsilon}{1+qI_j^*}\Big), \end{aligned}$$

where $j = 1, 2$, $\Psi = \mu + g + \delta$, $\theta = \mu + \omega$, and I_j^* satisfy the following equation:

$$I^{*2} + c_1(1 - R_1)I^* + c_0(1 - R_0) = 0, \tag{4.4}$$

where

$$\begin{aligned} c_0 &= \frac{\mu\theta(\Psi+\epsilon)}{qb(\mu\Psi+\omega\theta)}, \\ c_1 &= \frac{\mu b(\Psi+\epsilon) + \mu b\omega(\mu+\delta) + q\mu\theta\Psi}{qb(\mu\Psi+\omega\theta)}, \\ R_0 &= \frac{bA}{\mu\,(\Psi+\epsilon)}, \\ R_1 &= \frac{qb\theta A}{\mu b(\Psi+\epsilon) + \mu b\omega(\mu+\delta) + q\mu\theta\Psi}. \end{aligned}$$

Here R_0 is the basic reproduction number and the solutions for the equation (4.4) are

$$I_1^* = \frac{c_1(R_1 - 1) + \sqrt{\Delta}}{2}, \tag{4.5}$$

$$I_2^* = \frac{c_1(R_1 - 1) - \sqrt{\Delta}}{2}, \tag{4.6}$$

where

$$\Delta = c_1^2(1 - R_1)^2 - 4c_0(1 - R_0). \tag{4.7}$$

These solutions have two special cases: if $R_0 = 1$, then $\Delta > 0$, $I_1^* = 0$, $I_2^* = c_1(R_1 - 1)$, then there can be only one endemic equilibrium I_2^*; if $\Delta = 0$, then $I_1^* = I_2^* = c_1(R_1 - 1)/2$, so there can be only one endemic equilibrium, $I_1^* = I_2^*$. All equilibria will only exist in the physical world if $S > 0$, $I > 0$ and $R > 0$. The equilibrium point E_0 is physical since $A/\mu > 0$, and the equilibria E_1 and E_2 exist if the solutions (4.5) and (4.6) are not negative, which depends on the signs of R_0 and R_1. By considering the values of R_0 and R_1 we see that

1. A disease free equilibrium point E_0 always exists.
2. If $R_0 > 1$, there exists a unique endemic equilibrium point $E_1(S_1^*, I_1^*, R_1^*)$.
3. If $R_0 = 1$, $R_1 > 1$, there exists a unique endemic equilibrium $E_2 = (S_2^*, I_2^*, R_1^*)$ and a disease-free equilibrium $E_1 = (S_1^*, 0, R_1^*)$.
4. If $R_0 \leq 1$, $R_1 \leq 1$, no endemic equilibrium exists.
5. If $R_0 < 1$, $R_1 > 1$, and $\triangle > 0$, there exist two endemic equilibria $E_1 = (S_1^*, I_1^*, R_1^*)$ and $E_2 = (S_2^*, I_2^*, R_2^*)$.
6. If $R_0 < 1$, $R_1 > 1$, and $\triangle < 0$, no endemic equilibrium exists.

4.4 Stability of the Commensurate System

The local asymptotic stability of the commensurate system (4.2) around E_0 and E_1 has been studied in [52] and we summarise these results here. The local asymptotic stability analysis of the equilibrium points is investigated in the standard way by using the Jacobian matrix

$$J = \begin{pmatrix} -\mu - bI & -bS & \omega \\ bI & bS - \Psi - \dfrac{\epsilon}{(1+qI)^2} & 0 \\ 0 & g + \dfrac{\epsilon}{(1+qI)^2} & -(\mu + \omega) \end{pmatrix}. \tag{4.8}$$

By finding the eigenvalues λ_i, $i = 1, 2, 3$ of the Jacobian matrices $J(E_0)$, $J(E_1)$ and $J(E_2)$ and using the condition of stability for fractional systems, $|\arg \lambda_i| > \alpha\pi/2$, it was found that

1. If $R_0 < 1$ the disease free equilibrium E_0 is asymptotically stable, while if $R_0 > 1$ the disease free equilibrium E_0 is unstable.
2. If $R_0 = 1$, $R_1 \geq 1$ the disease free equilibrium E_0 is asymptotically stable.
3. E_1 and E_2 can be locally asymptotically stable if the roots of the characteristic equation of $J(E_1)$ and $J(E_2)$ satisfy $|\arg \lambda_i| > \alpha\pi/2$, $i = 1, 2, 3$.

In summary, for the commensurate system (4.2),

1. If $R_0 > 1$, then E_0 exists but is unstable, and a unique endemic equilibrium point E_1 exists and could be stable or unstable, depending on α.

2. If $R_0 = 1$, $R_1 \geq 1$ the disease free equilibrium E_0 exists and is stable, and a unique endemic equilibrium point E_1 exists and could be stable or unstable, depending on α.

3. If $R_0 \leq 1$, $R_1 \leq 1$, then E_0 exists but is unstable, and no endemic equilibrium exists.

4. If $R_0 < 1$, $R_1 > 1$, and $\triangle > 0$, then E_0 exists and is stable, and there exist two endemic equilibria E_1 and E_2 which could be stable or unstable, depending on α.

5. If $R_0 < 1$, $R_1 > 1$, and $\triangle < 0$, then E_0 exists and is stable, and no endemic equilibrium exists.

This behaviour is summarised in Figure 4.2.

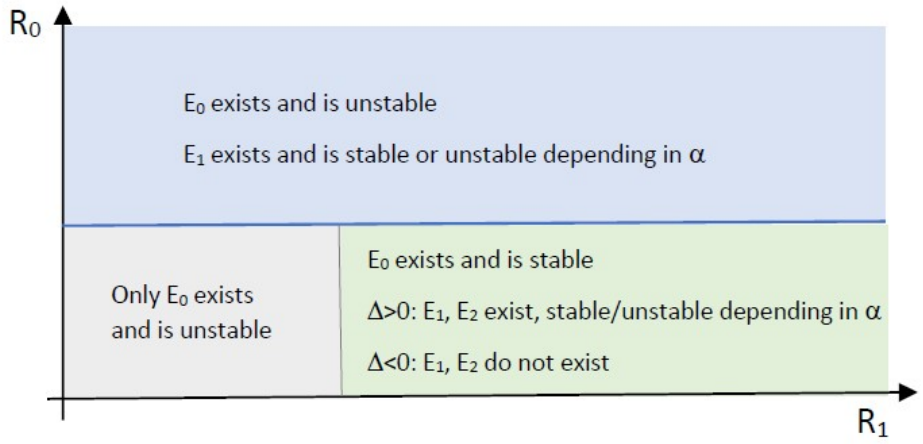

Figure 4.2: Summary plot of the existence and stability of states in the commensurate system.

4.5 Stability of the Incommensurate System

The local asymptotic stability of the incommensurate system (4.3) around the equilibrium points can be described using Lemma 2.5.2 and in this section we will find the analytical solution for the characteristic equation of the incommensurate

system for particular restrictions on α, β and γ. Specifically we consider the situation when α, β and γ are close to being equal.

The characteristic equation for the incommensurate system is

$$\begin{vmatrix} J_{11}-\lambda^{\alpha} & J_{12} & J_{13} \\ J_{21} & J_{22}-\lambda^{\beta} & J_{23} \\ J_{31} & J_{32} & J_{33}-\lambda^{\gamma} \end{vmatrix} = 0,$$

or equivalently,

$$(J_{11}-\lambda^{\alpha})(J_{22}-\lambda^{\beta})(J_{33}-\lambda^{\gamma}) - J_{23}J_{32}(J_{11}-\lambda^{\alpha}) - J_{13}J_{31}(J_{22}-\lambda^{\beta}) \\ -J_{12}J_{21}(J_{33}-\lambda^{\gamma}) + J_{12}J_{23}J_{31} + J_{13}J_{21}J_{32} = 0, \quad (4.9)$$

where J_{ij} are the elements of the Jacobian matrix (4.8). For the commensurate system we will assume α, β and γ are a rational number, so $\alpha = \beta = \gamma = n/p$ and by setting $\Lambda = \lambda^{\frac{1}{p}}$, we obtain

$$(J_{11}-\Lambda^{n})(J_{22}-\Lambda^{n})(J_{33}-\Lambda^{n}) - J_{23}J_{32}(J_{11}-\Lambda^{n}) - J_{13}J_{31}(J_{22}-\Lambda^{n}) \\ -J_{12}J_{21}(J_{33}-\Lambda^{n}) + J_{12}J_{23}J_{31} + J_{13}J_{21}J_{32} = 0. \quad (4.10)$$

Letting $\Delta = \Lambda^n$, we then have a cubic equation for Δ. The solution for the eigenvalues of the commensurate system, which we denote by Δ^*, are obtained from

$$\Delta^{*3} - (J_{22}+J_{11}+J_{33})\Delta^{*2} + (J_{11}J_{22}+J_{33}J_{22}+J_{33}J_{11} - J_{23}J_{32} - J_{13}J_{31} - J_{12}J_{21})\Delta^* \\ -J_{11}J_{22}J_{33} + J_{23}J_{32}J_{11} + J_{13}J_{31}J_{22} + J_{12}J_{21}J_{33} - J_{12}J_{23}J_{31} - J_{13}J_{21}J_{32} = 0. \quad (4.11)$$

We will now consider two cases, for which the system is nearly commensurate. Specifically we consider a case where the fractional orders of the infected and recovered populations are equal and only the susceptible fractional order is different. For this case we therefore set $\alpha = n/p$, $\beta = \gamma = m/p$. In the second case we consider all fractional orders to be different but related by $\alpha - \beta = \gamma - \alpha$ so that α, β and γ are in a geometric sequence. To simplify the analysis we also assume that α, β and γ are almost equal. In both cases we set p to be $p = 1/(\beta - \alpha)$.

In the first case we describe above we therefore have $\alpha = n/p$, $\beta = \gamma = m/p$, with $m = n+1$, then equation (4.9), with $\Lambda = \lambda^{\frac{1}{p}}$, is

$$(J_{11}-\Lambda^{n})(J_{22}-\Lambda^{n+1})(J_{33}-\Lambda^{n+1}) - J_{23}J_{32}(J_{11}-\Lambda^{n}) - J_{13}J_{31}(J_{22}-\Lambda^{n+1}) \\ -J_{12}J_{21}(J_{33}-\Lambda^{n+1}) + J_{12}J_{23}J_{31} + J_{13}J_{21}J_{32} = 0. \quad (4.12)$$

As in the commensurate system we set $\Delta = \Lambda^n$ so that $\Lambda^{n+1} = \Delta^{1+\frac{1}{n}}$, and set $\varepsilon = 1/n$, we obtain

$$(J_{11}-\Delta)(J_{22}-\Delta^{1+\varepsilon})(J_{33}-\Delta^{1+\varepsilon}) - J_{23}J_{32}(J_{11}-\Delta) - J_{13}J_{31}(J_{22}-\Delta^{1+\varepsilon}) \\ -J_{12}J_{21}(J_{33}-\Delta^{1+\varepsilon}) + J_{12}J_{23}J_{31} + J_{13}J_{21}J_{32} = 0. \quad (4.13)$$

If we assume that $\varepsilon = 1/n \ll 1$, i.e. small, so that the fractional orders are almost equal, then we can find solutions Δ by considering a perturbation [164] to the commensurate system,

$$\Delta = \Delta^* + \varepsilon\bar{\Delta}, \tag{4.14}$$

where Δ^* is a solution of eq.(4.11). Substituting (4.14) into (4.13), we have

$$\begin{aligned}\Big(J_{11} - \big(\Delta^* + \varepsilon\bar{\Delta}\big)\Big)\Big(J_{22} - \big(\Delta^* + \varepsilon\bar{\Delta}\big)^{1+\varepsilon}\Big)\Big(J_{33} - \big(\Delta^* + \varepsilon\bar{\Delta}\big)^{1+\varepsilon}\Big)\\ -J_{23}J_{32}\Big(J_{11} - \big(\Delta^* + \varepsilon\bar{\Delta}\big)\Big) - I_{13}J_{31}\Big(J_{22} - \big(\Delta^* + \varepsilon\bar{\Delta}\big)^{1+\varepsilon}\Big)\\ -J_{12}J_{21}\Big(J_{33} - \big(\Delta^* + \varepsilon\bar{\Delta}\big)^{1+\varepsilon}\Big) + J_{12}J_{23}J_{31} + J_{13}J_{21}J_{32} = 0.\end{aligned} \tag{4.15}$$

Taking Taylor expansion for $\big(\Delta^* + \varepsilon\bar{\Delta}\big)^{1+\varepsilon}$ about $\varepsilon = 0$, which is

$$\big(\Delta^* + \varepsilon\bar{\Delta}\big)^{1+\varepsilon} = \Delta^* + \big(\bar{\Delta} + \Delta^* \ln \Delta^*\big)\,\varepsilon + O(\varepsilon^2), \tag{4.16}$$

therefore, (4.15) can be written as

$$\begin{aligned}\Big(J_{11} - \big(\Delta^* + \varepsilon\bar{\Delta}\big)\Big)\Big(J_{22} - \Big(\Delta^* + \big(\bar{\Delta} + \Delta^* \ln \Delta^*\big)\,\varepsilon\Big)\Big)\\ \Big(J_{33} - \Big(\Delta^* + \big(\bar{\Delta} + \Delta^* \ln \Delta^*\big)\,\varepsilon\Big)\Big) - J_{23}J_{32}\Big(J_{11} - \big(\Delta^* + \varepsilon\bar{\Delta}\big)\Big)\\ -J_{13}J_{31}\Big(J_{22} - \Big(\Delta^* + \big(\bar{\Delta} + \Delta^* \ln \Delta^*\big)\,\varepsilon\Big)\Big) - J_{12}J_{21}\Big(J_{33} - \Big(\Delta^* + \big(\bar{\Delta} + \Delta^* \ln \Delta^*\big)\,\varepsilon\Big)\Big)\\ +J_{12}J_{23}J_{31} + J_{13}J_{21}J_{32} + O(\varepsilon^2) = 0.\end{aligned}$$

Equating terms of order $O(1)$ leads to the equation for Δ^* whereas terms of order $O(\varepsilon)$ leads to a solution for the first order perturbation of Δ^* due to the commensurate fractional orders,

$$\bar{\Delta} = \frac{\ln \Delta^*\Big(-2\Delta^{*3} + \Delta^{*2}\left(2J_{11} + J_{22} + J_{33}\right) + \Delta^*\left(-J_{11}J_{22} - J_{11}J_{33} + J_{13}J_{31} + J_{12}J_{21}\right)\Big)}{3\Delta^{*2} - 2\Delta^*\left(J_{11} + J_{22} + J_{33}\right) + J_{11}J_{22} + J_{22}J_{33} + J_{11}J_{33} - J_{23}J_{32} - J_{13}J_{31} - J_{12}J_{21}}. \tag{4.17}$$

In the second case we consider we let $\alpha = n/p$, $\beta = m/p$, $\gamma = r/p$, where $m = n+1$ and $r = n-1$. As in the previous case we have $\Lambda = \lambda^{\frac{1}{p}}$, $\Delta = \Lambda^n$ and set $\varepsilon = 1/n$ to obtain

$$\begin{aligned}\left(J_{11} - \Delta\right)\left(J_{22} - \Delta^{1+\varepsilon}\right)\left(J_{33} - \Delta^{1-\varepsilon}\right) - J_{23}J_{32}\left(J_{11} - \Delta\right) - J_{13}J_{31}\left(J_{22} - \Delta^{1+\varepsilon}\right)\\ -J_{12}J_{21}\left(J_{33} - \Delta^{1-\varepsilon}\right) + J_{12}J_{23}J_{31} + J_{13}J_{21}J_{32} = 0.\end{aligned} \tag{4.18}$$

Again using $\Delta = \Delta^* + \varepsilon\bar{\Delta}$, and taking Taylor expansion for $\big(\Delta^* + \varepsilon\bar{\Delta}\big)^{1+\varepsilon}$ and $\big(\Delta^* + \varepsilon\bar{\Delta}\big)^{1-\varepsilon}$ about $\varepsilon = 0$, we are able to find the first order perturbation to Δ^*

to be

$$\bar{\Delta} = \frac{\ln \Delta^* \Big(\Delta^{*2} \left(J_{33} - J_{22} \right) + \Delta^* \left(J_{11} J_{22} - J_{11} J_{33} + J_{13} J_{31} - J_{12} J_{21} \right) \Big)}{3\Delta^{*2} - 2\Delta^* \left(J_{11} + J_{22} + J_{33} \right) + J_{11} J_{22} + J_{22} J_{33} + J_{11} J_{33} - J_{23} J_{32} - J_{13} J_{31} - J_{12} J_{21}}. \tag{4.19}$$

Since $\Delta = \Lambda^n = \lambda^{\frac{n}{p}} = \lambda^\alpha$ and $\Delta^* = (\Lambda^*)^n = (\lambda^*)^{\frac{n}{p}} = (\lambda^*)^\alpha$, we have

$$\lambda^\alpha \;\; = \;\; (\lambda^*)^\alpha + \varepsilon \bar{\Delta}, \tag{4.20}$$

where $\bar{\Delta}$ is given by (4.17) or (4.19) and where λ^* is an eigenvalue solution of the commensurate system.

4.6 Stability Boundary

In this section, we concentrate on our approximate analytic eigenvalue solution, (4.20), and compare to the numerical solution of the original eigenvalue equation. The eigenvalues of the commensurate system are found from the cubic equation (4.11) and for the parameters we consider, there is one negative real eigenvalue and two complex. We are interested in $|\arg(\lambda^\alpha)|$ to study the stability of the equilibrium point and therefore we need only consider one of the complex solutions, $(\lambda^*)^\alpha = a + ib$, where a and b are related to the values of J_{ij} where $i, j = 1, 2, 3$. We can then write the solution for the eigenvalue of the incommensurate system as

$$\lambda^\alpha = (a + ib) + \varepsilon (a_1 + ib_1), \tag{4.21}$$

where a_1 and b_1 are the real and imaginary parts for either (4.17) or (4.19) which are related to the values of J_{ij}. The condition for stability, $|\arg\lambda| > \pi/2$, then leads to

$$\arg\left((a + \varepsilon a_1) + i\,(b + \varepsilon b_1)\right) = \tan^{-1}\frac{b + \varepsilon b_1}{a + \varepsilon a_1} = \tan^{-1}\left[\frac{b}{a} + \left(\frac{b_1}{a} - \frac{a_1 b}{a^2}\right)\varepsilon + O(\varepsilon^2)\right].$$

By using the Taylor series expansion for $\tan^{-1}$, we have

$$\arg\left((a + \varepsilon a_1) + i\,(b + \varepsilon b_1)\right) = \tan^{-1} G_1 + \frac{G_2}{1 + {G_1}^2}\varepsilon,$$

where $G_1 = b/a$ and $G_2 = (ab_1 - a_1 b)/a^2$. For the two cases that we consider, $\varepsilon = \beta/\alpha - 1$. In the first case $\gamma = \beta = n + 1/p$, and in the second case $\beta = n + 1/p$, $\gamma = n - 1/p$ and $\gamma = 2\alpha - \beta$. Therefore, the condition for the stability will then be

$$\left| \tan^{-1} G_1 + \frac{G_2}{1 + {G_1}^2}\left(\frac{\beta}{\alpha} - 1\right) \right| > \alpha\pi/2. \tag{4.22}$$

Equation (4.22) therefore gives us an approximation for the boundary $\beta(\alpha)$ of the stability region in the $\alpha\beta$ parameter plane, close to the critical order for the commensurate system α^*.

$$\beta(\alpha) = \alpha\left(H_1\alpha + H_2\right), \tag{4.23}$$

where

$$\begin{aligned} H_1 &= \frac{\pi}{2}\left(\frac{1+G_1^2}{G_2}\right), \\ H_2 &= 1 - \frac{1+G_1^2}{G_2}\tan^{-1} G_1. \end{aligned}$$

With $\bar{\Delta}$ given by (4.17) or (4.19), we can get two approximate analytical solutions $\beta = \beta_1(\alpha)$ and $\beta = \beta_2(\alpha)$ depending on the value of $\bar{\Delta}$ that is chosen.

In the next section we will determine the boundary of the stability region numerically in order to compare with (4.23) for the two cases of $\bar{\Delta}$ given by (4.17) or (4.19).

4.7 Numerical Solution

In this section, we will find the solution for the characteristic equation of the incommensurate system (4.9) numerically using Matlab and compare the stability boundary for a particular equilibrium point to the approximate analytical solutions (4.23).

El-Shahed and Alissa [52] studied the commensurate system (4.2), and chose parameters $A = 40$, $\mu = 0.6$, $b = 0.4$, $q = 0.3$, $\epsilon = 10$, $g = 5$, $\delta = 0.2$, and $\omega = 0.2$. For these parameters the equilibrium points are $E_0 = (66.7, 0, 0)$, $E_1 = (28.5, 2.6, 34.6)$ and $E_3 = (-53.2, -4.6, 125.9)$, and the eigenvalues are $\lambda_{1,2} = 0.311137 \pm 2.73893i$ and $\lambda_3 = -0.6$. In [52] it was found that the system (4.2) is asymptotically stable around E_1 for all fractional derivative orders in the interval $(0, \alpha^*)$ where α^* can be determined from the system parameters to be $\alpha^* = 0.92799$, and unstable for all fractional derivative orders that are greater than α^*. For the same parameters as above, we will study the incommensurate system (4.3) and investigate how the critical value α^* changes as β and γ are allowed to change.

Using the Matlab fsolve function and given the eigenvalue $\lambda_1 = 0.311137 + 2.73893i$ for the integer system ($\alpha = 1$, $\beta = 1$, $\gamma = 1$) at E_1 as an initial guess, which is the only eigenvalue (together with its conjugate) that will be affected by changes in fractional order, we will first vary the fractional orders individually

in order to observe their effects on λ_1. Figure 4.3 illustrates particular α, β and γ dependencies of the eigenvalue which in the integer system leads to instability. In Figure 4.3 (a, b) we see that varying the value of α, and using fixed values $\beta = \gamma = 1$, indicates the real part of the complex eigenvalue goes from positive to negative as α decreases. Hence, for a value of α less than a critical value $\alpha^* = 0.92799$, the system attains stability. Now considering equal integer orders for both the susceptible and recovered species, $\alpha = \gamma = 1$, we vary the fractional order of the infected population between $0 < \beta < 1$, see Figure 4.3 (c, d). Here we see that the real part of the eigenvalue is always positive and so the system (4.3) will never be stable around E_1 for this case. The final case when the values of the orders related to susceptible and infected populations are fixed to be $\alpha = \beta = 1$, and we vary γ, is shown in Figure 4.3 (e, f). As in the previous case, we see that the real part of the eigenvalue is always positive so that the system (4.3) will never be stable around E_1 for any value of γ while $\alpha = \beta = 1$.

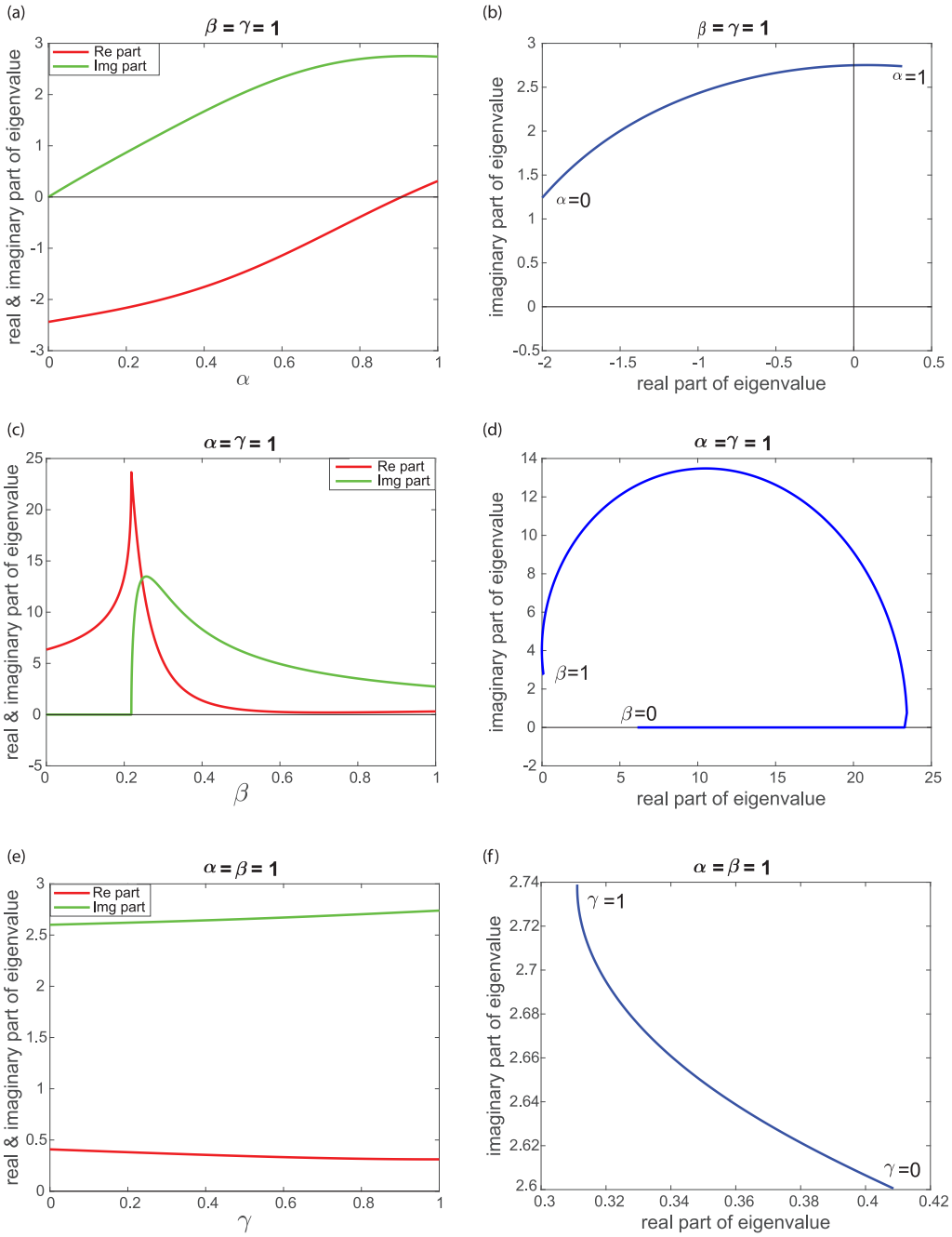

Figure 4.3: Numerical determination of one of the complex eigenvalues of the incommensurate system (4.3) at the equilibrium point E_1: (a) Real and imaginary parts of the complex eigenvalues as a function of α when $\beta = \gamma = 1$; (b) Corresponding Argand diagram for (a); (c) Real and imaginary parts of the complex eigenvalues as a function of β when $\alpha = \gamma = 1$; (d) Corresponding Argand diagram for (c); (e) Real and imaginary parts of the complex eigenvalues as a function of γ when $\alpha = \beta = 1$; (f) Corresponding Argand diagram for (e).

Although we could numerically investigate the stability of the equilibrium point E_1 for the full range of fractional orders $0 < \alpha, \beta, \gamma < 1$, here we wish to consider the accuracy of the two analytic approximations for the stability boundary $\beta(\alpha)$ for the cases previously mentioned. In the first case we consider $\alpha \neq \beta = \gamma$ and our analytic result (4.23) when $\bar{\Delta}$ is given by (4.17). The red line in Figure 4.4 indicates the approximate analytic solutions $\beta_1(\alpha)$ in this case. The results of varying both α and $\beta = \gamma$ are shown, where the green region indicates instability of the equilibrium point E_1, i.e. there is an eigenvalue with positive real part. The white region indicates stability of E_1, i.e. there are no positive eigenvalues. The blue line indicates the commensurate system $\alpha = \beta = \gamma$.

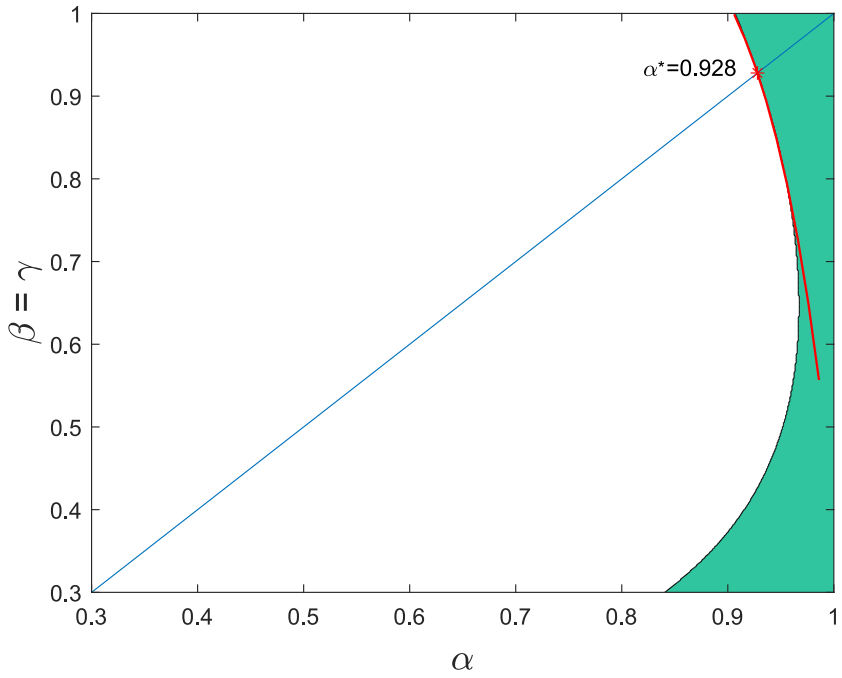

Figure 4.4: Stability region depending on the values of fractional derivative orders. The white region indicates stability around the equilibrium point E_1. The green region indicates instability around the equilibrium point E_1. The line $\alpha = \beta = \gamma$, i.e. the case of the commensurate system, is shown in blue as well as the critical value of α, i.e. the point α^* in red, below which the commensurate system achieves stability. The red line indicates the approximate analytical solution $\beta_1(\alpha)$.

As found in [52], for the commensurate system ($\alpha = \beta = \gamma$) the equilibrium point E_1 is unstable for $\alpha > \alpha^*$. However, the shape of the instability boundary shown in Figure 4.4 indicates that even for $\alpha > \alpha^*$ it is possible for the incommensurate system to be stable. Figure 4.5 illustrates an example of this situation. In Figure 4.5 we choose $\alpha = 0.93 > \alpha^*$, which leads to instability in the commensu-

rate system, as seen in Figure 4.5 (b). However, by reducing $\beta = \gamma$ below a critical value (β_3 as illustrated in Figure 4.5 (a)) the system can become stable about E_1, as seen in Figure 4.5 (c). Interestingly, the shape of the instability boundary in Figure 4.4 means that if the fractional orders β, γ are reduced even further (past β_2 as indicated in Figure 4.5 (a)) then instability occurs again, as seen in 4.5 (d).

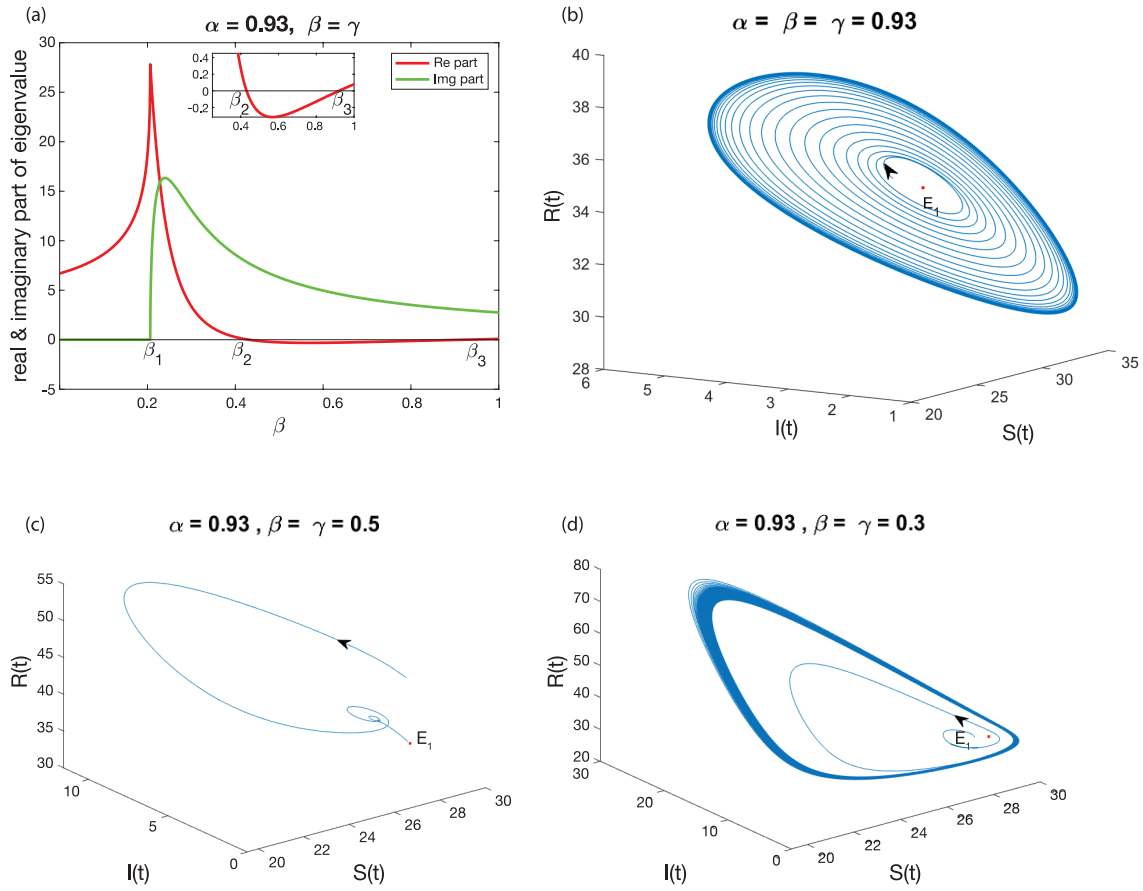

Figure 4.5: (a) Numerical determination of one of the complex conjugate eigenvalues associated with the incommensurate system (4.3) at equilibrium point E_1. The real part is shown as a red line and the imaginary part as a green line, while $\alpha = 0.93 > \alpha^*$. The real part of the eigenvalue is negative for $\beta_2 < \beta < \beta_3$. (b) For $\alpha = \beta = \gamma = 0.93$, the system is unstable around the equilibrium point. (c) For $\alpha = 0.93$ and $\beta = 0.5$, the incommensurate system is asymptotically stable around the equilibrium point. (d) For $\alpha = 0.93$ and $\beta = 0.3$, the incommensurate system is unstable around the equilibrium point.

In Figure 4.4 we have plotted the approximate analytical solution $\beta = \beta_1(\alpha)$ in order to confirm the accuracy of the perturbation approach. As Figure 4.4 demonstrates $\beta = \beta_1(\alpha)$ closely approximates the numerically determined stabil-

ity boundary, especially close to $\alpha = \beta = \alpha^*$, as expected. However, the form of $\beta = \beta_1(\alpha)$ does not show the re-entrant instability behaviour for low values of $\beta = \gamma$, as was demonstrated in Figure 4.5 (d). It may be that higher order terms in the perturbation series would lead to similar behaviour but we leave this for future investigations.

We now consider the second case discussed in Section 4.5, where we take into account the variation of both α and $\gamma = 2\alpha - \beta$ and our analytic result (4.23) when $\bar{\Delta}$ is given by (4.19). The red line in Figure 4.6 indicates the approximate analytic solutions $\beta_2(\alpha)$ in this case. As in Figure 4.4 the green region indicates instability of the equilibrium point E_1, i.e. there is an eigenvalue with positive real part, and the white region indicates stability of E_1.

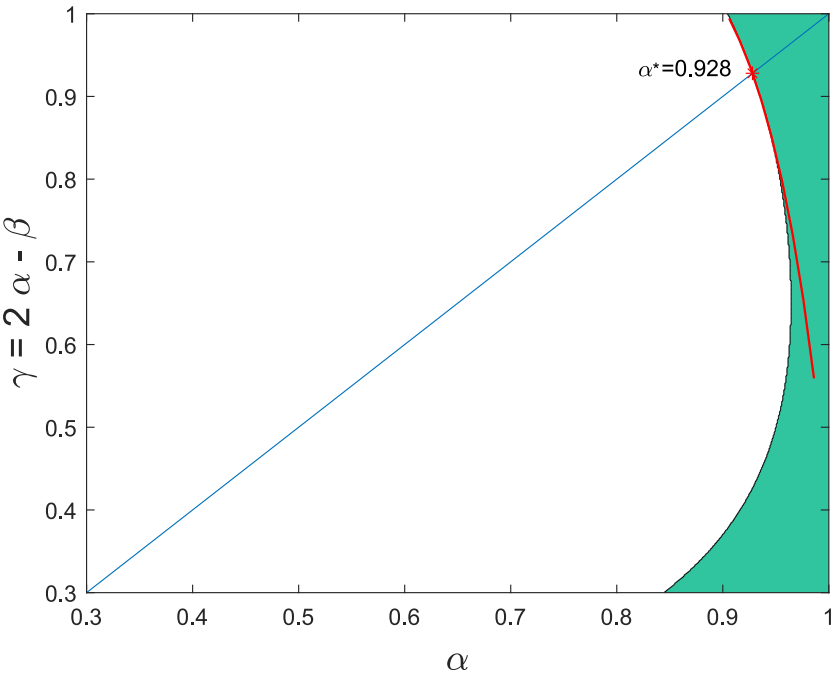

Figure 4.6: Stability regions depending on the values of fractional derivative orders. The white region indicates stability around the equilibrium point E_1. The green region indicates instability around the equilibrium point E_1. The line $\alpha = \beta = \gamma$, i.e. the case of the commensurate system, is shown in blue as well as the critical value of α, i.e. the point α^* in red, below which the commensurate system achieves stability. The red line indicates the approximate analytical solution $\beta_2(\alpha)$.

The stability boundary in Figure 4.6 show a very similar shape to Figure 4.4 and so the same conclusion can be drawn. As before, the approximation solution $\beta = \beta_2(\alpha)$ closely follows the numerical solution and confirms that $\beta = \beta_2(\alpha)$ closely approximates the stability boundary, especially near $\alpha = \beta = \gamma = \alpha^*$, as

expected.

4.8 Conclusion

In this chapter we have used perturbation theory to obtain approximate analytical solutions for the eigenvalues associated to the characteristic equation of the incommensurate system. We have considered two special cases for the values of the fractional orders, both close to the commensurate case, and used Matlab to obtain numerical solutions in order to plot the full stability boundary and compare to the analytic results. Through these studies we have developed a deeper understanding of how altering the fractional order can have a stabilising or destabilising effect. It is clear that given a system of three interacting species, we cannot immediately recognize whether reducing fractional orders leads to a stable or unstable state. We conclude by commenting that an incommensurate system would often be a more accurate model of a system than a commensurate model since the inherent memory effects can not be assumed to be the same for different species, or even different sub-populations of a single species.

Chapter 5

Travelling Waves

5.1 Introduction

Travelling waves have been widely studied since the first reaction-diffusion equations were introduced. Most of those models were concerned with the study of the propagation of a pattern that evolves in time and space. The study of a partial differential equation describing the evolution of such a pattern in a stable environment, including the heat equation and Fisher-KPP (KPP for Kolmogorov-Petrovsky-Piskunov) equation, was a key element to understanding more about various mechanisms related to wave propagation. The heat equation, also known as the diffusion equation, was established by Fourier to describe phenomena of heat propagation and temperature evolution. Fourier then sought to determine the value of the temperature, in a homogeneous environment, from a given initial distribution of temperature in time and space. The Fisher-KPP equation, was introduced in 1937 by the biologist Fisher [61] to describe the propagation of a new advantageous gene in a population. The same year, mathematicians Kolmogorov, Petrovski and Piscounov [95] were also interested in studying the speed of flames in combustion patterns. This equation includes a source-saturation point, whereas in the heat equation the dependent quantity propagates only by diffusion. Fisher's model was mainly concerned with a one-dimensional region, while Kolmogorov, Petrovski and Piscounov proposed an equation in two spatial dimensions. The first exact travelling wave solution was established by Ablowitz and Zeppetella [3] in 1979 through the Painlev approach. In 1999, Brazhnik and Tyson [149] established an explicit form of a travelling wave solution and managed to construct other similar solutions approximately in two dimensions. Sanchez-Garduno [135] sought to extend these preliminary results and establish more general results. In 1995, he considered a generalised reaction-diffusion equation and proved uniqueness for the travelling wave solution. Numerical simulations were also conducted, and sufficient conditions were found for the existence of front type solutions.

There are a huge number of phenomena in biology that show travelling waves,

i.e. chemical concentration, mechanical deformation, electrical signal etc. Winfree [165] includes a large number of examples of wave phenomena in biology, and Segel [138] deals with many aspects of wave motion. Other general books on reaction-diffusion equations, such as by Fife [58], Britton [27] and Grindrod [69], contain many examples of travelling wave solutions. At present, many research papers are concerned with travelling wave solutions of various PDEs. This interest has been stimulated by the observation of waves in several fields: tumor growth, population dynamics, ecology, epidemiology, biological invasions, as well as the spread of flames, chemical waves, etc. They are also used to describe the interaction between molecular diffusion, local growth and saturation. Thus, travelling waves remain a common phenomenon in multiple branches of knowledge, and are considered as solutions of PDEs that propagate with a constant speed, while maintaining their shape in space.

Biology and ecology are key areas of many studies of wave propagation. In fact, most of epizootic waves as well as cell invasion mechanisms and chemotaxis were investigated using reaction-diffusion equations, mainly the Fisher-KPP. Many authors have shown the existence of travelling wave solutions in such equations and revealed more information concerning their properties such as wave speed, stability and asymptotic behaviour. Against this background, the interactions and interchanges of information that describe prey-predator relationships have been incorporated into coherent mathematical models (i.e. [62]). The development of tumor cells was also the subject of many research papers (i.e. [103, 112]) and many studies were conducted on chemotaxis systems (i.e. [106]).

In many cases of the spread of any biological quantity, diffusion plays a crucial role. The standard diffusion equation in one space dimension is of the form

$$\frac{\partial u}{\partial t} = D\frac{\partial^2 u}{\partial x^2}, \tag{5.1}$$

for a chemical of concentration u, and diffusion constant D. In contrast to simple diffusion, when reaction kinetics and diffusion are coupled, travelling waves of chemical concentration can exist. These travelling waves can affect a biochemical change much faster than the diffusion processes governed by equation (5.1). The general form of a reaction-diffusion equation, in a one-dimensional scalar case, is

$$\frac{\partial u}{\partial t} = f(u) + D\frac{\partial^2 u}{\partial x^2}, \tag{5.2}$$

where $f(u)$ represents the reaction kinetics. One classic case of equation (5.2) is

$$\frac{\partial u}{\partial t} = ku(1-u) + D\frac{\partial^2 u}{\partial x^2}, \tag{5.3}$$

where k is a reaction rate. This equation was suggested by Fisher and is now referred to as the Fisher's equation.

A travelling wave is a wave which travels without change of shape, and so if a solution $u(x,t)$ represents a travelling wave, and the speed of propagation of this shape is a constant (denote by c), it will be of the form

$$u(x,t) = u(x-ct). \tag{5.4}$$

If we set $Z = x - ct$ we see that

$$\frac{\partial u}{\partial t} = -c\frac{du}{dZ}, \quad \frac{\partial u}{\partial x} = \frac{du}{dZ},$$

and so for the diffusion equation (5.1) we see that

$$D\frac{d^2u}{dZ^2} + c\frac{du}{dZ} = 0 \Rightarrow u(Z) = A + Be^{(-cZ/D)},$$

where A and B are integration constants. However, if u has to be bounded for all Z, B must be zero, and $u(Z) = A$ is not a wave solution. However, travelling wave solutions can be found in equation (5.2), depending on the form of the term $f(u)$.

In this chapter, we generalise the integer Fisher's equation that was studied by Fisher (1937) and prove that there are travelling wave solutions. In Section 5.3, we generalise an integer SIR model with spatial heterogeneity for random motion of rabid foxes that was studied by Murray [117]. In Section 5.4, we consider generalised space-time fractional SIR models and apply the (G'/G)-expansion method for finding travelling wave solutions using Jumarie's modified Riemann-Liouville derivative. A fractional transformation of coordinates has been utilised to convert the fractional order PDEs to ODEs.

5.2 Travelling Wave Solutions for Fisher's Equation

In the late 1930s, Kolmogorov, Petrovskii and Piskunov [95] were the first to investigate travelling wave solutions of a propagation model derived to describe gene evolution. Well ahead of its time, their work is the founding article on travelling wave theory in reaction-diffusion systems. Fisher [61] also introduced a model for the frequency of a new advantageous recessive gene in a diploid population, although this equation was first introduced by Fisher in [142]. He established that this equation would have a solution in the form of a travelling wave with steady speed. Kolmogorov, Petrovskii and Piskunov then verified the same result and extended their study to the long-term behaviour of the model. The integer Fisher's equation has the form,

$$\frac{\partial u}{\partial t} = ku(1-u) + D\frac{\partial^2 u}{\partial x^2}, \tag{5.5}$$

where k and D are positive parameters.

Since the time of Fisher, this equation has been used and extended by a large number of researchers. Here we highlight a few examples of these extensions but many more are provided in the review by Feng [56]. In terms of modified forms of Fisher's equation, authors have studied the stochastically perturbed Fisher's equation (i.e. [39]), Fisher's equation with cut-off parameter (i.e. [146]) where solutions were found for every considered value of the cut-off, and one-sided Fisher's equation (i.e. [94]). Other authors considered non-local version of Fisher's equation (i.e. [119, 167]), versions with time delay (i.e. [102, 182]) and other kinds of modified Fisher's equation (i.e. [139]). In terms of novel analytic methods, authors considered the Lie symmetry method (i.e. [56]), deployment of commutative ring theory (i.e. [57]) and the complex method (i.e. [171, 172]). Probabilistic approaches were also adopted to study travelling wave solutions of Fisher's equation (i.e.[73, 74]). In [40], a new modelling approach was studied, in which Fisher's equation was considered as a kinetic transport model. Other authors showed a particular interest in investigating characteristics of travelling wave profiles (i.e. [59, 60]).

Numerical approaches have been used to investigate travelling wave solutions of Fisher's equation. These works were based on a variety of computational approaches including finite difference and finite element methods. Establishing accurate and efficient numerical representation of solutions was the key element of the research. In [178], this problem was tackled using the discrete singular convolution (DSC) algorithm as a unified feature for studying Fisher's equation. In fact, the resulting DSC algorithm is a crucial computationally feasible method to predict the long-term behaviour of the travelling wave.

In the next section, we will consider the integer Fisher's equation (5.5), repeating the classical analysis of the stability of travelling waves [117]. In section 5.2.2 we then consider a fractional form of Fisher's equation, showing that a classical solution of the integer equation can be transformed to a solution of the fractional Fisher's equation.

5.2.1 Travelling Wave Solutions for Integer Fisher's Equation

In this section, we will consider the integer Fisher's equation (5.5), which after suitable non-dimensionalisation

$$t^* = kt, \quad x^* = x\Big(\frac{k}{D}\Big)^{\frac{1}{2}}, \tag{5.6}$$

becomes

$$\frac{\partial u}{\partial t} = u(1-u) + \frac{\partial^2 u}{\partial x^2}. \tag{5.7}$$

In the spatially homogeneous situation, the steady states are $u = 0$ and $u = 1$, which suggests that we should look for solutions (5.7) for which $0 \leq u \leq 1$. Indeed negative values of u often have no physical meaning. Using the substitution $Z = x - ct$, equation (5.7) becomes

$$u'' + cu' + u(1-u) = 0, \tag{5.8}$$

where $'$ denotes d/dZ.

A typical wave solution will be where u at one extreme, say as $Z \to -\infty$, is at one steady state and as $Z \to \infty$ it is at the other. We therefore have an eigenvalue problem to determine the value, or values, of c such that a nonnegative solution u of equation (5.8) exists and which satisfies

$$\lim_{Z\to\infty} u(Z) = 0, \quad \lim_{Z\to-\infty} u(Z) = 1. \tag{5.9}$$

By studying equation (5.8) for u in the (u, v) phase plane where

$$u' = v, \quad v' = -cv - u(1-u), \tag{5.10}$$

we see that the stability of the two equilibrium points for (u, v), namely, $(0, 0)$ and $(1, 0)$, is determined by the Jacobian, J, given by

$$J = \begin{pmatrix} \dfrac{\partial f}{\partial u} & \dfrac{\partial f}{\partial v} \\ \\ \dfrac{\partial g}{\partial u} & \dfrac{\partial g}{\partial v} \end{pmatrix} = \begin{pmatrix} 0 & 1 \\ -1+2u & -c \end{pmatrix}. \tag{5.11}$$

At the equilibrium point $(0, 0)$ we find the eigenvalues of the Jacobian

$$det(J - \lambda I) = det \begin{pmatrix} -\lambda & 1 \\ -1 & -c-\lambda \end{pmatrix} = \lambda^2 + c\lambda + 1 = 0, \tag{5.12}$$

so that

$$\lambda_\pm = \frac{-c \pm \sqrt{c^2 - 4}}{2}. \tag{5.13}$$

If $c^2 < 4$, then the eigenvalues λ are complex and hence the point $(0, 0)$ is a stable spiral. However, travelling waves are not possible in the case of a stable spiral since in this situation the quantity I would oscillate between positive and negative values. Since I must be non-negative to remain physical, this case does not correspond to a physically realistic travelling wave. However, if $c^2 \geq 4$, then the eigenvalues λ are both real and negative, so $(0, 0)$ is a stable node and travelling

wave solutions are possible.

At the equilibrium point $(1, 0)$, the eigenvalues are derived from

$$det(J - \lambda I) = det \begin{pmatrix} -\lambda & 1 \\ 1 & -c - \lambda \end{pmatrix} = \lambda^2 + c\lambda - 1 = 0, \tag{5.14}$$

so that

$$\lambda_{\pm} = \frac{-c \pm \sqrt{c^2 + 4}}{2}, \tag{5.15}$$

which are always real with one positive and one negative. The point $(1, 0)$ is therefore a saddle point.

A travelling wave with the wave travelling from the region where $u = 0$ to the region where $u = 1$ is therefore possible for $c^2 \geq 4$. However, it is only for a few special cases of the equation and the initial conditions that an analytic form of the solution is known. In the next section we consider one of these examples.

5.2.2 Travelling Wave Solutions for Space-Time Fractional Fisher's Equation

In this section we generalise the non-dimensionalised Fisher's equation (5.7) by the following space-time fractional differential equation,

$$\frac{\partial^{\alpha} u}{\partial t^{\alpha}} = u(1 - u) + \frac{\partial^{2\beta} u}{\partial x^{2\beta}}, \tag{5.16}$$

where $0 < \alpha, \beta \leq 1$, are the fractional orders of the Jumarie's modified Riemann-Liouville time and space derivatives defined in Definition (2.2.5) respectively. We seek travelling wave solutions with the following transformation

$$Z = \frac{x^{\beta}}{\Gamma(\beta + 1)} - \frac{ct^{\alpha}}{\Gamma(\alpha + 1)}, \tag{5.17}$$

with the particular initial condition $u(x, 0) = \left(1 + e^{x^{\beta}/\sqrt{6}\Gamma(\beta+1)}\right)^{-2}$. This initial condition has been selected to allow a simple solution, but it is expected that a travelling wave would also emerge for a general initial condition. Equation (5.16) can then be written as

$$\frac{\partial^2 u}{\partial Z^2} + c\frac{\partial u}{\partial Z} + u(1 - u) = 0, \tag{5.18}$$

and from [5], the solution is

$$u(Z) = \frac{1}{(1 + e^{Z/\sqrt{6}})^2}, \tag{5.19}$$

if $c = 5/\sqrt{6} \cong 2.04$. Therefore, the solution of equation (5.16) is

$$u(x,t) = \left(1 + e^{\frac{1}{\sqrt{6}}\left(\frac{x^\beta}{\Gamma(\beta+1)} - \frac{ct^\alpha}{\Gamma(\alpha+1)}\right)}\right)^{-2}. \tag{5.20}$$

Figure 5.1(a) shows the solution $u(Z)$, which is also equivalent to the initial condition $u(x,0)$ as a function of x. The transition from the solution $u = 1$ for $Z \to -\infty$ and $u = 0$ for $Z \to \infty$ is clear. In Figure 5.1(b) we have plotted $u(x,t)$ for $t = 2$ and for different values of α and β. If we set $u = 1/2$ to be the mid-point of the travelling wave, where $Z = \sqrt{6}\ln(\sqrt{2}-1)$, then we can also consider the slope of the wave front at that point. See Figure 5.1(c).

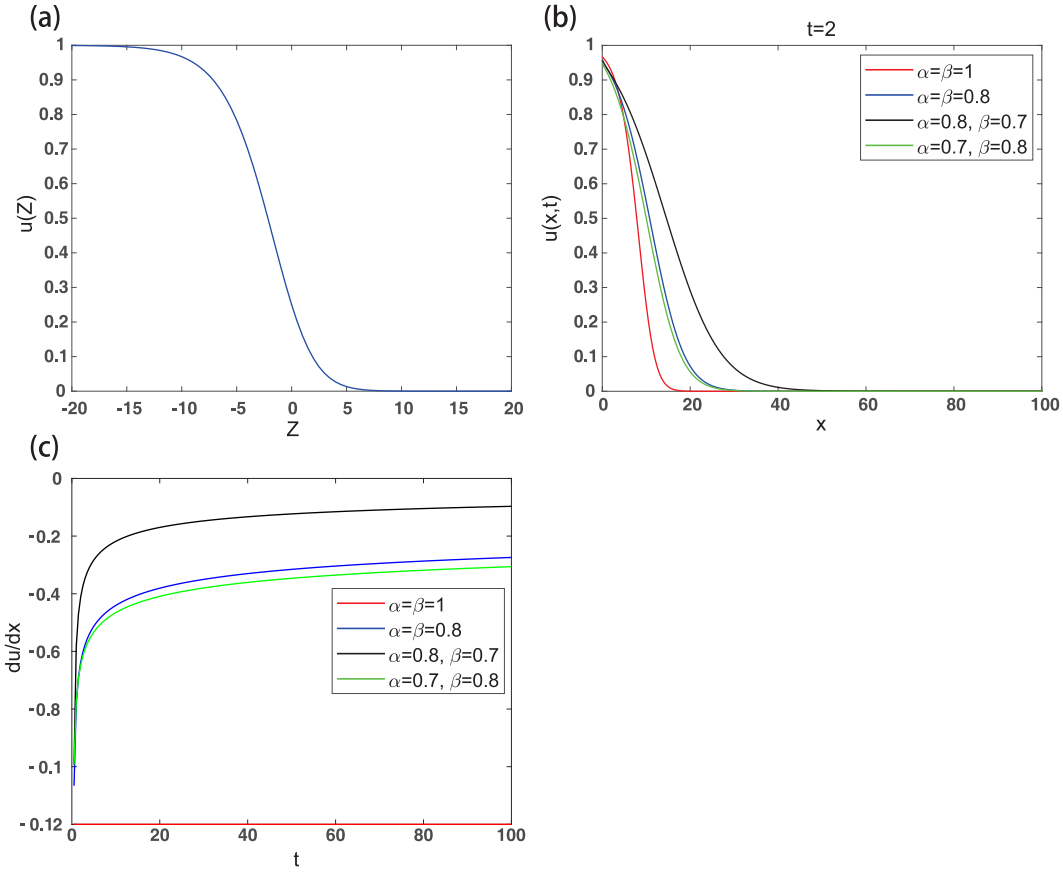

Figure 5.1: (a) The solution $u(Z)$ of Fisher's equation. (b) The solution $u(x,t)$ when $t = 2$ for different values of α and β. (c) The slope of $u(x,t)$ at the point $Z = \sqrt{6}\ln(\sqrt{2}-1)$ (the mid-point of the wave) for different values of α and β.

From Figure 5.1(b) we see that, for a fixed time t, the position of the center of the travelling wave, i.e. the point where $u = 1/2$, $Z = \sqrt{6}\ln(\sqrt{2}-1)$, is dependent

on both α and β. We can find the location of the center of the travelling wave by setting $Z = \sqrt{6}\ln(\sqrt{2}-1)$ in (5.17) to obtain

$$x(t) = \left(\Gamma(\beta+1)\Big(\sqrt{6}\ln(\sqrt{2}-1) + \frac{ct^{\alpha}}{\Gamma(\alpha+1)}\Big)\right)^{\frac{1}{\beta}}. \tag{5.21}$$

We can also calculate the speed of the travelling wave through the derivative of $x(t)$

$$v(t) = \frac{dx}{dt} = \frac{1}{\beta}\left(\left(\sqrt{6}\ln(\sqrt{2}-1) + \frac{ct^{\alpha}}{\Gamma(\alpha+1)}\right)\Gamma(\beta+1)\right)^{\frac{1}{\beta}-1}\left(\frac{c\alpha t^{\alpha-1}}{\Gamma(\alpha+1)}\Gamma(\beta+1)\right). \tag{5.22}$$

We plot $x(t)$ as a function of time for different α and β in Figure 5.2 (a, c, e). Figure 5.2 (b, d, f) shows the speeds $v(t)$ of the situations in Figure 5.2 (a, c, e) . In Figure 5.2(b) we see that for $\alpha = \beta$, the speed of the travelling wave increases as time increases and then tends to constant speed, and that speed increases as $\alpha = \beta$ decreases. In Figure 5.2 (d, f) we see that, if $\alpha > \beta$, the speed of the travelling wave increases as time increases whereas for $\alpha < \beta$, the speed of the travelling wave decreases. This critical dependence on the sign of $\alpha - \beta$ is unexpected. The fractional order α may be linked to a memory effect and β is often used to describe multiscale inhomogeneity in space. That the difference $\alpha - \beta$ may determine if the travelling wave accelerates or decelerates is interesting and would be worthy of further investigation, both experimental and theoretical.

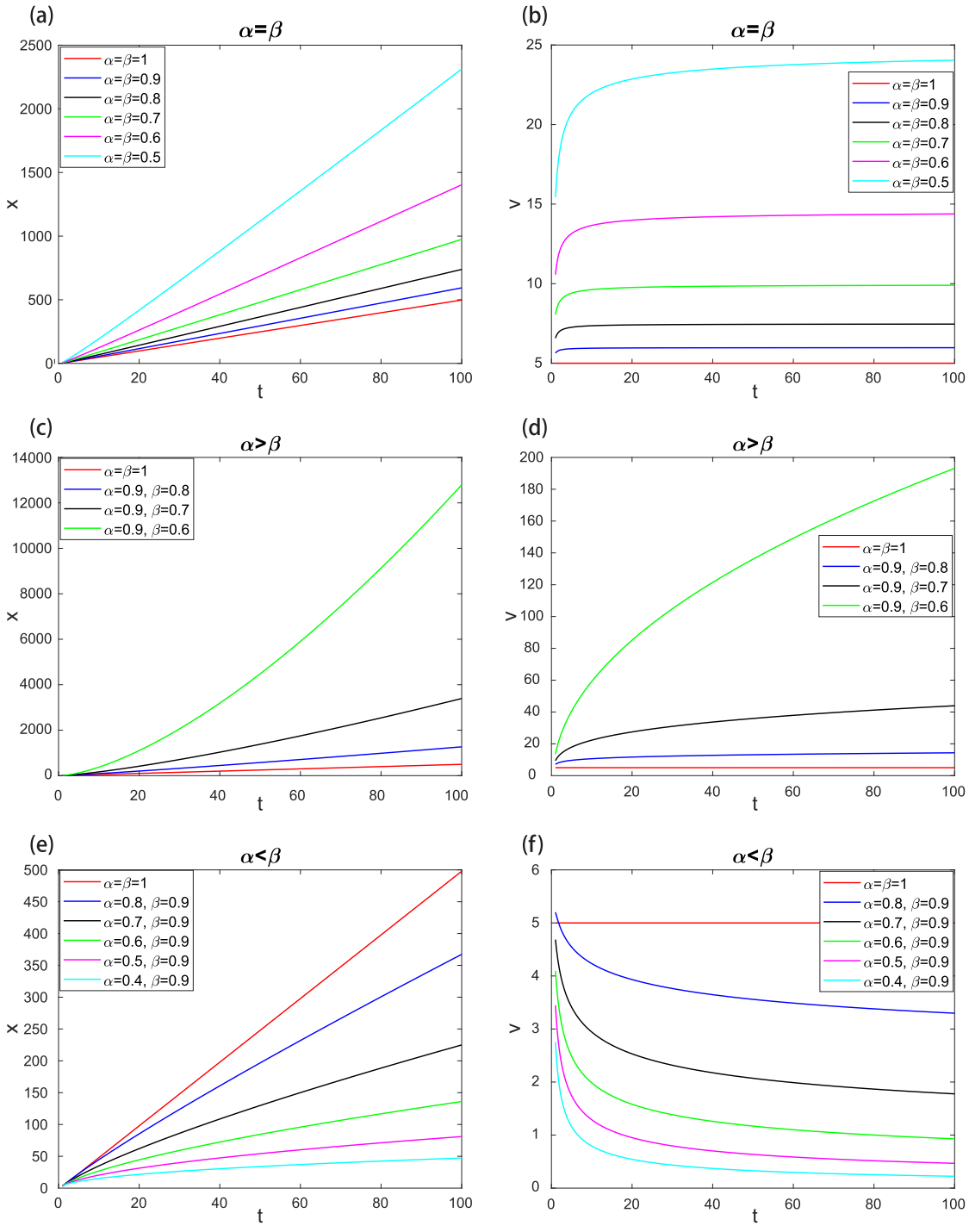

Figure 5.2: (a), (c) and (e) are the locations $x(t)$ of the travelling wave when $\alpha = \beta$, $\alpha > \beta$, $\alpha < \beta$ respectively. (b), (d) and (f) are the speeds of the travelling wave when $\alpha = \beta$, $\alpha > \beta$, $\alpha < \beta$ respectively.

5.3 Travelling Waves Solutions for SIR Models

As discussed in Chapter 2, SIR models are used in epidemiology to predict the behaviour of an infectious disease within a population. This type of model was first introduced by Kermack and McKendrik [90] in the form of a reaction-diffusion system with three compartments, susceptible individuals, S, infected individuals, I, and recovered individuals, R. Each one of these variables refers to a specific part of the total population and their size may fluctuate over time.

The dynamics of SIR models have been explored extensively and considerable progress has been achieved to understand and predict the spread of diseases. In terms of delay in travelling waves in SIR models, Wang and Wu [160] analysed the general SIR model with a time delay to investigate existence and non-existence of travelling wave solutions to show whether a disease can spread. Time delay effects on the minimum wave speed was also considered in [99]. Minimum wave speed in a diffusive non-local model was also a subject of studies done by Bo et al. [24], where they considered a system of differential equations with non-local delays and proved the existence of travelling wave solutions. More recently, Wu and Zhou [166] considered the effect of non-local delayed transmission on diffusive SIR models with a standard incidence rate. Many authors established the existence of travelling wave solutions and studied their asymptotic behaviour by using Schauder's fixed point theorem (i.e.[98, 159, 166, 168]).

In this section, we consider a relatively standard integer SIR model with spatial heterogeneity, and first show that there are travelling wave solutions for this model. We then generalise this integer SIR model to be a space-time fractional SIR model and consider new solutions, and the effects of the fractional derivative orders.

5.3.1 Travelling Wave Solutions for an Integer SIR Model

SIR model for the spread of rabies in foxes, which included a model of random movement of infected foxes is given in [117],

$$\frac{\partial S}{\partial t} = -rIS, \tag{5.23}$$

$$\frac{\partial I}{\partial t} = D\frac{\partial^2 I}{\partial x^2} + rIS - aI, \tag{5.24}$$

$$\frac{\partial R}{\partial t} = aI, \tag{5.25}$$

where it is assumed that infected foxes move in a one-dimensional spatial domain $x \in (-\infty, \infty)$. Applying the non-dimensionalisation,

$$I_* = \frac{I}{S_0}, \quad S_* = \frac{S}{S_0}, \quad x = \sqrt{\frac{D}{rS_0}}x, \quad t_* = rS_0 t, \quad \lambda = \frac{a}{rS_0}, \tag{5.26}$$

Since the S and I equations do not involve R we may consider the solutions to only the first two equations,

$$\frac{\partial S}{\partial t} = -IS, \tag{5.27}$$

$$\frac{\partial I}{\partial t} = \frac{\partial^2 I}{\partial x^2} + I(S - \lambda). \tag{5.28}$$

Then, we seek travelling wave solutions with

$$S(x,t) = S(Z), I(x,t) = I(Z), \tag{5.29}$$

where $Z = x - ct$ and $c > 0$ is the wave speed. Substituting into (5.27) and (5.28) gives

$$cS' - IS = 0, \tag{5.30}$$

$$cI' + I'' + I(S - \lambda) = 0. \tag{5.31}$$

We now assume that $S \to 1$, $I \to 0$, as $Z \to \infty$ and $S \to 0$, $I \to 0$, as $Z \to -\infty$, so that we move from a state with no infections $(S, I) = (1, 0)$ to a state where, after the whole population has become infected and then recovered, we have everyone recovered so that $(S, I) = (0, 0)$.
Linearising (5.31) about $S = 1$ and $I = 0$ we obtain

$$I'' + cI' + I(1 - \lambda) = 0, \tag{5.32}$$

and consider the stability of the $(S, I) = (1, 0)$ state. Setting $v = I'$ we see that (5.32) is equivalent to the system $v = I'$, $v' = -cv - I(1 - \lambda)$, and the Jacobian is then

$$J = \begin{bmatrix} 0 & 1 \\ \lambda - 1 & -c \end{bmatrix}.$$

The eigenvalues of the Jacobian are found to be

$$\mu = \frac{-c \pm \sqrt{c^2 - 4(1 - \lambda)}}{2},$$

so that if $\lambda > 1$, we have one positive real μ and one negative real μ so that the state $(S, I) = (1, 0)$ is unstable;
if $\lambda < 1$ and $c < 2\sqrt{1 - \lambda}$, we have $\mu = -c/2 \pm iM$ and hence the equilibrium point is a stable spiral;

if $\lambda < 1$ and $c > 2\sqrt{1-\lambda}$, we have $\mu = -c/2 \pm M$ with $M < c/2$ and hence the equilibrium point is a stable node;
if $\lambda < 1$ and $c = 2\sqrt{1-\lambda}$, we have $\mu = -\sqrt{1-\lambda}$ and hence the equilibrium point is a stable node.
Therefore, a travelling wave solution exists for $\lambda < 1$ and wave speeds, $c \geq 2\sqrt{1-\lambda}$.

We will now consider the possible existence of travelling wave solutions in fractional derivative SIR models, i.e. one where there is a form of memory, modelled by the fractional derivative in time, and possibly multiscale spatial effects modelled by fractional derivative in space coordinates.

5.3.2 Travelling Wave Solutions for Space-Time Fractional SIR Models

Additional spatial gradients can be included in both the susceptible and infected populations. For instance, in [117] the following system is shown to exhibit travelling waves,

$$\begin{aligned} \frac{\partial S}{\partial t} &= \frac{\partial^2 S}{\partial x^2} - IS, \\ \frac{\partial I}{\partial t} &= \frac{\partial^2 I}{\partial x^2} + I(S-\lambda). \end{aligned}$$

We might first consider a fractional form of these equations by replacing all time derivatives by Caputo derivatives of order $\alpha < 1$,

$$\begin{aligned} \frac{\partial^\alpha S}{\partial t^\alpha} &= \frac{\partial^2 S}{\partial x^2} - IS, \\ \frac{\partial^\alpha I}{\partial t^\alpha} &= \frac{\partial^2 I}{\partial x^2} + I(S-\lambda). \end{aligned} \tag{5.33}$$

We can now seek travelling wave solutions with $S(x,t) = S(Z)$, $I(x,t) = I(Z)$, with

$$Z = x - ct^\alpha/\Gamma(\alpha+1), \tag{5.34}$$

where $c > 0$ is the wave speed, and use the same boundary conditions as before. The model is then written as

$$c\frac{d^\alpha S}{dZ^\alpha} + \frac{d^2 S}{dZ^2} - IS = 0, \tag{5.35}$$

$$c\frac{d^\alpha I}{dZ^\alpha} + \frac{d^2 I}{dZ^2} + I(S-\lambda) = 0. \tag{5.36}$$

Linearising equation (5.36) about $S = 1$ and $I = 0$ we get

$$c\frac{d^\alpha I}{dZ^\alpha} + \frac{d^2 I}{dZ^2} + I(1-\lambda) \;=\; 0. \tag{5.37}$$

As before the stability of the solution is determined from the eigenvalues, μ, of the associated Jacobian leading to

$$c\mu^\alpha + \mu^2 + (1-\lambda) \;=\; 0. \tag{5.38}$$

There are travelling wave solutions for the system if this equilibrium point is a stable node, which implies the solutions of (5.38) are real and negative, i.e. $\mu = -R$, for $R \in \mathbb{R}$, $R > 0$, so that

$$c(-1)^\alpha (R)^\alpha + (R)^2 + (1-\lambda) \;=\; 0.$$

However, for real solutions we must have $(-1)^\alpha$ real, which implies $\alpha = 0, \pm 1, \pm 2, ...$, i.e. α is not a fractional order, and so there are no travelling wave solutions.

If we additionally include fractional spatial derivatives the situation changes. When

$$\begin{aligned} \frac{\partial^\alpha S}{\partial t^\alpha} &= \frac{\partial^{2\beta} S}{\partial x^{2\beta}} - IS, \\ \frac{\partial^\alpha I}{\partial t^\alpha} &= \frac{\partial^{2\beta} I}{\partial x^{2\beta}} + I(S-\lambda), \end{aligned} \tag{5.39}$$

we can seek travelling wave solutions with $S(x,t) = S(Z)$, $I(x,t) = I(Z)$, where

$$Z = \frac{x^\beta}{\Gamma(\beta+1)} - \frac{ct^\alpha}{\Gamma(\alpha+1)}, \tag{5.40}$$

where $c > 0$ is the wave speed. The model can then be written as

$$c\frac{d^\alpha S}{dZ^\alpha} + \frac{d^{2\beta} S}{dZ^{2\beta}} - IS \;=\; 0, \tag{5.41}$$

$$c\frac{d^\alpha I}{dZ^\alpha} + \frac{d^{2\beta} I}{dZ^{2\beta}} + I(S-\lambda) \;=\; 0. \tag{5.42}$$

Again, linearising equation (5.42) about $S = 1$ and $I = 0$ we get

$$c\frac{d^\alpha I}{dZ^\alpha} + \frac{d^{2\beta} I}{dZ^{2\beta}} + I(1-\lambda) \;=\; 0, \tag{5.43}$$

and so the eigenvalues, μ, of the Jacobian satisfy

$$c\mu^\alpha + \mu^{2\beta} + (1-\lambda) \;=\; 0. \tag{5.44}$$

The equilibrium point will be a stable node when $\mu = -R$, for $\mathbb{R} \in R$, $R > 0$, so that

$$c(-1)^{\alpha}(R)^{\alpha} + (-1)^{2\beta}(R)^{2\beta} + (1-\lambda) = 0.$$

Setting $(-1)^{\alpha} = e^{i\alpha\pi} = \cos(\alpha\pi) + i\sin(\alpha\pi)$, and $(-1)^{2\beta} = e^{2i\beta\pi} = \cos(2\beta\pi) + i\sin(2\beta\pi)$, we therefore have two equations

$$\begin{aligned} cR^{\alpha}\cos(\alpha\pi) + R^{2\beta}\cos(2\beta\pi) + (1-\lambda) &= 0, \\ cR^{\alpha}\sin(\alpha\pi) + R^{2\beta}\sin(2\beta\pi) &= 0. \end{aligned}$$

Solving these two equations together, we find the conditions for travelling waves solutions are

$$\begin{aligned} R &= \Big(\frac{(\lambda-1)\sin(\alpha\pi)}{\sin((\alpha+2\beta)\pi)}\Big)^{\frac{1}{2\beta}}, \\ c &= -\frac{\sin(2\beta\pi)}{\sin(\alpha\pi)}\Big(\frac{(\lambda-1)\sin(\alpha\pi)}{\sin((\alpha+2\beta)\pi)}\Big)^{1-\frac{\alpha}{2\beta}}. \end{aligned}$$

In the next section we will consider specific forms of the travelling wave solutions of the form of (5.40).

5.4 Travelling Wave Solutions by using the (G'/G)-Expansion Method

Nonlinear evolution equations, such as those found in SIR models, are often found in descriptions of physical systems, and finding exact solutions of these evolution equations is essential to understanding the behaviour of the physical systems. A large number of methods for finding solutions have been proposed and we list these here for further reference: the (G'/G)-expansion method and the new generalised (G'/G)-expansion method (i.e. [7, 11, 19, 23, 155, 170]), the sub-equation method and the modified sub-equation method (i.e. [13, 18, 114, 176]), the modified simple equation method (i.e. [87, 88, 169, 173, 174]), the modified Kudryashov method (i.e. [51, 79]), the Exp-function method and the generalised Exp-function method (i.e. [20, 179]), the functional variable method (i.e. [34]), the first integral method (i.e. [1]), the modified trial equation method (i.e. [28]), the Jacobi elliptic function expansion method (i.e. [101, 143]), the homotopy perturbation method (i.e. [65]), the tanh-function method and the modified extended tanh method (i.e. [122, 140]), the sine-cosine method (i.e. [9]), the variational iteration method (i.e. [80]), the spline collocation method (i.e. [10]), the solitary wave ansatz method (i.e. [71]), the Fourier transform method (i.e. [121]), the Q-function method (i.e. [36, 37]),

as well as the Khater method (i.e. [91]).

In this section we first consider the generalised space-time fractional SIR model in Section (5.4.1),

$$\frac{\partial^\alpha S}{\partial t^\alpha} = -IS, \tag{5.45}$$

$$\frac{\partial^\alpha I}{\partial t^\alpha} = \frac{\partial^{2\beta} I}{\partial x^{2\beta}} + I(S - \lambda_1), \tag{5.46}$$

where the spatial derivative is present only in the infected fox population and where $0 < \alpha, \beta \leq 1$, are the fractional orders of Jumarie's modified Riemann-Liouville time and space derivatives defined in Definition (2.2.5) respectively. We introduce the G'/G-expansion method using this system of equations, although, as we see below, we eventually find that no travelling wave solutions are possible.

We then consider the generalised space-time fractional SIR model in Section (5.4.2)

$$\frac{\partial^\alpha S}{\partial t^\alpha} = \frac{\partial^{2\beta} S}{\partial x^{2\beta}} - IS, \tag{5.47}$$

$$\frac{\partial^\alpha I}{\partial t^\alpha} = \frac{\partial^{2\beta} I}{\partial x^{2\beta}} + I(S - \lambda_1), \tag{5.48}$$

where the spatial derivative is present in both the susceptible and infected fox populations and using the G'/G-expansion method, we find forms of the travelling wave solutions.

The form of fractional derivative, that of Jumarie [84], is used for two important properties: firstly that the derivative of a constant is zero, so that stability of equilibria can be easily undertaken, which is not possible with the Riemann-Liouville derivative; and secondly so that the later introduction of a travelling coordinate does not introduce space-dependent terms, which the Caputo derivative would.

5.4.1 The First Generalised Space-Time Fractional SIR Model

Considering first the system of equations (5.45) and (5.46), we again use the substitute (5.40) to obtain

$$cS' - IS = 0, \tag{5.49}$$

$$I'' + cI' + I(S - \lambda_1) = 0, \tag{5.50}$$

and will now use the G'/G-expansion method described in Section 2.7.

We now suppose that the solutions for S and I can be expressed as

$$S(Z) = \sum_{i=0}^{m_1} \alpha_i \left(\frac{G'}{G}\right)^i,$$

$$I(Z) = \sum_{i=0}^{m_2} \beta_i \left(\frac{G'}{G}\right)^i,$$

where $G = G(Z)$ satisfies $G'' + \lambda G' + \mu G = 0$ and where α_i, β_i, and c are arbitrary constants. By calculating the homogeneous balance between the highest order derivatives and nonlinear term in the equations (5.50), we find that $m_1 = 2$ and $m_2 = 1$, so that

$$S(Z) = \alpha_0 + \alpha_1 \frac{G'}{G} + \alpha_2 \left(\frac{G'}{G}\right)^2, \tag{5.51}$$

$$I(Z) = \beta_0 + \beta_1 \frac{G'}{G}. \tag{5.52}$$

To determine these constants α_0, α_1, α_2, β_0, β_1 we substitute (5.51) and (5.52) into equations (5.49) and (5.50) and collect all the terms with the same power of (G'/G) to obtain

$$\begin{aligned}
-\alpha_0\beta_0 - c\alpha_1\mu &= 0,\\
-\alpha_0\beta_1 - \alpha_1\beta_0 - c\alpha_1\lambda - 2c\alpha_2\mu &= 0,\\
-\alpha_1\beta_1 - \alpha_2\beta_0 - c\alpha_1 - 2c\alpha_2\lambda &= 0,\\
-\alpha_2\beta_1 - 2c\alpha_2 &= 0,\\
\beta_1\lambda\mu - c\beta_1\mu + \alpha_0\beta_0 - \lambda_1\beta_0 &= 0,\\
\beta_1\lambda^2 + 2\beta_1\mu - c\beta_1\lambda + \alpha_0\beta_1 + \alpha_1\beta_0 - \lambda_1\beta_1 &= 0,\\
\beta_1\lambda - c\beta_1 + \alpha_1\beta_1 + \alpha_2\beta_0 &= 0,\\
\beta_1 + \alpha_2\beta_1 &= 0.
\end{aligned}$$

Solving these equations we find

$$\begin{aligned}
\beta_0 &= -\lambda c - c^2, \quad \beta_1 = -2c, \quad \lambda_1 = 0, \quad \mu = (\lambda^2 - c^2)/4,\\
\alpha_0 &= (-\lambda^2 + 2c\lambda - c^2)/2, \quad \alpha_1 = -2\lambda + 2c, \quad \alpha_2 = -2.
\end{aligned}$$

From solving $G''(Z) + \lambda G'(Z) + \mu G(Z) = 0$, we have

$$\frac{G'}{G} = \frac{-\lambda}{2} + \frac{\sqrt{\lambda^2 - 4\mu}}{2}\left(\frac{C_1 \sinh\left(Z\sqrt{\lambda^2 - 4\mu}/2\right) + C_2 \cosh\left(Z\sqrt{\lambda^2 - 4\mu}/2\right)}{C_1 \cosh\left(Z\sqrt{\lambda^2 - 4\mu}/2\right) + C_2 \sinh\left(Z\sqrt{\lambda^2 - 4\mu}/2\right)}\right), \tag{5.53}$$

where C_1 and C_2 are integration constants, but since $\lambda^2 - 4\mu = c^2 > 0$ we have

$$\frac{G'}{G} = \frac{-\lambda}{2} + \frac{c}{2}\left(\frac{C_1 \sinh\Big(Zc/2\Big) + C_2 \cosh\Big(Zc/2\Big)}{C_1 \cosh\Big(Zc/2\Big) + C_2 \sinh\Big(Zc/2\Big)}\right). \tag{5.54}$$

Substituting (5.54) into (5.51) and (5.52), we have

$$\begin{aligned} S(Z) &= c^2\Bigg(\left(\frac{C_1 \sinh(cZ/2) + C_2 \cosh(cZ/2)}{C_1 \cosh(cZ/2) + C_2 \sinh(cZ/2)}\right) - \\ &\quad \frac{1}{2}\left(\frac{C_1 \sinh(cZ/2) + C_2 \cosh(cZ/2)}{C_1 \cosh(cZ/2) + C_2 \sinh(cZ/2)}\right)^2 - \frac{1}{2}\Bigg), \end{aligned} \tag{5.55}$$

$$I(Z) = -c^2\left(1 + \left(\frac{C_1 \sinh(cZ/2) + C_2 \cosh(cZ/2)}{C_1 \cosh(cZ/2) + C_2 \sinh(cZ/2)}\right)\right). \tag{5.56}$$

With the initial conditions $S(0) = S_0$, $I(0) = I_0$, we have

$$S_0 = c^2\Big(\Big(\frac{C_2}{C_1}\Big) - \frac{1}{2}\Big(\frac{C_2}{C_1}\Big)^2 - \frac{1}{2}\Big), \tag{5.57}$$

$$I_0 = -c^2\Big(1 + \Big(\frac{C_2}{C_1}\Big)\Big), \tag{5.58}$$

and we can solve for the unknown constants, C_2/C_1 and c from which we can find four values for the wave speed c,

$$c = \pm\frac{1}{2}\sqrt{-S_0 - 2I_0 \pm \sqrt{S_0^2 + 4I_0 S_0}}, \tag{5.59}$$

However, since $\sqrt{S_0^2 + 4I_0 S_0} < S_0 + 2I_0$, all the values of c are complex, showing that no travelling wave solutions of this form are possible in this model.

5.4.2 The Second Generalised Space-Time Fractional SIR Model

We now consider the system of equations (5.47) and (5.48) in a similar way. After the transformation to the Z coordinate we have

$$S'' + cS' - IS = 0, \tag{5.60}$$

$$I'' + cI' + I(S - \lambda_1) = 0, \tag{5.61}$$

and suppose that the solutions can be expressed as polynomials of (G'/G). Calculating the homogeneous balance between the highest order derivatives and nonlinear term in the equations (5.61), then leads to $m_1 = m_2 = 2$, and so

$$S(Z) = \alpha_0 + \alpha_1 \frac{G'}{G} + \alpha_2 \left(\frac{G'}{G}\right)^2, \tag{5.62}$$

$$I(Z) = \beta_0 + \beta_1 \frac{G'}{G} + \beta_2 \left(\frac{G'}{G}\right)^2, \tag{5.63}$$

where α_0, α_1, α_2, β_0, β_1, β_2 and c are arbitrary constants. Substituting into equations (5.60) and (5.61) and collecting all terms with the same power of (G'/G), then gives

$$\begin{aligned}
\alpha_1\mu\lambda + 2\alpha_2\mu^2 - c\alpha_1\mu - \alpha_0\beta_0 = 0,\\
\alpha_1\lambda^2 + 6\alpha_2\lambda\mu + 2\alpha_1\mu - c\alpha_1\lambda - 2c\alpha_2\mu - \alpha_0\beta_1 - \alpha_1\beta_0 = 0,\\
3\alpha_1\lambda + 8\alpha_2\mu + 4\alpha_2\lambda^2 - c\alpha_1 - 2c\alpha_2\lambda - \alpha_0\beta_2 - \alpha_1\beta_1 - \alpha_2\beta_0 = 0,\\
2\alpha_1 + 10\alpha_2\lambda - 2c\alpha_2 - \alpha_1\beta_2 - \alpha_2\beta_1 = 0,\\
6\alpha_2 - \alpha_2\beta_2 = 0,\\
\beta_1\mu\lambda + 2\beta_2\mu^2 - c\beta_1\mu + \alpha_0\beta_0 - \lambda_1\beta_0 = 0,\\
\beta_1\lambda^2 + 6\beta_2\lambda\mu + 2\beta_1\mu - c\beta_1\lambda - 2c\beta_2\mu + \alpha_0\beta_1 + \alpha_1\beta_0 - \lambda_1\beta_1 = 0,\\
3\beta_1\lambda + 8\beta_2\mu + 4\beta_2\lambda^2 - c\beta_1 - 2c\beta_2\lambda + \alpha_0\beta_2 + \alpha_1\beta_1 + \alpha_2\beta_0 - \lambda_1\beta_2 = 0,\\
2\beta_1 + 10\beta_2\lambda - 2c\beta_2 + \alpha_1\beta_2 + \alpha_2\beta_1 = 0,\\
6\beta_2 + \alpha_2\beta_2 = 0.
\end{aligned}$$

Solving these equations we find $c = 5\lambda$, $\mu = \lambda_1 = \alpha_1 = \beta_0 = \beta_1 = 0$, $\beta_2 = 6$, $\alpha_0 = 6\lambda^2$ and $\alpha_2 = -6$. It should be noted here that a solution of this form is only possible if $\lambda_1 = 0$, i.e. if the susceptible population never recovers and therefore we assume that the disease remains dormant in the body. Since $\mu = 0$, so that $\lambda^2 - 4\mu = \lambda^2 = (c/5)^2 > 0$, we have $G = C_1 + C_2 e^{-cZ/5}$, and $(G'/G) = -cC_2 e^{-cZ/5}/\Big(5(C_1 + C_2 e^{-cZ/5})\Big)$. Substituting these into equations (5.62) and (5.63), we have

$$S(Z) = \frac{6c^2 C_1(C_1 + 2C_2 e^{-cZ/5})}{25(C_1 + C_2 e^{-cZ/5})^2}, \tag{5.64}$$

$$I(Z) = \frac{6c^2 C_2^2 e^{-2cZ/5}}{25(C_1 + C_2 e^{-cZ/5})^2}. \tag{5.65}$$

Note that $\lim_{Z\to\infty} S(Z) = 6c^2/25$, $\lim_{Z\to-\infty} S(Z) = 0$, $\lim_{Z\to\infty} I(Z) = 0$ and
$\lim_{Z\to-\infty} I(Z) = 6c^2/25$. Using the initial conditions $S(0) = S_0$, $I(0) = I_0$, then

$$S_0 = \frac{6c^2 C_1(C_1 + 2C_2)}{25(C_1 + C_2)^2}, \tag{5.66}$$

$$I_0 = \frac{6c^2C_2^2}{25(C_1+C_2)^2}, \tag{5.67}$$

and knowing that $S_0 + I_0 = 1$, allows us to solve the two equations and for C_2/C_1 and c^2, giving

$$\frac{C_2}{C_1} = \frac{I_0 \pm \sqrt{I_0}}{S_0}, \quad c^2 = \frac{25}{6}. \tag{5.68}$$

Two of the solutions above, those with $C_2/C_1 < 0$, lead to populations that contain singularities. However, there are still two possible travelling wave solutions of (G'/G) polynomial form,

$$S_{1,2}(Z) = \frac{S_0\left(S_0 + 2(I_0+\sqrt{I_0})e^{\pm Z/\sqrt{6}}\right)}{\left(S_0 + (I_0+\sqrt{I_0})e^{\pm Z/\sqrt{6}}\right)^2}, \tag{5.69}$$

$$I_{1,2}(Z) = \frac{(I_0+\sqrt{I_0})^2 e^{\pm 2Z/\sqrt{6}}}{\left(S_0 + (I_0+\sqrt{I_0})e^{\pm Z/\sqrt{6}}\right)^2}, \tag{5.70}$$

Figure 5.3 shows plots of these travelling wave solutions for $S_0 = I_0 = 0.5$, in Figure 5.3(a), the disease turned the susceptible (S decreased) into infectious (I increased), by moving the travelling wave to the left, and in Figure 5.3(b) the wave moves to the right.

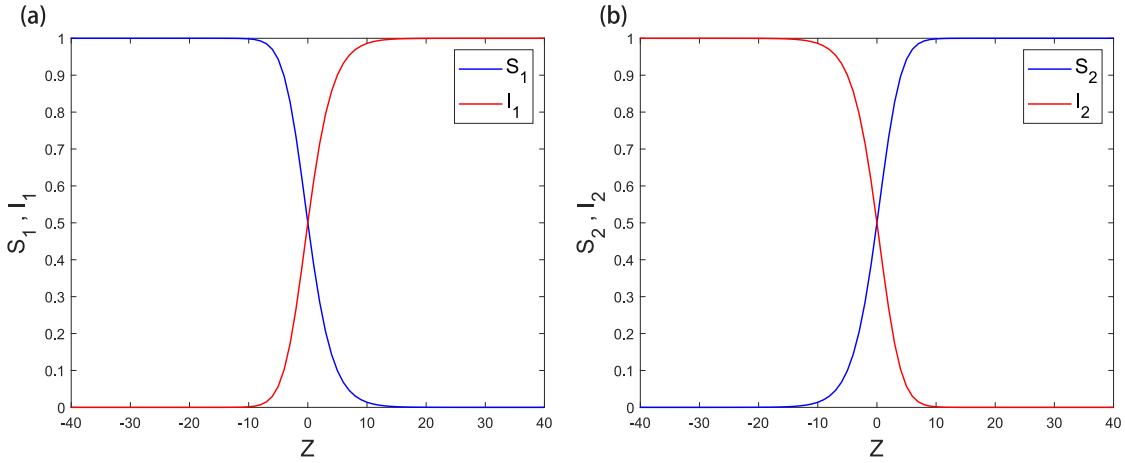

Figure 5.3: Plots of (a) S_1 and I_1 and (b) S_2 and I_2, the travelling wave solutions in eqs (5.69) and (5.70), when $S_0 = I_0 = 0.5$.

Without loss of generality, we now consider only the solution S_2, I_2, the travelling wave moving in the positive Z direction. If we define the location of the travelling wave front, $x = x_{\rm f}$, as the point at which $S_2 = I_2 = 0.5$, then we find

$$Z = -\sqrt{6}\ln\left((1+\sqrt{2})\left(\frac{1}{\sqrt{I_0}} - 1\right)\right), \tag{5.71}$$

and the location of the travelling wave front is

$$x_{\rm f} = \left(\frac{5\Gamma(\beta+1)}{\sqrt{6}\Gamma(\alpha+1)}t^{\alpha} - \sqrt{6}\Gamma(\beta+1)\ln\left((1+\sqrt{2})\left(\frac{1}{\sqrt{I_0}}-1\right)\right)\right)^{\frac{1}{\beta}}. \quad (5.72)$$

We note here that, due to the fractional derivative being defined only for $x > 0$, i.e. we assume that in the region $x < 0$ the S and I populations are constant, the expression in eq. (5.72) is also only defined for $x_{\rm f} > 0$. The plots of the location $x_{\rm f}$ of the travelling wave front are shown in Figure 5.4 (a), (c) and (e).

The speed and acceleration of the travelling wave front (S_2, I_2), are therefore

$$\begin{aligned}
v_{\rm f}(t) &= \frac{1}{\beta}\frac{5\alpha\Gamma(\beta+1)}{\sqrt{6}\Gamma(\alpha+1)}t^{\alpha-1}\left(\frac{5\Gamma(\beta+1)}{\sqrt{6}\Gamma(\alpha+1)}t^{\alpha} - \sqrt{6}\Gamma(\beta+1)\ln\left((1+\sqrt{2})\left(\frac{1}{\sqrt{I_0}}-1\right)\right)\right)^{\frac{1}{\beta}-1},\\
a_{\rm f}(t) &= \frac{1}{\beta}\frac{5\alpha(\alpha-1)\Gamma(\beta+1)}{\sqrt{6}\Gamma(\alpha+1)}t^{\alpha-2}\left(\frac{5\Gamma(\beta+1)}{\sqrt{6}\Gamma(\alpha+1)}t^{\alpha} - \sqrt{6}\Gamma(\beta+1)\times\right.\\
&\quad \left.\times\ln\left((1+\sqrt{2})\left(\frac{1}{\sqrt{I_0}}-1\right)\right)\right)^{\frac{1}{\beta}-1} + \frac{1}{\beta}\left(\frac{1}{\beta}-1\right)\left(\frac{5\alpha\Gamma(\beta+1)}{\sqrt{6}\Gamma(\alpha+1)}t^{\alpha-1}\right)^{2}\\
&\quad \left(\frac{5\Gamma(\beta+1)}{\sqrt{6}\Gamma(\alpha+1)}t^{\alpha} - \sqrt{6}\Gamma(\beta+1)\ln\left((1+\sqrt{2})\left(\frac{1}{\sqrt{I_0}}-1\right)\right)\right)^{\frac{1}{\beta}-2}.
\end{aligned}$$

The plots of the speed $v_{\rm f}$ of the travelling wave front are shown in Figure 5.4 (b), (d) and (f).

It is particularly interesting to note that if $\alpha = \beta$, then $v_{\rm f} = (c)^{\frac{1}{\beta}}$, so that $v_{\rm f}$ is constant. Also, if $\alpha \neq \beta$, and since $\Gamma(\beta+1) = \beta\Gamma(\beta)$, and $\Gamma(\alpha+1) = \alpha\Gamma(\alpha)$, we have

$$v_{\rm f} = \left(\frac{c\Gamma(\beta)}{\Gamma(\alpha)}\right)^{\frac{1}{\beta}}\left(\frac{\beta}{\alpha}\right)^{\left(\frac{1}{\beta}-1\right)} t^{\left(\frac{\alpha}{\beta}-1\right)}.$$

Therefore

$$v'_{\rm f} = \left(\frac{c\Gamma(\beta)}{\Gamma(\alpha)}\right)^{\frac{1}{\beta}}\left(\frac{\beta}{\alpha}\right)^{\left(\frac{1}{\beta}-1\right)}\left(\frac{\alpha}{\beta}-1\right)t^{\left(\frac{\alpha}{\beta}-2\right)},$$

and so if $\alpha > \beta$, then $v'_{\rm f} > 0$, and if $\alpha < \beta$, then $v'_{\rm f} < 0$. We have therefore shown that if $\alpha = \beta$, the speed $v_{\rm f}$ of the travelling wave solution is constant (see Figure 5.4 (b)). If $\alpha > \beta$, the speed $v_{\rm f}$ of the travelling wave solution increases with time

(see Figure 5.4 (d)), and if $\alpha < \beta$, the speed v_{f} of the travelling wave solution decreases (see Figure 5.4 (f)).

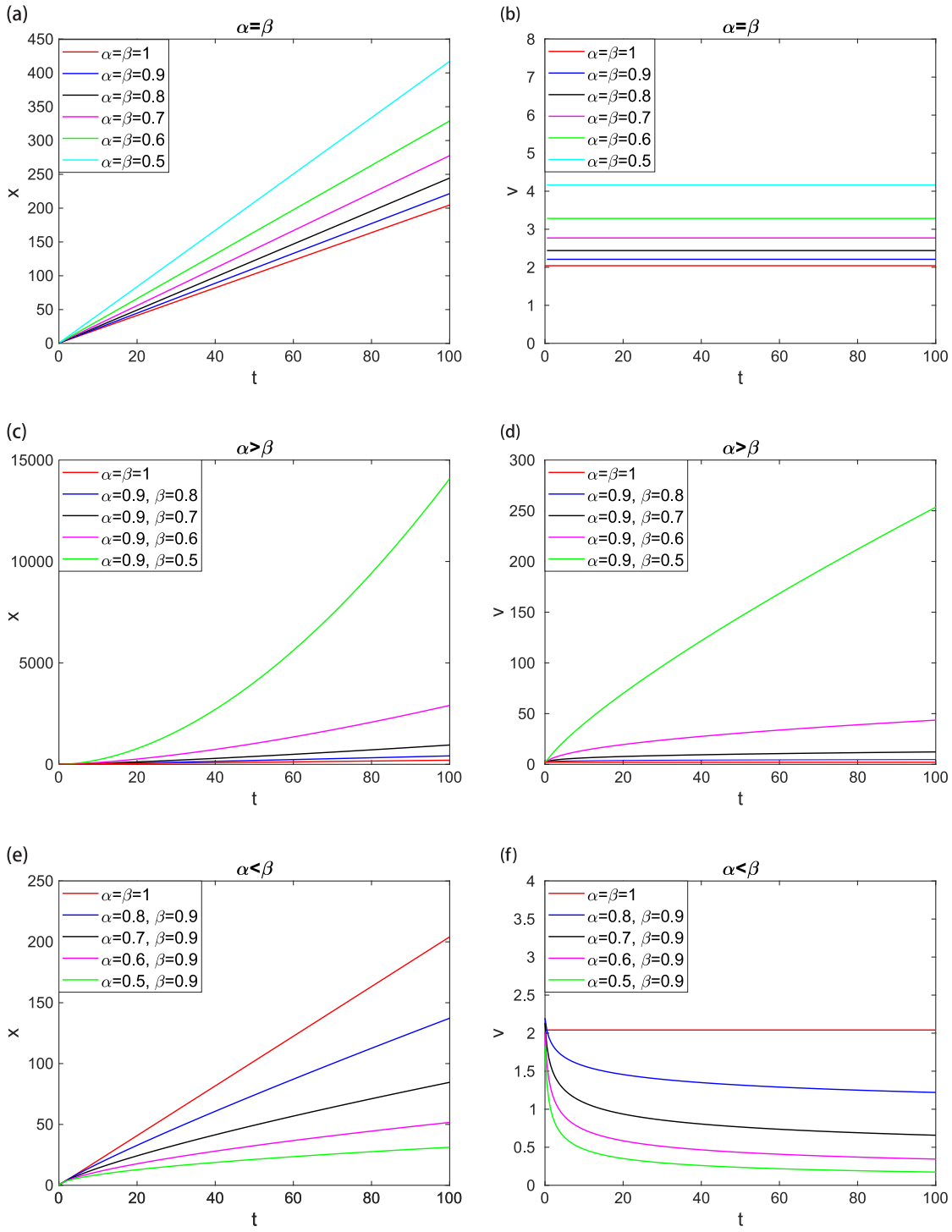

Figure 5.4: (a), (c) and (e) are the location $x_{\mathrm{f}}(t)$ of the front travelling wave solution (S_2, I_2) when $\alpha = \beta$, $\alpha > \beta$ and $\alpha < \beta$ respectively. (b), (d) and (f) are the speed $v_{\mathrm{f}}(t)$ of the front travelling wave solution (S_2, I_2) when $\alpha = \beta$, $\alpha > \beta$ and $\alpha < \beta$ respectively, with $S_0 = I_0 = 0.5$.

It should be noted that further generalisations of the travelling wave system can easily be incorporated. For instance, since the recovered equation is not coupled to those for S and I, we may use the solution for the travelling waves in S and I in a number of different R equations. Two example R equations are

$$\frac{\partial^\alpha R}{\partial t^\alpha} = \lambda_1 I,$$

and

$$\frac{\partial^\alpha R}{\partial t^\alpha} = \frac{\partial^{2\beta} R}{\partial x^{2\beta}} + \lambda_1 I,$$

both of which can readily be solved given the solution for I. Furthermore, generalisations to two spatial dimensions can also be incorporated. In this case we consider the system

$$\begin{aligned} \frac{\partial^\alpha S}{\partial t^\alpha} &= \left(\frac{\partial^{2\beta} S}{\partial x^{2\beta}} + \frac{\partial^{2\gamma} S}{\partial y^{2\gamma}}\right) - IS, \\ \frac{\partial^\alpha I}{\partial t^\alpha} &= \left(\frac{\partial^{2\beta} I}{\partial x^{2\beta}} + \frac{\partial^{2\gamma} I}{\partial y^{2\gamma}}\right) + I(S - \lambda_1), \end{aligned} \tag{5.73}$$

where $0 < \alpha, \beta, \gamma \leq 1$, In a similar way as in the preceding section, we seek travelling wave solutions of the form $S(x, y, t) = S(Z), \quad I(x, y, t) = I(Z)$, where

$$Z = \frac{k_x x^\beta}{\Gamma(\beta + 1)} + \frac{k_y y^\gamma}{\Gamma(\gamma + 1)} - \frac{c t^\alpha}{\Gamma(\alpha + 1)}, \tag{5.74}$$

where k_x, k_y are unknown parameters. This leads to equations similar to eqs (5.60) and (5.61)

$$(k_x^2 + k_y^2)S'' + cS' - IS = 0, \tag{5.75}$$

$$(k_x^2 + k_y^2)I'' + cI' + I(S - \lambda_1) = 0. \tag{5.76}$$

A suitable rescaling of S, I and c, by the factor $(k_x^2 + k_y^2)$, then leads to exactly eqs (5.60) and (5.61) and the solutions are then, again for $\lambda_1 = 0$,

$$S_{1,2}(Z) = \frac{S_0\Big(S_0 + 2(I_0 + \sqrt{I_0})e^{\pm Z/(\sqrt{6}(k_x^2+k_y^2))}\Big)}{(k_x^2 + k_y^2)\Big(S_0 + (I_0 + \sqrt{I_0})e^{\pm Z/(\sqrt{6}(k_x^2+k_y^2))}\Big)^2}, \tag{5.77}$$

$$I_{1,2}(Z) = \frac{(I_0 + \sqrt{I_0})^2 e^{\pm 2Z/(\sqrt{6}(k_x^2+k_y^2))}}{(k_x^2 + k_y^2)\Big(S_0 + (I_0 + \sqrt{I_0})e^{\pm Z/(\sqrt{6}(k_x^2+k_y^2))}\Big)^2}. \tag{5.78}$$

The location of the travelling wave front is again defined as the locations where $S = I$, but this is now a curve in the xy-plane defined by

$$Z = -\sqrt{6}(k_x^2 + k_y^2) \ln\left((1 + \sqrt{2})\left(\frac{1}{\sqrt{I_0}} - 1\right)\right), \tag{5.79}$$

which, using (5.79), is the line

$$y = \left(\frac{\Gamma(\gamma+1)}{k_y}\right)^{\frac{1}{\gamma}} \left(-\frac{k_x x^\beta}{\Gamma(\beta+1)} + \frac{ct^\alpha}{\Gamma(\alpha+1)} - \sqrt{6}(k_x^2+k_y^2)\ln\left((1+\sqrt{2})\left(\frac{1}{\sqrt{I_0}}-1\right)\right)\right)^{\frac{1}{\gamma}}. \tag{5.80}$$

Given that we must have $x > 0$ and $y > 0$ for the fractional derivatives to be valid, we see that the travelling wave front enters the region $x > 0$, $y > 0$ only after the time

$$t = \left(\frac{\sqrt{6}\Gamma(\alpha+1)}{c}(k_x^2+k_y^2)\ln\left((1+\sqrt{2})\left(\frac{1}{\sqrt{I_0}}-1\right)\right)\right)^{\frac{1}{\alpha}}, \tag{5.81}$$

and that the front enters the region at the origin $(x, y) = (0, 0)$.

We now consider four cases: (a) $\beta = \gamma = 1$; (b) $\beta = \gamma \neq 1$; (c) $\beta > \gamma$; (d) $\beta < \gamma$. For Case (a), $\beta = \gamma = 1$, the equation of the contour line is

$$y = -\frac{k_x}{k_y}x + \frac{c}{k_y\Gamma(\alpha+1)}t^\alpha - \frac{\sqrt{6}}{k_y}(k_x^2+k_y^2)\ln\left((1+\sqrt{2})\left(\frac{1}{\sqrt{I_0}}-1\right)\right), \tag{5.82}$$

i.e. a straight line (see Figure 5.5 (a)). In Case (b), $\beta = \gamma \neq 1$, the equation of the contour line is

$$y = \left(-\frac{k_x}{k_y}x^\beta + \frac{c\Gamma(\beta+1)}{k_y\Gamma(\alpha+1)}t^\alpha - \frac{\sqrt{6}\Gamma(\beta+1)}{k_y}(k_x^2+k_y^2)\ln\left((1+\sqrt{2})\left(\frac{1}{\sqrt{I_0}}-1\right)\right)\right)^{\frac{1}{\beta}}. \tag{5.83}$$

For the last two cases, $\beta > \gamma$ and $\beta < \gamma$ no simplification is possible. However, in the special cases $\gamma = 0$ and $\beta = 0$, respectively, we see that equivalent one dimensional cases are recovered, namely

$$x = \left(\frac{\Gamma(\beta+1)}{k_x}\right)^{\frac{1}{\beta}} \left(-k_y + \frac{ct^\alpha}{\Gamma(\alpha+1)} - \sqrt{6}(k_x^2+k_y^2)\ln\left((1+\sqrt{2})\left(\frac{1}{\sqrt{I_0}}-1\right)\right)\right)^{\frac{1}{\beta}}, \tag{5.84}$$

and

$$y = \left(\frac{\Gamma(\gamma+1)}{k_y}\right)^{\frac{1}{\gamma}} \left(-k_x + \frac{ct^\alpha}{\Gamma(\alpha+1)} - \sqrt{6}(k_x^2+k_y^2)\ln\left((1+\sqrt{2})\left(\frac{1}{\sqrt{I_0}}-1\right)\right)\right)^{\frac{1}{\gamma}}. \tag{5.85}$$

Plots of the travelling wave fronts in each of the above cases are included in Figure. 5.5.

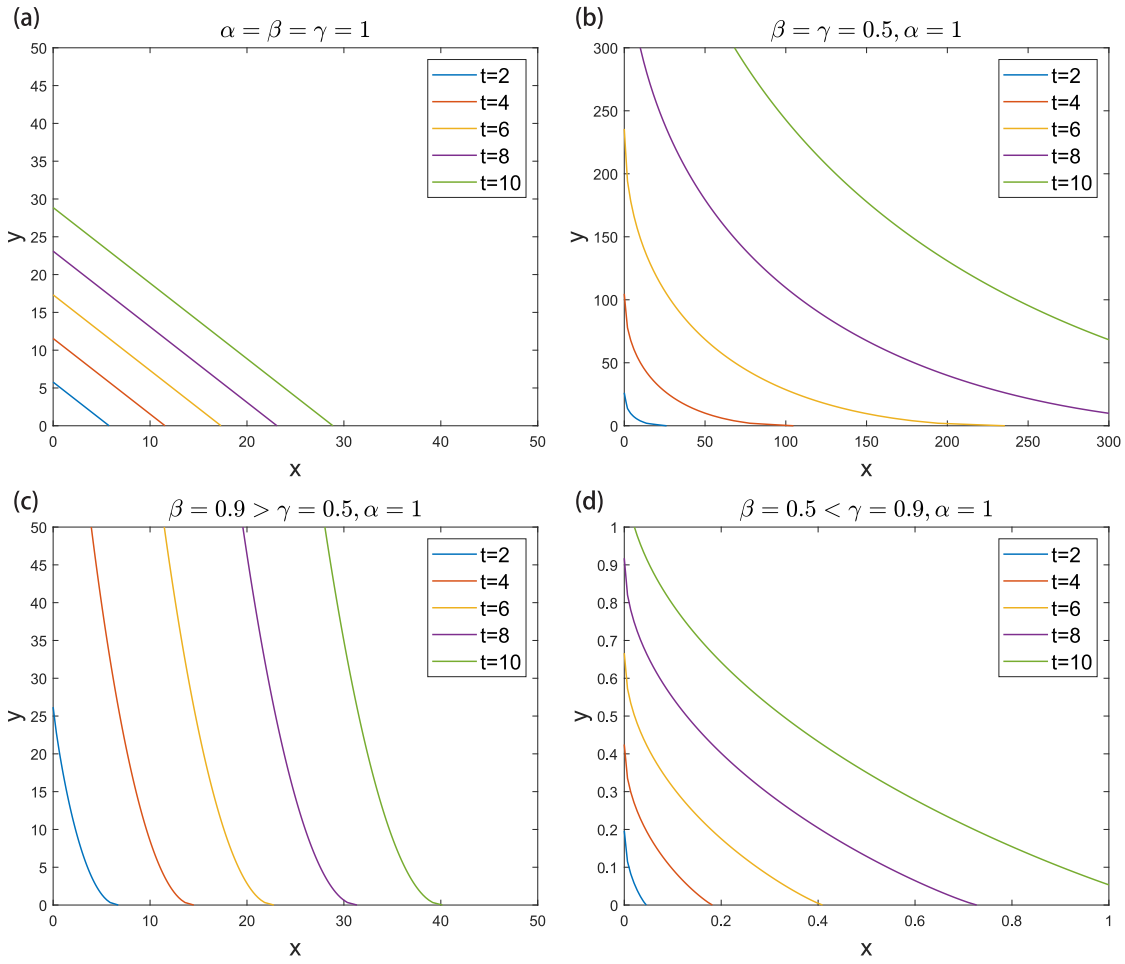

Figure 5.5: The location of the travelling wave front in the xy-plane when (a) $\alpha = \beta = \gamma = 1$, (b) $\beta = \gamma = 0.5$, $\alpha = 1$, (c) $\beta = 0.9 > \gamma = 0.5$, $\alpha = 1$, (d) $\beta = 0.5 < \gamma = 0.9$, $\alpha = 1$, for $0 < t < 10$. The initial conditions are $I_0 = 0.16$, $S_0 = 0.84$.

5.5 Conclusion

In this chapter we have considered various aspects of travelling wave behaviour in fractional differential systems. The use of fractional time derivatives has previously been justified through an attempt to model memory in both material science and in a biological context, and in our situation we see that for non-integer derivatives restricts the possibility of finding travelling waves. For a fractional Fisher's equation we found that, for a time derivative fractional order α and a space derivatives fractional order β, if $\alpha < \beta$, the speed $v(t)$ of the front travelling wave solution

$u(x,t)$ decreases in time, and conversely, if $\alpha > \beta$ the travelling wave accelerates. It would be interesting to consider these situations further particularly if altering the order of the spatial fractional diffusion could be used to show the progress of a travelling wave. This would have important consequences for real-life situations such as the spread of diseases. We have also considered the generalisation of an integer SIR model with spatial heterogeneity and proved that there may be travelling wave solutions by using the (G'/G)-expansion method. In a similar way to Fisher's equation, we found changing the fractional order can accelerate or decelerate the travelling wave. We have also seen, for two dimensional travelling waves, anisotropic spatial diffusion (i.e. $\beta \neq \gamma$) will lead to nonlinear wave front shapes. Again, it would be interesting to consider if such behaviour would be seen in real-life situations. Of course, there can be other possible solutions to the models described in this Chapter. Not all solutions are of the travelling wave type. For instance, solutions which are non-local, with the emergence of infection occurring at periodic points in space, or constant spatial solutions, where the infection emergences everywhere at the same time, are all possible. However, experience in the outbreak of diseases show that initial infection occurs locally and then spreads out, in a wave-like fashion. For this reason we have have concentrated in this Chapter on travelling wave solutions.

Chapter 6

Conclusion

6.1 Overall Conclusions

In this thesis, we considered fractional derivatives to study various diseases models, in order to capture the memory effect of individuals on the stability of the systems. Chapter 2 provides a brief review of some mathematical principles of fractional calculus and describes the methods that we used in this thesis. In Chapter 3 we studied a fractional order tumor model and its properties, and found that the stability of the system is affected by changing the model's fractional order. We also studied the parameter dependence of the critical value of the fractional order. To investigate the transition from a monostable to a bistable system, we considered an epidemiological model of susceptible, infected and recovered individuals (an SIR model). Crucially we found that variation of the fractional order as well as the other system parameters, gives the possibility of transitioning from a monostable system to a bistable system. The transient behaviour for this fractional system, in particular the dependence of trajectories on the initial states was identified. In addition, we also found that the observed domains of attraction for the two stable equilibrium points change by changing the fractional order, which is very important because if a disease state is unstable then memory can stabilise it.

Chapter 4 provides a broader and more complete investigation of this previous SIR model, by extending the model to be an incommensurate fractional order system. This might be a more accurate model because each of the species in this model has different memory which is more realistic than a commensurate system. Using the incommensurate system, we have shown that a stable equilibrium point can become an unstable point by decreasing the fractional order. This is an unexpected result since within the commensurate system decreasing the fractional order will only change an unstable point to be a stable point. To investigate this behaviour further, we used perturbation theory to find approximate analytical solutions for the characteristic equation of the incommensurate system, when the values of the fractional orders are close to the commensurate case. We also found

numerical solutions of the full system and showed that the stability boundary compared very well with the analytic solutions. We therefore found that reducing fractional orders may stabilise or destabilise the system. These results are again important because increased memory effects can stabilise or destabilise the system.

In Chapter 5 we have investigated various aspects of travelling wave behaviour in fractional differential equation systems. In this chapter we consider the fractional time derivative modelling a memory effect in a biological system and the spatial fractional system modelling multiscale inhomogeneities in the medium the travelling wave is moving through. We found that non-integer order derivatives can restrict the possibility of travelling waves unless there were non-integer derivatives in both time and space variables. In the fractional Fisher's equation we found that if the fractional time derivative α was less than the fractional space derivative β, the speed of the travelling wave solution decreases with time, and conversely, the travelling wave speed increases if $\alpha > \beta$. The study of these situations provides a more realistic picture of a biological system moving through a complex environment, and can have consequences for real human life situations, such as the spread of diseases. In this study, we also considered the generalization of a simple SIR model, by incorporating spatial heterogeneity to study the spread of diseases. We used the G'/G-expansion method to find travelling wave solutions, and in a similar way to Fisher's equation, we have shown that changing the fractional order can consequently accelerate or decelerate the travelling wave. In a two-dimensional travelling waves we have also shown that anisotropic spatial diffusion will lead to nonlinear wave fronts. It would be interesting to consider whether the behaviour obtained in our study would be the same in real-life situations.

6.2 Future Work and Extensions

Based on the obtained results in Chapter 3, the fine structure of the boundaries of the domain of attraction could be an extension for the future, although this investigation will depend on the value of t_{end}. It would be interesting to find, for example, fractal domains of attraction similar to those uncovered in systems of delay-differential equations [145]. This is only speculation at the moment, particularly without a completely satisfactory link between a fractional derivative model and the model of memory function. However, an understanding of the alterations in the domains of attraction as a function of α may provide a useful tool for comparison between practical work and theoretical models.

Regarding Chapter 4, given the complicated stability boundaries we have found, there are many new methods that could be used to control chaotic incommensurate fractional order systems such as using feedback control. Studying the global stability of the incommensurate fractional order systems could then be investigated.

In terms of Chapter 5, due to lack of time, many different methods to construct travelling wave solutions for space-time fractional differential equation models have been left as future work. Finally, travelling wave solutions for incommensurate space-time fractional models could also be investigated.

In short, although our study provided a deeper understanding of the effects of commensurate and incommensurate fractional derivatives in diseases systems, further investigation of these systems and their consequences for real-life situations would prove very interesting.

Bibliography

[1] M. Abdoon et al. First integral method: a general formula for nonlinear fractional Klein-Gordon equation using advanced computing language. *American Journal of Computational Mathematics*, 5:127–134, 2015.

[2] N. Abel. Solution de quelques problèmes à l'aide d'intégrales définies. *Oeuvres*, 1:11–27, 1881.

[3] M. Ablowitz and A. Zeppetella. Explicit solutions of Fisher's equation for a special wave speed. *Bulletin of Mathematical Biology*, 41:835–840, 1979.

[4] M. Agarwal and A. Bhadauria. A generalised prey-predator type model of immunogenic cancer with the effect of immunotherapy. *International Journal of Engineering, Science and Technology*, 5:66–84, 2013.

[5] D. Ağırseven and T. Öziş. An analytical study for Fisher type equations by using homotopy perturbation method. *Computers & Mathematics with Applications*, 60:602–609, 2010.

[6] E. Ahmed and A. Elgazzar. On fractional order differential equations model for nonlocal epidemics. *Physica A: Statistical Mechanics and its Applications*, 379:607–614, 2007.

[7] M. Akbar, N. Ali, and R. Roy. Closed form solutions of two time fractional nonlinear wave equations. *Results in Physics*, 9:1031–1039, 2018.

[8] T. Akman Yıldız, S. Arshad, and D. Baleanu. Optimal chemotherapy and immunotherapy schedules for a cancer-obesity model with Caputo time fractional derivative. *Mathematical Methods in the Applied Sciences*, 41:9390–9407, 2018.

[9] G. Akram and F. Batool. Solitary wave solutions of the Schäfer-Wayne short-pulse equation using two reliable methods. *Optical and Quantum Electronics*, 49:1–9, 2017.

[10] G. Akram and H. Tariq. An exponential spline technique for solving fractional boundary value problem. *Calcolo*, 53:545–558, 2016.

[11] A. Al-Shawba, K. Gepreel, F. Abdullah, and A. Azmi. Abundant closed form solutions of the conformable time fractional Sawada-Kotera-Ito equation using (G'/G)-expansion method. *Results in Physics*, 9:337–343, 2018.

[12] Z. Alqahtani, M. El-Shahed, and N. Mottram. Derivative-order-dependent stability and transient behaviour in a predator-prey system of fractional differential equations. *Letters in Biomathematics*, 6:32–49, 2019.

[13] J. Alzaidy. Fractional sub-equation method and its applications to the space-time fractional differential equations in mathematical physics. *British Journal of Mathematics & Computer Science*, 3:153–163, 2013.

[14] B. Anderson, J. Jackson, and M. Sitharam. Descartes' rule of signs revisited. *The American Mathematical Monthly*, 105:447–451, 1998.

[15] K. Atkinson, W. Han, and D. Stewart. *Numerical Solution of Ordinary Differential Equations*, volume 108. John Wiley & Sons, 2011.

[16] I. Baba. A fractional-order bladder cancer model with BCG treatment effect. *Computational and Applied Mathematics*, 38:1–8, 2019.

[17] E. Balcı, İ. Öztürk, and S. Kartal. Dynamical behaviour of fractional order tumor model with Caputo and conformable fractional derivative. *Chaos, Solitons & Fractals*, 123:43–51, 2019.

[18] D. Baleanu, M. Inc, A. Yusuf, and A. Aliyu. Lie symmetry analysis, exact solutions and conservation laws for the time fractional Caudrey-Dodd-Gibbon-Sawada-Kotera equation. *Communications in Nonlinear Science and Numerical Simulation*, 59:222–234, 2018.

[19] A. Bekir and Ö. Güner. Exact solutions of nonlinear fractional differential equations by (G'/G)-expansion method. *Chinese Physics B*, 22:1–6, 2013.

[20] A. Bekir, Ö. Güner, and A. Cevikel. Fractional complex transform and exp-function methods for fractional differential equations. In *Abstract and Applied Analysis*, volume 2013. Hindawi, 2013.

[21] A. Bekir, O. Guner, and A. Cevikel. The exp-function method for some time-fractional differential equations. *IEEE/CAA Journal of Automatica Sinica*, 4:315–321, 2016.

[22] A. Bhrawy and A. Alofi. An accurate spectral Galerkin method for solving multiterm fractional differential equations. *Mathematical Problems in Engineering*, 2014:1–9, 2014.

[23] Z. Bin. (G'/G)-expansion method for solving fractional partial differential equations in the theory of mathematical physics. *Communications in Theoretical Physics*, 58:623–630, 2012.

[24] W. Bo, G. Lin, and B. Xiong. Minimal wave speed on a diffusive SIR model with nonlocal delays. *Electronic Journal of Differential Equations*, 2018:1–11, 2018.

[25] M. Bonkile, A. Awasthi, C. Lakshmi, V. Mukundan, and V. Aswin. A systematic literature review of Burgers' equation with recent advances. *Pramana*, 90:1–21, 2018.

[26] C. Bonnet and J. Partington. Analysis of fractional delay systems of retarded and neutral type. *Automatica*, 38:1133–1138, 2002.

[27] N. Britton. *Reaction-Diffusion Equations and their Applications to Biology.* Academic Press, 1986.

[28] H. Bulut and Y. Pandir. Modified trial equation method to the nonlinear fractional Sharma-Tasso-Olever equation. *International Journal of Modeling and Optimization*, 3:353–357, 2013.

[29] R. Caponetto. *Fractional Order Systems: Modeling and Control Applications*, volume 72. World Scientific Publishing, 2010.

[30] M. Caputo. Linear models of dissipation whose Q is almost frequency independent. *Annals of Geophysics*, 19:383–393, 1966.

[31] M. Caputo. Linear models of dissipation whose Q is almost frequency independent—II. *Geophysical Journal International*, 13:529–539, 1967.

[32] R. Casagrandi, L. Bolzoni, S. Levin, and V. Andreasen. The SIRC model and influenza A. *Mathematical Biosciences*, 200:152–169, 2006.

[33] F. Castiglione and B. Piccoli. Cancer immunotherapy, mathematical modeling and optimal control. *Journal of Theoretical Biology*, 247:723–732, 2007.

[34] Y. Çenesiz, O. Tasbozan, and A. Kurt. Functional Variable Method for conformable fractional modified KdV-ZK equation and Maccari system. *Tbilisi Mathematical Journal*, 10:118–126, 2017.

[35] H. Chen, W. Chen, and B. Chen. Robust synchronization of incommensurate fractional-order chaotic systems via second-order sliding mode technique. In *Proceedings of the 32nd Chinese Control Conference*, pages 3147–3151, 2013.

[36] J. Choi, H. Kim, and R. Sakthivel. On certain exact solutions of diffusive predator-prey system of fractional order. *Chinese Journal of Physics*, 54:135–146, 2016.

[37] J. Choi, H. Kim, and R. Sakthivel. Exact travelling wave solutions of reaction-diffusion models of fractional order. *Journal of Applied Analysis and Computation*, 7:236–248, 2017.

[38] S. Choi, B. Kang, and N. Koo. Stability for Caputo fractional differential systems. *Abstract and Applied Analysis*, 2014:1–6, 2014.

[39] J. Conlon and C. Doering. On travelling waves for the stochastic Fisher-Kolmogorov-Petrovsky-Piscunov equation. *Journal of Statistical Physics*, 120:421–477, 2005.

[40] C. Cuesta, S. Hittmeir, and C. Schmeiser. Traveling waves of a kinetic transport model for the KPP-Fisher equation. *SIAM Journal on Mathematical Analysis*, 44:4128–4146, 2012.

[41] R. Culshaw and S. Ruan. A delay-differential equation model of HIV infection of CD4+ T-cells. *Mathematical Biosciences*, 165:27–39, 2000.

[42] S. Damarla and M. Kundu. Novel hybrid function operational matrices of fractional integration: An application for solving multi-order fractional differential equations. *arXiv preprint arXiv:1801.06973*, 2018.

[43] R. J De Boer. *Modeling Population Dynamics: a Graphical Approach*. 2006.

[44] L. De Pillis and A. Radunskaya. The dynamics of an optimally controlled tumor model: A case study. *Mathematical and Computer Modelling*, 37:1221–1244, 2003.

[45] W. Deng, C. Li, and J. Lü. Stability analysis of linear fractional differential system with multiple time delays. *Nonlinear Dynamics*, 48:409–416, 2007.

[46] K. Diethelm, N. Ford, and A. Freed. A predictor-corrector approach for the numerical solution of fractional differential equations. *Nonlinear Dynamics*, 29:3–22, 2002.

[47] K. Diethelm, N. Ford, and A. Freed. Detailed error analysis for a fractional Adams method. *Numerical Algorithms*, 36:31–52, 2004.

[48] Y. Ding and H. Ye. A fractional-order differential equation model of HIV infection of CD4+ T-cells. *Mathematical and Computer Modelling*, 50:386–392, 2009.

[49] M. Du, Z. Wang, and H. Hu. Measuring memory with the order of fractional derivative. *Scientific Reports*, 3:1–3, 2013.

[50] A. Edwin. *Modeling and analysis of a two prey-one predator system with harvesting, Holling Type II and ratio-dependent responses*. PhD thesis, Doctoral Dissertation, Makerere University, 2010.

[51] S. Ege and E. Misirli. The modified Kudryashov method for solving some fractional-order nonlinear equations. *Advances in Difference Equations*, 2014:1–13, 2014.

[52] M. El-Shahed and F. Alissa. A fractional-order model for computer viruses propagation with saturated treatment rate. *Nonlinear Analysis and Differential Equations*, 4:583–595, 2016.

[53] M. El-Shahed and A. Alsaedi. The fractional SIRC model and influenza A. *Mathematical Problems in Engineering*, 2011:1–9, 2011.

[54] A. Erdélyi, W. Magnus, F. Oberhettinger, and F. Tricomi. Higher transcendental functions. *New York*, 1, 1955.

[55] L. Euler. De progressionibus transcendentibus seu quarum termini generales algebraice dari nequeunt. *Commentarii academiae scientiarum Petropolitanae*, pages 36–57, 1738.

[56] Z. Feng. Traveling waves to a reaction-diffusion equation. *Discrete & Continuous Dynamical Systems Supplement*, 12:382–390, 2007.

[57] Z. Feng, S. Zheng, and D. Gao. Traveling wave solutions to a reaction-diffusion equation. *Zeitschrift Für Angewandte Mathematik und Physik*, 60:756–773, 2009.

[58] P. Fife. Mathematical Aspects of Reacting and Diffusing. *Systems, Sppinger-Verlag, Heidelberg*, 1979.

[59] D. Finkelshtein, Y. Kondratiev, and P. Tkachov. Doubly nonlocal Fisher-KPP equation: Existence and properties of traveling waves. *arXiv preprint arXiv:1804.10258*, pages 1–30, 2018.

[60] D. Finkelshtein, Y. Kondratiev, and P. Tkachov. Doubly nonlocal Fisher-KPP equation: Speeds and uniqueness of traveling waves. *Journal of Mathematical Analysis and Applications*, 475:94–122, 2019.

[61] R. Fisher. The wave of advance of advantageous genes. *Annals of Eugenics*, 7:355–369, 1937.

[62] R. Gardner. Existence of travelling wave solutions of predator–prey systems via the connection index. *SIAM Journal on Applied Mathematics*, 44:56–79, 1984.

[63] R. Garrappa. On linear stability of predictor-corrector algorithms for fractional differential equations. *International Journal of Computer Mathematics*, 87:2281–2290, 2010.

[64] R. Garrappa. Trapezoidal methods for fractional differential equations: Theoretical and computational aspects. *Mathematics and Computers in Simulation*, 110:96–112, 2015.

[65] K. Gepreel. The homotopy perturbation method applied to the nonlinear fractional Kolmogorov-Petrovskii-Piskunov equations. *Applied Mathematics Letters*, 24:1428–1434, 2011.

[66] J. Gómez-Aguilar, M. López-López, V. Alvarado-Martínez, D. Baleanu, and H. Khan. Chaos in a cancer model via fractional derivatives with exponential decay and Mittag-Leffler law. *Entropy*, 19:681, 2017.

[67] G. González-Parra, A. Arenas, and B. Chen-Charpentier. A fractional order epidemic model for the simulation of outbreaks of influenza A (H1N1). *Mathematical Methods in the Applied Sciences*, 37:2218–2226, 2014.

[68] R. Gorenflo and F. Mainardi. Essentials of fractional calculus. 2000.

[69] P. Grindrod. *The Theory and Applications of Reaction-Diffusion Equations: Patterns and Waves*. Clarendon Press, 1996.

[70] A. Grunwald. Uber 'begrente' Derivationen und deren Anwedung. *Zangew Math und Phys*, 12:441–480, 1867.

[71] O. Guner and A. Bekir. Solving nonlinear space-time fractional differential equations via Ansatz method. *Computational Methods for Differential Equations*, 6:1–11, 2018.

[72] E. Hairer, C. Lubich, and M. Schlichte. Fast numerical solution of weakly singular Volterra integral equations. *Journal of Computational and Applied Mathematics*, 23:87–98, 1988.

[73] J. Harris, S. Harris, and A. Kyprianou. Further probabilistic analysis of the Fisher-Kolmogorov-Petrovskii-Piscounov equation: One sided travelling-waves. 42:125–145, 2006.

[74] S. Harris. Travelling-waves for the FKPP equation via probabilistic arguments. *Proceedings of the Royal Society of Edinburgh Section A: Mathematics*, 129:503–517, 1999.

[75] J. He, S. Elagan, and Z. Li. Geometrical explanation of the fractional complex transform and derivative chain rule for fractional calculus. *Physics Letters A*, 376:257–259, 2012.

[76] J. Heffernan, R. Smith, and L. Wahl. Perspectives on the basic reproductive ratio. *Journal of the Royal Society Interface*, 2:281–293, 2005.

[77] H. Hethcote. *Applied Mathematical Ecology*. Springer, 1989.

[78] H. Hethcote and J. Van Ark. Modeling HIV transmission and AIDS in the United States. *Lecture Notes in Biomathematics*, 95, 1991.

[79] K. Hosseini and R. Ansari. New exact solutions of nonlinear conformable time-fractional Boussinesq equations using the modified Kudryashov method. *Waves in Random and Complex Media*, 27:628–636, 2017.

[80] M. Inc. The approximate and exact solutions of the space-and time-fractional Burgers equations with initial conditions by variational iteration method. *Journal of Mathematical Analysis and Applications*, 345:476–484, 2008.

[81] M. Ishteva. *Properties and applications of the Caputo fractional operator*. PhD thesis, Department of Mathematics, University of Karlsruhe, Karlsruhe, 2005.

[82] O. Iyiola and F. Zaman. A fractional diffusion equation model for cancer tumor. *AIP Advances*, 4:107121, 2014.

[83] Z. Jiao and Y. Chen. Stability analysis of fractional-order systems with double noncommensurate orders for matrix case. *Fractional Calculus and Applied Analysis*, 14:436–453, 2011.

[84] G. Jumarie. Modified Riemann-Liouville derivative and fractional Taylor series of nondifferentiable functions further results. *Computers & Mathematics with Applications*, 51:1367–1376, 2006.

[85] G. Jumarie. Table of some basic fractional calculus formulae derived from a modified Riemann-Liouville derivative for non-differentiable functions. *Applied Mathematics Letters*, 22:378–385, 2009.

[86] G. Jumarie. *Fractional Differential Calculus for Non-Differentiable Functions: Mechanics, Geometry, Stochastics, Information Theory*. LAP Lambert Academic Publishing, 2013.

[87] M. Kaplan, A. Akbulut, and A. Bekir. Solving space-time fractional differential equations by using modified simple equation method. *Communications in Theoretical Physics*, 65:563–568, 2016.

[88] M. Kaplan, M. Koparan, and A. Bekir. Regarding on the exact solutions for the nonlinear fractional differential equations. *Open Physics*, 14:478–482, 2016.

[89] G. Kaur and N. Ahmad. On study of immune response to tumor cells in prey-predator system. *International Scholarly Research Notices*, 2014:1–8, 2014.

[90] W. Kermack and A. McKendrick. A contribution to the mathematical theory of epidemics. *Royal Society*, 115:700–721, 1927.

[91] M. Khater, A. Seadawy, and D. Lu. Elliptic and solitary wave solutions for Bogoyavlenskii equations system, couple Boiti-Leon-Pempinelli equations system and Time-fractional Cahn-Allen equation. *Results in Physics*, 7:2325–2333, 2017.

[92] A. Kilbas, H. Srivastava, and J. Trujillo. *Theory and Applications of Fractional Differential Equations*. Elsevier, 2006.

[93] V. Kiryakova. A long standing conjecture failed. *Transform Methods and Special Functions, Varna*, 96:579–588, 1998.

[94] R. Knobloch. One-sided FKPP travelling waves in the context of homogeneous fragmentation processes. *arXiv preprint arXiv:1204.0758*, pages 1–30, 2012.

[95] A. Kolmogorov. Étude de l'équation de la diffusion avec croissance de la quantité de matière et son application à un problème biologique. *Bull. Univ. Moskow, Ser. Internat., Sec. A*, 1:1–25, 1937.

[96] A. Letnikov. Theory of differentiation of fractional order. *Mat. Sb*, 3:1868, 1868.

[97] R. Levins, T. Awerbuch, U. Brinkmann, I. Eckardt, P. Epstein, N. Makhoul, C. de Possas, C. Puccia, A. Spielman, and M. Wilson. The emergence of new diseases. *American Scientist*, 82:52–60, 1994.

[98] W. Li, F. Yang, et al. Traveling waves for a nonlocal dispersal SIR model with standard incidence. *Journal of Integral Equations and Applications*, 26:243–273, 2014.

[99] Y. Li, W. Li, and G. Lin. Traveling waves of a delayed diffusive SIR epidemic model. *Communications on Pure & Applied Analysis*, 14:1001–1022, 2015.

[100] Z. Li and J. He. Fractional complex transform for fractional differential equations. *Mathematical and Computational Applications*, 15:970–973, 2010.

[101] S. Liu, Z. Fu, S. Liu, and Q. Zhao. Jacobi elliptic function expansion method and periodic wave solutions of nonlinear wave equations. *Physics Letters A*, 289:69–74, 2001.

[102] S. Ma. Traveling wavefronts for delayed reaction-diffusion systems via a fixed point theorem. *Journal of Differential Equations*, 171:294–314, 2001.

[103] J. Malinzi, P. Sibanda, and H. Mambili-Mamboundou. Response of immunotherapy to tumour-TICLs interactions: a travelling wave analysis. *Abstract and Applied Analysis*, 2014:1–11, 2014.

[104] T. Malthus. An essay on the principle of population as it affects the future improvement of society, with remarks on the speculations of Mr Godwin, M. *Condorcet, and Other Writers. London: J. Johnson*, 1798.

[105] J. Manafian and M. Lakestani. A new analytical approach to solve some of the fractional-order partial differential equations. *Indian Journal of Physics*, 91:243–258, 2017.

[106] M. Mansour. Traveling wave solutions of a nonlinear reaction-diffusion-chemotaxis model for bacterial pattern formation. *Applied Mathematical Modelling*, 32:240–247, 2008.

[107] A. Marchaud. *Sur les dérivées et sur les différences des fonctions de variables réelles*. PhD thesis, impr. Gauthier-Villars, 1927.

[108] P. Martens. How will climate change affect human health? The question poses a huge challenge to scientists. Yet the consequences of global warming of public health remain largely unexplored. *American Scientist*, 87:534–541, 1999.

[109] R. Martínez-Guerra, C. Pérez-Pinacho, G. Gómez-Cortés, and J. Cruz-Victoria. Synchronization of incommensurate fractional order system. *Applied Mathematics and Computation*, 262:260–266, 2015.

[110] D. Matignon. Stability properties for generalized fractional differential systems. *ESAIM: Proceedings*, 5:145–158, 1998.

[111] D. Matignon and C. Prieur. Asymptotic stability of linear conservative systems when coupled with diffusive systems. *ESAIM: Control, Optimisation and Calculus of Variations*, 11:487–507, 2005.

[112] A. Matzavinos and M. Chaplain. Travelling-wave analysis of a model of the immune response to cancer. *Comptes Rendus Biologies*, 327:995–1008, 2004.

[113] D. Mohammed. Numerical solution of fractional integro-differential equations by least squares method and shifted Chebyshev polynomial. *Mathematical Problems in Engineering*, 2014:1–6, 2014.

[114] S. Mohyud-Din, T. Nawaz, E. Azhar, and M. Akbar. Fractional sub-equation method to space-time fractional Calogero-Degasperis and potential Kadomtsev-Petviashvili equations. *Journal of Taibah University for Science*, 11:258–263, 2017.

[115] S. Momani and S. Hadid. Lyapunov stability solutions of fractional integrodifferential equations. *International Journal of Mathematics and Mathematical Sciences*, 2004:2503–2507, 2004.

[116] C. Monje, Y. Chen, B. Vinagre, D. Xue, and V. Feliu-Batlle. *Fractional-Order Systems and Controls: Fundamentals and Applications*. Springer Science & Business Media, 2010.

[117] J. Murray. *Mathematical Biology II: Spatial Models and Biomedical Applications*. Springer New York, 2001.

[118] J. Murray. *Mathematical Biology: I. An Introduction*, volume 17. Springer Science & Business Media, 2007.

[119] G. Nadin, B. Perthame, and M. Tang. Can a traveling wave connect two unstable states? The case of the nonlocal Fisher equation. *Comptes Rendus Mathematique*, 349:553–557, 2011.

[120] K. Oldham and J. Spanier. *The Fractional Calculus Theory and Applications of Differentiation and Integration to Arbitrary Order*. Academic Press, 1974.

[121] K. Owolabi. Efficient numerical simulation of non-integer-order space-fractional reaction-diffusion equation via the Riemann-Liouville operator. *The European Physical Journal Plus*, 133:1–16, 2018.

[122] E. Parkes and B. Duffy. An automated tanh-function method for finding solitary wave solutions to non-linear evolution equations. *Computer Physics Communications*, 98:288–300, 1996.

[123] J. Patade and S. Bhalekar. A novel numerical method for solving Volterra integro-differential equations. *International Journal of Applied and Computational Mathematics*, 6:1–19, 2020.

[124] I. Petras. Stability of fractional-order systems with rational orders: A survey. *Fractional Calculus & Applied Analysis*, 12:269–298, 2009.

[125] I. Podlubny. *Fractional Differential Equations: an Introduction to Fractional Derivatives, Fractional Differential Equations, to Methods of their Solution and Some of their Applications*. Elsevier, 1998.

[126] I. Podlubny. Geometric and physical meaning of fractional derivative. *Fractional Calculus & Applied Analysis*, pages 1311–045, 2002.

[127] S. Pooseh, H. Rodrigues, and D. Torres. Fractional derivatives in dengue epidemics. *AIP Conference Proceedings*, 1389:739–742, 2011.

[128] M. Razvan and S. Yasaman. Global analysis of an sais model. *Journal of Biological Dynamics*, 6:457–474, 2012.

[129] F. Rihan. Numerical modeling of fractional-order biological systems. *Abstract and Applied Analysis*, 2013:1–11, 2013.

[130] F. Rihan, A. Hashish, F. Al-Maskari, M. Hussein, E. Ahmed, M. Riaz, and R. Yafia. Dynamics of tumor-immune system with fractional-order. *Journal of Tumor Research*, 2:109–115, 2016.

[131] B. Ross. Fractional calculus and its applications. 1974. *Lecture Notes in Mathematics*, 457, 1974.

[132] Z. Ruo-Xun and Y. Shi-Ping. Adaptive stabilization of an incommensurate fractional order chaotic system via a single state controller. *Chinese Physics B*, 20:1–8, 2011.

[133] J. Sabatier, C. Farges, and J. Trigeassou. A stability test for non-commensurate fractional order systems. *Systems & Control Letters*, 62:739–746, 2013.

[134] S. Samko, A. Kilbas, and O. Marichev. *Fractional Integrals and Derivatives*. Gordon and Breach Science Publishers, 1993.

[135] F. Sanchezgarduno and P. Maini. Traveling wave phenomena in some degenerate reaction-diffusion equations. *Journal of Differential Equations*, 117:281–319, 1995.

[136] R. Sarkar and S. Banerjee. Cancer self remission and tumor stability-a stochastic approach. *Mathematical Biosciences*, 196:65–81, 2005.

[137] R. Sarkar and S. Banerjee. A time delay model for control of malignant tumor growth. *National Conference on Nonlinear Systems and Dynamics*, 1:1–5, 2006.

[138] L. Segel. *Mathematical Models in Molecular Cellular Biology*. CUP Archive, 1980.

[139] M. Shakeel. Travelling wave solution of the Fisher-Kolmogorov equation with non-linear diffusion. *Applied Mathematics*, pages 148–160, 2013.

[140] M. Shallal, H. Jabbar, and K. Ali. Analytic solution for the space-time fractional Klein-Gordon and coupled conformable Boussinesq equations. *Results in Physics*, 8:372–378, 2018.

[141] B. Singh and P. Kumar. Fractional variational iteration method for solving fractional partial differential equations with proportional delay. *International Journal of Differential Equations*, 2017:1–12, 2017.

[142] R. Sir and R. Fisher. *The Genetical Theory of Natural Selection: a Complete Variorum Edition*. Oxford University Press, 1999.

[143] E. Tala-Tebue, Z. Djoufack, A. Djimeli-Tsajio, and A. Kenfack-Jiotsa. Solitons and other solutions of the nonlinear fractional Zoomeron equation. *Chinese Journal of Physics*, 56:1232–1246, 2018.

[144] M. Tavazoei and M. Haeri. Chaotic attractors in incommensurate fractional order systems. *Physica D: Nonlinear Phenomena*, 237:2628–2637, 2008.

[145] S. Taylor and S. Campbell. Approximating chaotic saddles for delay differential equations. *Physical Review E*, 75:046215, 2007.

[146] A. Tisbury, D. Needham, and A. Tzella. The Evolution of Travelling Waves in a KPP Reaction-Diffusion Model with Cut-off Reaction Rate. I. Permanent Form Travelling Waves. *arXiv preprint arXiv:1805.01878*, 2018.

[147] P. Tong, Y. Feng, and H. Lv. Euler's method for fractional differential equations. *Wseas Transactions on Mathematics*, 12:1146–1153, 2013.

[148] P. Turchin. *Complex Population Dynamics: a Theoretical/Empirical Synthesis*. Princeton University Press, 2003.

[149] J. Tyson and P. Brazhnik. On traveling wave solutions of Fisher's equation in two spatial dimensions. *SIAM Journal on Applied Mathematics*, 60:371–391, 2000.

[150] E. Ucar, N. Özdemir, and E. Altun. Fractional order model of immune cells influenced by cancer cells. *Mathematical Modelling of Natural Phenomena*, 14:1–12, 2019.

[151] R. Upadhyay, S. Kumari, and A. Misra. Modeling the virus dynamics in computer network with SVEIR model and nonlinear incident rate. *Journal of Applied Mathematics and Computing*, 54:485–509, 2017.

[152] B. Van der Waerden. *Algebra*. Springer Science & Business Media, 2003.

[153] M. Veselinova, H. Kiskinov, and A. Zahariev. Stability analysis of neutral linear fractional system with distributed delays. *Filomat*, 30:841–851, 2016.

[154] N. Vitanov and M. Ausloos. Knowledge epidemics and population dynamics models for describing idea diffusion. In *Models of Science Dynamics*, pages 69–125. Springer, 2012.

[155] M. Wang, X. Li, and J. Zhang. The (G'/G)-expansion method and travelling wave solutions of nonlinear evolution equations in mathematical physics. *Physics Letters A*, 372:417–423, 2008.

[156] W. Wang. Backward bifurcation of an epidemic model with treatment. *Mathematical Biosciences*, 201:58–71, 2006.

[157] W. Wang. Epidemic models with nonlinear infection forces. *Mathematical Biosciences & Engineering*, 3:267, 2006.

[158] W. Wang and S. Ruan. Bifurcations in an epidemic model with constant removal rate of the infectives. *Journal of Mathematical Analysis and Applications*, 291:775–793, 2004.

[159] X. Wang, H. Wang, and J. Wu. Traveling waves of diffusive predator-prey systems: Disease outbreak propagation. *Discrete & Continuous Dynamical Systems-A*, 32:3303–3324, 2012.

[160] Z. Wang and J. Wu. Travelling waves of a diffusive Kermack-McKendrick epidemic model with non-local delayed transmission. *Proceedings of the Royal Society A: Mathematical, Physical and Engineering Sciences*, 466:237–261, 2010.

[161] H. Weiss. *A Mathematical Introduction to Population Dynamics*. IMPA, 2009.

[162] H. Weyl. Bemerkungen zum begriff des differentialquotienten gebrochener ordnung. *Zürich. Naturf. Ges*, 62:296–302, 1917.

[163] K. Wilkie and P. Hahnfeldt. Mathematical models of immune-induced cancer dormancy and the emergence of immune evasion. *Interface Focus*, 3:20130010, 2013.

[164] H. Wilson and J. Rallison. Short wave instability of co-extruded elastic liquids with matched viscosities. *Journal of Non-Newtonian Fluid Mechanics*, 72:237–251, 1997.

[165] A. Winfree. *The Geometry of Biological Time*, volume 12. Springer Science & Business Media, 2001.

[166] K. Wu and K. Zhou. Traveling waves in a nonlocal dispersal SIR model with standard incidence rate and nonlocal delayed transmission. *Mathematics*, 7:1–22, 2019.

[167] H. Yagisita. Existence and nonexistence of traveling waves for a nonlocal monostable equation. *arXiv preprint arXiv:0810.3317*, pages 925–953, 2008.

[168] J. Yang, S. Liang, and Y. Zhang. Travelling waves of a delayed SIR epidemic model with nonlinear incidence rate and spatial diffusion. *PloS one*, 6, 2011.

[169] M. Younis. A new approach for the exact solutions of nonlinear equations of fractional order via modified simple equation method. *Applied Mathematics*, 5:1927–1932, 2014.

[170] M. Younis and A. Zafar. Exact solution to nonlinear differential equations of fractional order via (G'/G)-expansion method. *Applied Mathematics*, 5:1–6, 2014.

[171] W. Yuan, Q. Chen, J. Qi, and Y. Li. The general traveling wave solutions of the Fisher equation with degree three. *Advances in Mathematical Physics*, 2013:1–6, 2013.

[172] W. Yuan, B. Xiao, Y. Wu, and J. Qi. The general traveling wave solutions of the Fisher type equations and some related problems. *Journal of Inequalities and Applications*, 2014:1–15, 2014.

[173] E. Zayed, Y. Amer, and A. Al-Nowehy. The modified simple equation method and the multiple exp-function method for solving nonlinear fractional Sharma-Tasso-Olver equation. *Acta Mathematicae Applicatae Sinica, English Series*, 32:793–812, 2016.

[174] E. Zayed and H. SA. Modified simple equation method and its applications for some nonlinear evolution equations in mathematical physics. *International Journal of Computer Applications*, 67:39–44, 2013.

[175] J. Zhang, J. Jia, and X. Song. Analysis of an SEIR epidemic model with saturated incidence and saturated treatment function. *The Scientific World Journal*, 2014:1–12, 2014.

[176] S. Zhang and H. Zhang. Fractional sub-equation method and its applications to nonlinear fractional PDEs. *Physics Letters A*, 375:1069–1073, 2011.

[177] X. Zhang and X. Liu. Backward bifurcation of an epidemic model with saturated treatment function. *Journal of Mathematical Analysis and Applications*, 348:433–443, 2008.

[178] S. Zhao and G. Wei. Comparison of the discrete singular convolution and three other numerical schemes for solving Fisher's equation. *SIAM Journal on Scientific Computing*, 25:127–147, 2003.

[179] B. Zheng. Exp-function method for solving fractional partial differential equations. *The Scientific World Journal*, 2013:1–9, 2013.

[180] Z. Zhonghua and S. Yaohong. Qualitative analysis of a SIR epidemic model with saturated treatment rate. *Journal of Applied Mathematics and Computing*, 34:177–194, 2010.

[181] L. Zhou and M. Fan. Dynamics of an SIR epidemic model with limited medical resources revisited. *Nonlinear Analysis: Real World Applications*, 13:312–324, 2012.

[182] X. Zou. Delay induced traveling wave fronts in reaction-diffusion equations of KPP-Fisher type. *Journal of Computational and Applied Mathematics*, 146:309–321, 2002.